https://doi.org/10.5194/egusphere-2026-971
Preprint. Discussion started: 6 March 2026

Compound Drivers and Spatial Connectivity led to the Devastating Debris Flood in the Village of La Bérarde, June 2024, French Alps

Simon Filhol[1], Clement Misset[2], Noélie Bontemps[3], Diego Cusicanqui[3], Emmanuel Paquet[4], Marie Dumont[1], Olivier Gagliardini[5], Pascal Lacroix[3], Simon Gascoin[6], Guillaume Thirel[6], Julien Brondex[5], Pascal Hagenmuller[1], Eric Larose[3], Philipp Schoeneich[7], Denis Roy[8], Emmanuel Thibert[5], Nicolas Eckert[5], Felix de Montety[7], Robin Mainieri[3], Alexandre Hauet[4], Frédéric Gottardi[4], Johan Berthet[9], Alexandre Baratier[9], Frédéric Liébault[5], Małgorzata Chmiel[10], Guillaume Piton[5], Guillaume Chambon[5], Guillaume James[11], Philippe Frey[5], Philip Deline[12], Laurent Astrade[12], Christian Vincent[5], Dominique Laigle[13], Alain Recking[13], Fatima Karbou[1], Adrien Mauss[14], Mylène Bonnefoy-Demongeot[5], Firmin Fontaine[5], Mickael Langlais[3], Etienne Berthier[15], and Antoine Blanc[16]

[1]Météo-France, CNRS, Université Grenoble Alpes, Université Toulouse, CNRM, Centre d'Études de la Neige, 38000 Grenoble, France
[2]Office National des Forêts, Délégation Nationale aux Risques Naturels, Pole RTM, 38000 Grenoble, France
[3]Institut des Sciences de la Terre (ISTerre), CNES, CNRS, IRD, Université Grenoble Alpes, Université Savoie Mont Blanc, Université Gustave Eiffel, 38000 Grenoble, France
[4]EDF-DTG, 38950 St Martin le Vinoux, France
[5]Institut des Géosciences de l'Environnement (IGE), CNRS, IRD, INRAE, Université Grenoble Alpes, 38000 Grenoble, France
[6]CESBIO, Université de Toulouse, CNES, CNRS, INRAE, IRD, 31000 Toulouse, France
[7]Laboratoire Pacte, Université Grenoble Alpes, 38000 Grenoble, France
[8]Météo-France, Direction Inter-régionale Centre-Est, 38000 Grenoble, France
[9]Styx4D, 73370 Le Bourget du Lac, France
[10]Observatoire de la Côte d'Azur, Université Côte d'Azur, CNRS, IRD, Géoazur, Sophia Antipolis 06560 Valbonne, France
[11]Université Grenoble Alpes, Inria, CNRS, Grenoble INP, LJK, 38000 Grenoble, France
[12]EDYTEM, Université Savoie Mont-Blanc, CNRS, 73000 Chambéry, France
[13]Université Grenoble Alpes, CNRS, IRD, INRAE, Grenoble-INP, IGE, 38000 Grenoble, France
[14]Météo-France, Centre de Météorologie Spatiale (CMS), Lannion, 22300, France
[15]Observatoire Midi-Pyrénées, Université de Toulouse, LEGOS (CNES/CNRS/IRD/UT3), 31000 Toulouse, France
[16]Office National des Forêts, service de Restauration des Terrains de Montagne de l'Isère, 38000 Grenoble, France

Correspondence: Simon Filhol (simon.filhol@meteo.fr)

Abstract.

On the evening of June 21, 2024, a debris flood inundated the village of La Bérarde, located at the heart of the Écrins mountain range in the French Alps. More than 200 000 m^3 of materials were deposited in place of the village. People were evacuated on time but many buildings were destroyed and buried. The event was understood to be driven by a 10-year return period rain alongside to a 20-year snowmelt, the drainage of a supra-glacial lake, with potentially more internal water storage in the Bonne Pierre glacier. While we do not have direct observation of the supraglacial lake drainage, we found a number of evidences pointing to the role it likely had in destabilizing and triggering sediment transport from the Bonne Pierre fan. This

https://doi.org/10.5194/egusphere-2026-971
Preprint. Discussion started: 6 March 2026

work required an interdisciplinary approach to establish the set of scientific elements to reconstruct the event's chronology and rarity. We found that the combination of moderate magnitude drivers is not sufficient to explain the impacts observed. The location of the village on an alluvial fan directly connected to the source of sediments, was also key to understand the magnitude of the impacts. This event took place in a region particularly sensitive to climate change, where physical processes of the cryosphere at play are subject to alteration in a changing climate (*e.g.* precipitation amount and phase). The recent paradigm of compound events helps reconsidering the nature of this event and suggests possible approaches in anticipating new up-coming compound events in an era in which the Alps are entering a new paraglacial adjustments. Nevertheless, compound events remain difficult to forecast as they may be generated by diverse set of combination of low to moderate magnitude hazards associated to specific geographical, geomorphological, cryospheric, and meteorological onsets.

1 Introduction

Individual hazards result from a variety of interacting physical processes that take place on a broad range of time and spatial scales. Often not identified as extreme when occurring separately, they may become extreme when colluding in time and space (AghaKouchak et al., 2020). For instance, a heat wave may lead to a drought, drying the vegetation to the point it may burn by fire, so that a subsequent intense rain would easily mobilize ashes and soil to form a debris flow. Such event was observed to build up from 2012 to 2016 and unleashed a devastating debris flow in January 2018 in Montecito, California, USA, leading to the deadliest debris flow of California (AghaKouchak et al., 2020). Thinking hazards in a broader and interconnected manner in relation to their reach in impacts is recent and referred to by the terms compound events - compound hazards in the literature (Zscheischler et al., 2018; AghaKouchak et al., 2020; Zscheischler et al., 2020; IPCC-AR6, 2023). Prior studies may refer to the similar concept of multi-hazards (Kappes et al., 2012; Pescaroli and Alexander, 2018).

This broader analysis redefines the relevant time periods to include for the *prior-during-post* event sequence, using a multi-disciplinary approach to apprehend an event. Analog to a holistic approach, analyzing catastrophic events using the paradigm of compound events allows deciphering which are the drivers involved in the triggering of an extreme event, how these drivers interacted together, and lastly how the mitigation response and long-term impacts may have profound implications for human societies. The terminology can be loosely defined, and some compound events are also referred to as cascading hazards. Here we will restrict the term cascading hazard to one event leading consecutively to another, rather than to co-occurring hazards that may bear a variety of independent drivers.

The hazards induced by the degradation of the cryosphere (due to climate change) in the high alpine areas find their origin where glaciers, snow and permafrost are retreating, and may propagate to lower elevations driven by gravity and potentially cascading processes (Keiler et al., 2010; Haeberli et al., 2017; Stoffel et al., 2024). The inherent cascading nature of hazards due to the elevation gradient in mountainous regions may reach lower elevations by triggering a chain of hazards such as, for

https://doi.org/10.5194/egusphere-2026-971
Preprint. Discussion started: 6 March 2026

instance, a rock avalanche damming a river, subsequently releasing an outburst flood. A striking recent example of such an event is the ice and rockfall event in the Chamoli region of the Himalayas, an event that killed more than 200 people, triggered by the detachment of a rock and ice volume of 27×10^6 m^3 (Shugar et al., 2021; Cook et al., 2021). The detached mixture of rock, ice and water collapsed, blocked the next valley so that a 700-m-long lake formed, and transformed into an extraordinary large and mobile debris flow. Such cascading types of hazards are not new, but are expected to become more frequent as the cryosphere recedes in the regions of highest elevations (Kääb et al., 2005; Haeberli et al., 2017; Pörtner et al., 2019). While the scientific community integrated well concepts related to cascading hazards given striking recent examples (e.g. Chamoli), we are yet to investigate and analyze risks under the more recent framework of compound events (Zscheischler et al., 2018). Starting from the critical point of failure of a given system, the paradigm of compound events will search for pathways and combination of hazards that may become threatening.

Communities living within mountain ranges or downstream are already experiencing an increase in risks to infrastructure, livelihoods, and transport and communication networks in direct response to the cryospheric response of high-altitude regions to climate change (Keiler et al., 2010; Haeberli et al., 2017; Pörtner et al., 2019; Mani et al., 2023; Stoffel et al., 2024) . The consequences of the decaying cryosphere in regions with broad elevation ranges will become more and more intricate, with a broad variety of processes interacting, and therefore more complex to assess the full range of threats these communities may becomes exposed to. The case exposed herein, we think is a striking example of how the paradigm of compound events may bring an additional insights for risk management.

On June 21, 2024, a debris flood devastated the small village of La Bérarde (6.292°E, 44.933°N) (Fig. 1 and 2) at the heart of the Écrins mountain range in the French Alps (Fig. 3a and b, and Fig. A1), destroying buildings and roads, by depositing hundreds of thousands of cubic meters of sediments (Fig. A2). The event was initiated by intense rain, 104 mm in 48 hours, caused by the advection of a warm and humid air mass directly from the Mediterranean Sea. The rain fell over an above normal snow cover (*i.e.* twice as thick) in the Étançons catchment. During the event, a supra-glacial lake drained as well. The Étançons river change course going through the old village. No human life was lost, but people were evacuated by helicopter, in a life-threatening situation for some of them. Many buildings were impacted. Debris floods, a sediment rich flood, eroding, transporting and depositing material, are known to be significant threat to humans and infrastructure, yet they remain difficult to apprehend in terms of occurrence and extent of their potential damage (Church and Jakob, 2020). The origin of the debris floods can be varied but important to identify and to understand in order to better forecast, to improve preparedness and to plan mitigation for subsequent events.

The village of La Bérarde is centuries old and iconic given its unique location deep inside the Vénéon valley, surrounded by prestigious peaks like the Barre des Écrins (4102 m a.s.l.) or the peak of La Meije (3983 m a.s.l.). In the 1880s, painter Laurent Guétal captured with his monumental oil painting the uniqueness of the place, and most elements involved in this event by depicting the steep and tall mountains, the rushing water streams besides housing, and the central role of rocks, glaciers and snow in this mountainous landscape (Fig. 2). A few years later, Ernest Hareux complemented the depiction of this place with the illustrations of the book *La Meije et les Écrins* (Baud-Bovy, 1907). From both art corpus, a feeling of grandeur of the landscape in respect to the smallness of the human's infrastructure emerges. It is during that same period that La Bérarde

https://doi.org/10.5194/egusphere-2026-971
Preprint. Discussion started: 6 March 2026

Figure 1. Photo of the village La Bérarde before (June 3, 2021) and after (June 22, 2024) the debris flood event. Photo credits: ONF-RTM.

Figure 2. La Bérarde, oil painting ($1.2 \cdot 2.8$ m) by Abbot Laurent Guétal, 1882, Art Museum of Grenoble.

became the departure to some prestigious alpine routes. This increased attention in the second half of the 19th Century placed the small village of La Bérarde at a pivotal place for alpinism and in the heart of many.

Built on the alluvial fan of the Les Étançons torrent, the village of La Bérarde was geographically constrained by both the steep surrounding terrain, and the many natural hazards it generates (*i.e.* landslide, rockfall, snow avalanche, flooding), that result from terrain steepness all around the valley. On the alluvial fan, the village was considered to be in an area of lower risk exposure (Fig. A3). The catchment upstream of La Bérarde is of peculiar geography with multiple glaciers, permafrost terrain, and long lying snowpack. Located in the South-western part of the Alps, the catchment is particularly exposed to heavy precipitation during southerly winds bringing humid air directly from the Mediterranean Sea (Blanchet et al., 2021; Blanc et al., 2022b). To reflect this contextual complexity of natural hazards to which the village is exposed, the objective of this

https://doi.org/10.5194/egusphere-2026-971
Preprint. Discussion started: 6 March 2026

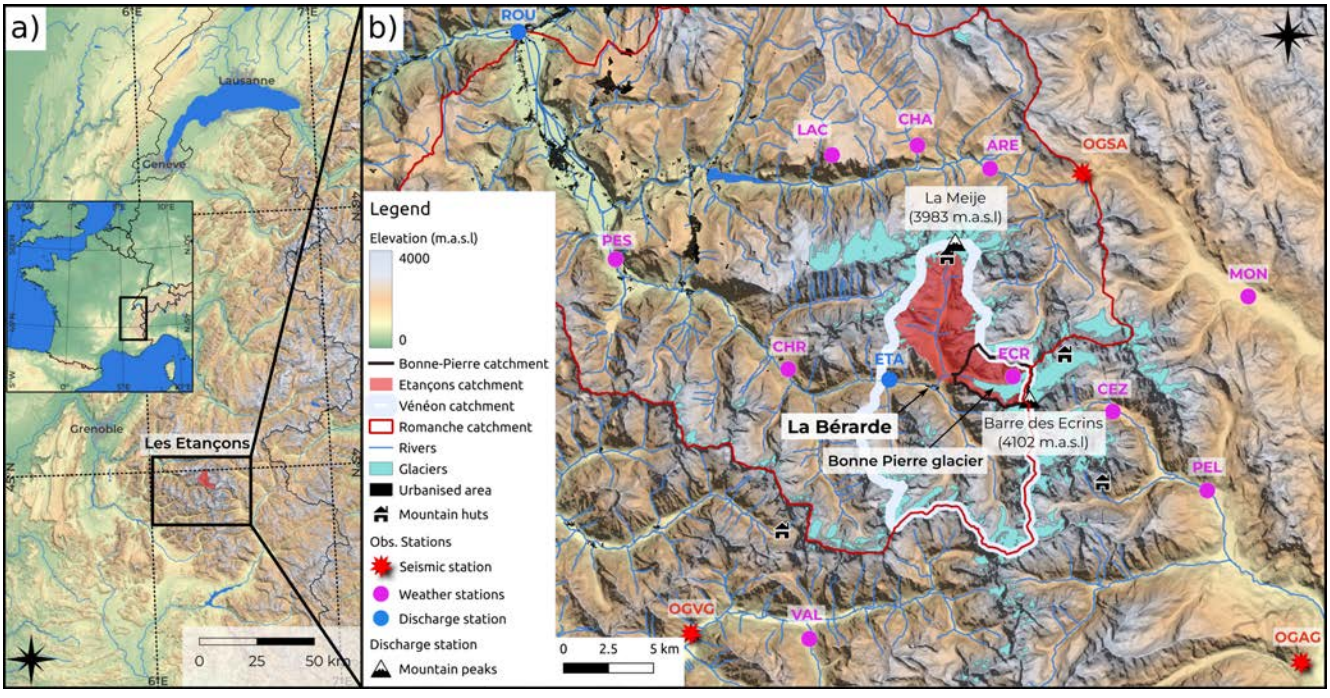

Figure 3. a) Location of the watershed Les Étançons (in red) and the village of La Bérarde within the western European Alps. **b)** Regional map indicating the watersheds of interest (*e.g.* Les Étançons (red shading), Bonne-Pierre (black line), and of the Vénéon river at Saint-Christophe-en-Oisans, Les Étages (white line)), urbanized areas (black), glaciers (delineation from 2022, Rabatel and Klee 2022) and location of interest (*e.g.* monitoring stations, mountain huts, mountain peaks of interest). All acronyms description of the observation stations are in Appendice A4.

paper is to reconsider the event of June 21 in light of the contemporary literature on compound events, sediment connectivity in a landscape undergoing paraglacial adjustments.

Following the event at La Bérarde, many questions needed answers. What had happened? What were the drivers triggering the hazards? How rare and exceptional was this event? Can the paradigm of compound event help us understand further the roots of this event? In what respect may we link this event to climate change? Some of these questions rapidly found first element of answers during the hindcast analysis requested by the French state services, which brought an interdisciplinary team together (Blanc et al., 2024). With this study, we recollect, strengthen and contextualize the main elements (*i.e.* water contribution, frequency analysis, chronology reconstruction) of this hindcast analysis to the international scientific community. We think important not only to report, but also to qualify the rarity of the event, and to attempt to dissect the possible compound nature of the event. This work involves a team from public and private institutions, spreading over research and operational activities. The learning of this work will directly seep into regional future decision making and nourish our understanding in identifying the upcoming of analogous risk situation.

https://doi.org/10.5194/egusphere-2026-971
Preprint. Discussion started: 6 March 2026

2 Site, data, and method description

2.1 Site description

The village of La Bérarde is located at 1700 m a.s.l. at the heart of the high alpine massif of Les Écrins, south east of the city of Grenoble (Fig. 3a). Les Écrins, the second highest mountain range of the French Alps, is made of crystalline rocks, with the presence of many glaciers (Fig. 3). The village is built in the middle of the alluvial fan of the torrent Les Étançons. This torrent has a drainage area of 34.4 km^2 ranging from 1700 to 4000 m a.s.l. with a mean elevation of 2788 m a.s.l.

Glaciers cover 6.2 % of the catchment (Fig A1) and the largest one is the Bonne Pierre glacier with a surface area of 1.74 km^2, a length of 3508 m and its front located at an altitude of 2400 m (Rabatel and Klee, 2023b). This glacier is characterized by an almost total debris cover over the glacier tongue and numerous glacial meltwater ponds on its surface (section 4.3).

The catchment splits into two branches, the upper Étançons torrent (V, Fig. 4) and the Bonne Pierre torrent (I + II). The upper Étançons torrent is fed by numerous active sediment sources and shows several braiding reaches along its 3 km-long valley with a slope $\approx 5-9$ %. Its catchment is about 2.5 larger than the Bonne Pierre torrent, its main tributary. The Bonne Pierre torrent is steeper (20-40 %). Both meet at the inlet of a narrow, 12-25 % steep canyon (III) exiting 500 m downstream on the alluvial fan (IV) where La Bérarde is built. The Étançons torrent, prior to June 21, 2024, had an incised channel several meters deep into the fan, located to the north-west part of the fan. This channel had a slope decreasing progressively from 9 to 7 % before reaching the Vénéon river.

Within the Bonne Pierre branch, three main sectors of erosion and deposition of materials can be distinguished (Mainieri et al., 2025): (i) the proglacial margin of the Bonne Pierre glacier (part I in Fig. 4), which constitutes one of the two primary sources of material during the flood of June 21, 2024; (ii) the Bonne Pierre proglacial cone (part II), located in between the proglacial margin and the confluence with the Étançons torrent, is normally a transit zone, but provided a second main source of material during the flood; and (iii) the Bérarde alluvial fan (part IV), at the exit of the canyon (part III) was the main deposition.

The proglacial margin (part I) exhibits several latero-frontal moraines. The largest of them extends E-W on the northern side of the proglacial margin, as a large right-lateral moraine (Fig. 4). Datings from this moraine show ages ranging from 4.25 $\pm$ 0.44 ka to 2.09 $\pm$ 0.10 ka for the outermost and innermost ridges, respectively. Le Roy et al. (2017) date the last glacier advance of the Little Ice Age (LIA), around 1850-60 CE. This prominent moraine ridge is thus the result of the accretion of multiple glacier re-advances during the whole Holocene, as elsewhere in the Alps. The bumpy shape of the margin results from the deposition of abundant surficial debris cover and suggests a rapid glacier retreat of about 1 km between 1860 and 1890 (averaging a front retreat of approximately 5.5 m yr^{-1}), after which the front stabilized its position during the 20th Century (Le Roy et al., 2017). Since 1820, the glacier has lost around 100 ha, about 55 % of its maximum surface area (Gardent, 2014).

Part II, here designated as a "progacial cone", has the shape of an alluvial fan with a steep slope ($\approx$27 %). It was built by glacio-fluvial processes. The main channel runs on the left edge of the cone and is the only channel connecting to the Etançons torrent. In the apical zone, the bedrock outcrops at shallow depth, and the upper half of the channel is incised into the bedrock. On the right bank, overflow channels form a braided system covering the rest of the cone and serving as deposition zone, barely

https://doi.org/10.5194/egusphere-2026-971
Preprint. Discussion started: 6 March 2026

connected to the main river. During the event, erosion occurred mainly along the main channel, uncovering what seems to be a buried bedrock gorge.

In comparison to the Étançons catchment size, the alluvion fan of La Bérarde (part IV) has a relatively small size. The relatively fast flowing Vénéon river at the fan base, provides an efficient evacuation of materials brought by the Étançons torrent onto the fan. Its small size exacerbated the effects of the 2024 flood, during which material were deposited over almost the entire surface of the fan. Prior to the event, the channel ran along the right margin of the fan, making a sharp turn to the right in the apical zone. The channel was deeply incised into the fan and formed a wide channel, especially at the turn. The central and left parts of the fan (where the village is built) were therefore disconnected from the torrential activity. The fan is truncated at the base by the lateral erosion of the Vénéon river. The position of the channel and of the village are documented since at least the 18th Century by old maps, and all historically reported torrential events were confined in the incised channel (Sect. 6.1). All these elements suggest that an event similar to that of 2024 has not occurred for several centuries.

Annual precipitation for the area reaches on average 987±166 mm per year for the period 1991-2020. Over those years, the maximum 48 h precipitation observed was on August 29, 2020, with 148 mm recorded. Typically, the 48 h yearly maximums at Saint-Christophe-en-Oisans (CHR) occur from August to November. Since 1964, the 48 h yearly maximums occurring at CHR typically in May, June or July have an average precipitation of 65±11 mm, with the maximum recorded for this season on May 15, 1983, of 83 mm. From June 19 to 21, 2024, the gauge recorded a total of 104 mm in 48 h.

2.2 Monitoring networks

Within and surrounding the Étançons catchment, there are several autonomous stations recording meteorological observations, river discharge, snow, and seismic signals (Fig. 3b, Table A1). Even though the Étançons torrent was not instrumented with a discharge gauge, the closest one is located 3.5 km downstream of La Bérarde, on the Vénéon river at les Étages (ETA, 6.252°E, 44.937°N). At this location, the Vénéon river drains a larger area of 104 km^2 (Fig. 3b). This station got destroyed during the flood peak. As this dataset is key to the hydrological modeling, there was a careful assessment until when this measurement can be trusted (Sect. 5.1), and what is the likely maximum discharge peak based on drift wood and other clues left by the peak discharge. An extra discharge gauging station located on the Romanche river (of which the Vénéon is a tributary) at Pont Rouge (ROU, 6.013°E, 45.116°N, Fig. 3b) was used in the hydrological analysis. It drains an area of 804 km^2 with multiple dam reservoirs and water intakes.

A network of various weather observations is also available within and around the catchment. One of them, the weather station *Nivose-Écrins* (ECR), is located inside the Étançons catchment right aside of the Bonne Pierre glacier recording air temperature, wind speed and direction, and snow depth since 1983 (44.9369°N 6.3461°E, 2970 m a.s.l.). Downstream of the catchment, the weather station of Saint-Christophe-en-Oisans (CHR) records precipitation among other atmospheric variables since 1963 (44.9458°N 6.1883°E, 1564 m a.s.l.). Precipitations were recorded at other locations around the Écrins mountain range by other autonomous weather stations, and manual monitoring of precipitation at the local mountain huts (Fig. 3b, Table A1). The French national precipitation radar system captured in part (one radar was in maintenance) the precipitation

https://doi.org/10.5194/egusphere-2026-971
Preprint. Discussion started: 6 March 2026

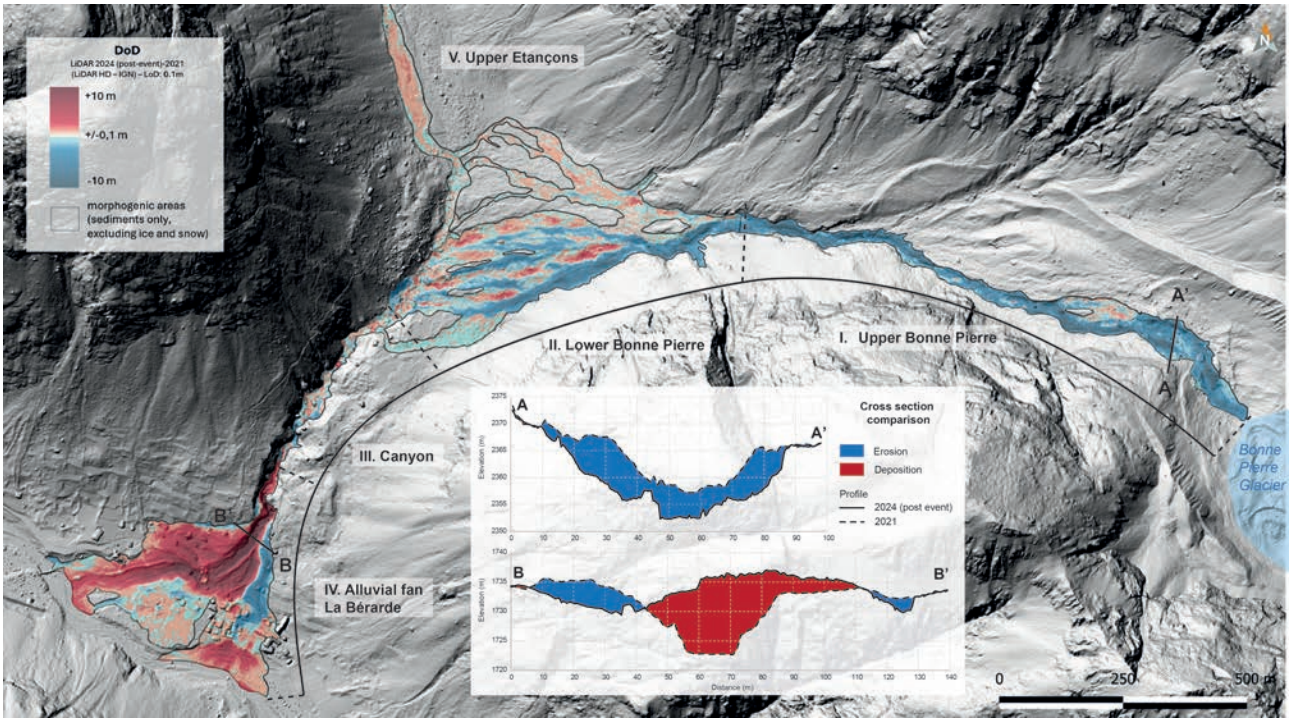

Figure 4. Topographical changes based on airborne lidar in between the dates June-July 2021 and June 2024. Blue zones indicate erosion, and red zones indicate deposition. Section AA' shows the large erosion of the cross section in the upstream part of the Bonne Pierre torrent channel, section BB' shows the massive deposition at the fan apex in the deeply incised channel and on the Étançons alluvial fan. Note that a limit of detection of changes of ±30 cm is considered on the map.

field every hour (Champeaux et al., 2011). Radar and *in-situ* precipitation data from this network of weather observation (Fig. 3b) were used to better estimate the precipitation fields in space and time.

Glaciological observations for the Glacier Blanc, across the ridge on the east from Bonne Pierre, relies on the Glacioclim program from which we extracted the annual mass balance (Sect. 8).

Lastly, the three seismic stations from the network Epos-France (1962), FR.OGAG (44.7878°N, 6.5397°E), FR.OGSA (45.0368°N, 6.4009°E) and FR.OGVG (44.8152°N, 6.1123°E), recorded the seismic signals linked to the flooding event on June 21. These stations are located 13 km to the north of the Étançons catchment (OGSA), 25 km south east close to the Durance river (OGAG), and 20 km to the south west beside the Séveraisse river (OGVG).

2.3 Reanalysis datasets

To complement and obtain a broader perspective on the meteorological situation, we used two reanalysis datasets. The ERA5 reanalysis (Hersbach et al., 2020) was used to examine the synoptic situation of the upper atmosphere prior and during the event (Sect. 4.1). Data were downloaded directly from the Copernicus Data Store https://cds.climate.copernicus.eu/ for the

https://doi.org/10.5194/egusphere-2026-971
Preprint. Discussion started: 6 March 2026

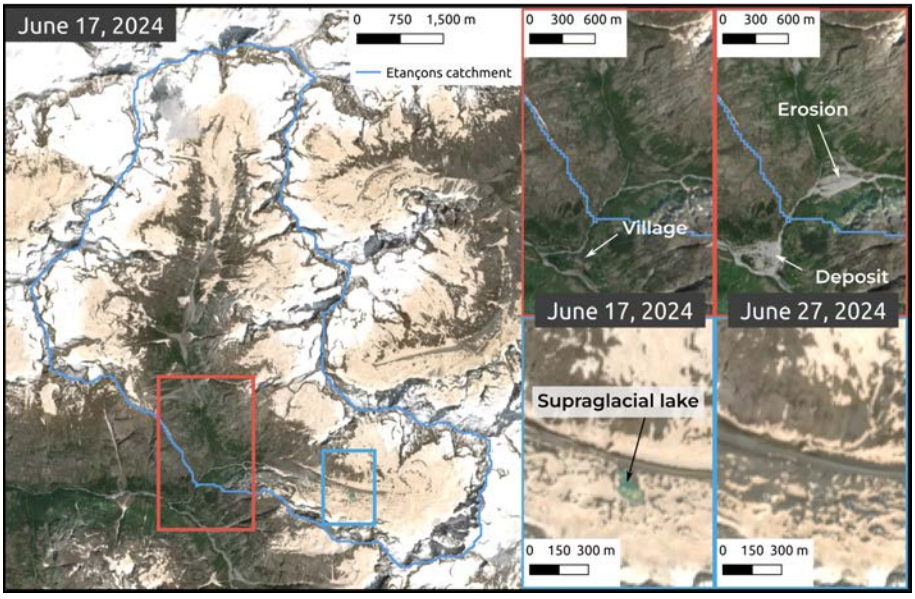

Figure 5. Sentinel-2 image on June 17, 2024, prior to the event, showing a watershed largely covered in snow of a brownish color due to Saharan dust deposits. Boxes orange and blue show detail of the alluvial fan and of the supra-glacial lake of Bonne Pierre before and after the event based on Sentinel-2 images, June 17 and 27 respectively. Notice the lake disappearance, the retreat of the snowline, and the zones where sediment has been either eroded or deposited.

dates showed in the analysis. ERA5 comes at a spatial resolution of 0.25°, at an hourly timestep. ERA5 assimilates a large amount of observation such as *in-situ* air temperature, precipitation and products derived from satellite data. ERA5 is widely used and recognized for its quality (Lavers et al., 2022; Monteiro and Morin, 2023).

Specific to the French Alps, the reanalysis S2M (Vernay et al., 2022) is produced by Météo-France for a wide range of applications (*i.e.* initially for avalanche forecasting). S2M is a suite of tools starting by the downscaling scheme SAFRAN (Durand et al., 2009) followed by the land surface model Surfex (Masson et al., 2013). SAFRAN combines data from global numerical weather prediction models (ERA-40 reanalysis from 1958 to 2002, ARPEGE from 2002 to 2021), downscaled to an abstraction of the French Alps at the scale of mountain ranges for eight aspects and slopes of 0, 20 and 40°at every 300 m elevation bin. SAFRAN provides all necessary forcings to drive the Surfex model, that itself includes the CROCUS snow model (Vionnet et al., 2012). This toolchain, readily available at Météo-France, could accurately estimate snow mass and historical snowmelt rate, after projection of the abstracted geometry onto the Étançons catchment. For this study, we used the timeseries of the massif Oisans at an hourly timestep to derive all data presented hereafter.

2.4 Geospatial data

The surface geomorphology of the Bonne Pierre Glacier was mapped from airborne and spaceborne multispectral optical data. We used aerial orthomosaics from the Institut national de l'information géographique et forestière (IGN; BD ORTHO®) and,

https://doi.org/10.5194/egusphere-2026-971
Preprint. Discussion started: 6 March 2026

for the most recent dates, orthomosaics from the satellites SPOT, Pléiades, and Pléiades Neo (Pneo). All orthomosaics have 0.2–1.5 m spatial resolution, enabling consistent delineation of supra-glacial ponds and their evolution from 2003 to 2024. Details about spatial resolution are described in Table A2.

Surface-elevation change was quantified from two airborne lidar digital elevation models (DEMs): (i) an IGN LiDAR HD (acquired on August 21, 2021) DEM derived from classified ground points and resampled to 1 m (Cusicanqui, 2024), and (ii) a 1 m resampled lidar DEM acquired by SINTEGRA (acquired on July 11, 2024) (Blanc et al., 2024). In addition, stereo-derived DEMs from the satellites Pléiades (acquired on September 13 2014, August 12 2018) and Pléiades Neo (acquired on July 4 2024) were generated to assess catchment-scale changes, following the automated workflow of Berthier et al. (Table A2 2014). Horizontal and vertical biases in stereo DEMs were corrected with the Nuth and Kääb (2011) approach, using the 2021 lidar DEM as a reference, and additional low-frequency undulating biases due to the unmodeled attitude error ("jitter") were minimized with the method of Deschamps-Berger et al. (2020).

2.5 Method

Characterizing the event to confidently identifying and quantifying the preconditioning drivers, and reconstructing the event chronology, an interdisciplinary approach was necessary given the breath of data types to collect, interpret and intersect. Disciplines are ranging from meteorology, geomorphology, hydrology, hydrodynamics, glaciology, remote sensing, natural hazards, statistics to history. The rich discussions emanating from the range of perspectives that offer such broad range of disciplines were helpful in confronting point of views to incrementally unfold a consensus on what has happened and what remains unclear to this date. Given that each discipline used established state-of-the-art tools to process and interpret data, we chose for clarity to include concise method descriptions directly where relevant and further methodological details in appendices rather than an extensive methodological section herein. Nevertheless, the goal of this study in combining a large amount of varied information is to clearly differentiate among facts and deduced information from model outputs (*i.e.* relying on some assumptions). Expert knowledge is finally brought into the discussion section (Sect. 7) to interpret and contextualize in broader terms the event itself and its ramification (*i.e.* role of climate change, compound nature of the event, etc.).

Throughout the study, we aggregated contributions of precipitation and snowmelt to 48 h period. This is deliberate choice as such a time frame encompasses the flood events, and the peak snowmelt and rainfall leading to the event too. 48 h is also the time frame at which the snowmelt and rainfall contribution are of historical significance (Sect. 6.2).

3 Impact of the event

3.1 Human and infrastructure impacts

No casualties were reported. The rescue teams evacuated 114 people by helicopter in the morning of June 21 after they had taken refuge outside the village or on roofs overnight. Sixty-six buildings have been impacted, of which 16 have been destroyed or completely buried during the event (Fig. 1 and A2b-c). The NW part of the village was mainly affected by

https://doi.org/10.5194/egusphere-2026-971
Preprint. Discussion started: 6 March 2026

material deposition, while the SE part (the older part) was affected by both direct incision and scouring from a newly created river channel, as well as large amounts of material deposits (Fig. 4). Roads and bridges on the alluvial fan have also been eroded or buried like other networks (water supply, sewage, electricity, etc.).

3.2 Geomorphological changes

Field surveys, videos shot during the event, and witnesses suggest that the event at the village can be qualified as a debris flood (Church and Jakob, 2020), *i.e.*, a two-phase water/sediment flow with highly concentrated bedload. Although meter size boulders were transported, no surge was observed. From all available pictures and videos with sufficient quality, we observed that the flow remained biphasic. Boulders and cobbles covering the fan did not show sand or gravel recovering since they were washed away by the flows. Deposits on the alluvial fan at the village showed some stratification. However, in the lower part of the Bonne Pierre torrent channel (part II in Fig. 4), we could observe some evidence of en-masse flows with boulder levees, typical of debris flows, as well as sand and gravel covering deposited boulders. This is another evidence that during at least part of the event, boulders, cobbles, gravel, sand and water were transported in a monophasic mixture. This combination of upstream debris flow and downstream debris flood led to large geomorphological changes on the Étançons torrent. Changes were quantified by differencing of digital elevation models (DEM) acquired before and after the event by lidar surveys on June-July 2021 and June 2024 (Fig. 4, Sect. A3). We applied the morphological method by Vericat et al. (2017) using the Difference of DEM (DoD) to quantify the sediment budget (Table 1).

We can separate the sediment cascade into five parts (Fig. 4). The upper part of the Bonne Pierre branch (Part I), just downstream of the glacier front, is a steep proglacial margin from which around 200 000 m^3 were eroded. Bed incision reached up to 10-m deep, not only entrenching the channel but widening it too. The lower Bonne Pierre part (part II) consists of a proglacial fan, from which about 100 000 m^3 were eroded with, for its southern side, a mean erosion of 5 m along the channel. The approximate volume of 300 000 m^3 was transported from the upper and lower parts of the Bonne Pierre branch with high efficiency into the canyon (part III) downstream of the confluence between the Bonne Pierre and the upper Étançons torrents (part V). At the canyon exit, around 230 000 m^3 of material were deposited on the alluvial fan of Les Étançons (Part IV) leading to many damages in the Bérarde village (Sect. 3.1). It first filled the wide and deep channel along the right side of the fan, where most of the material was deposited, before spreading over the whole fan surface. Towards the end of the flood and during the following days, a new channel incised the east side of the alluvial fan, leading to an erosion of roughly 30,000 m^3 and the formation of a small fan at the new confluence with the Vénéon river.

The upper Étançons torrent (upstream of the confluence with the Bonne Pierre torrent) shows bed reworking of its long braiding reaches. However, the estimated volume of sediment exported is negligible in comparison to the volume eroded along the Bonne Pierre torrent. We note that the sediment budget is not complete in this part of the catchment, as the post-event lidar does not cover the upper Étançons where some snow was remaining at the date of the post-event lidar survey. Thus, we expect an underestimation of the eroded volume from this part of the catchment. Though, according to field observations (Mainieri et al., 2025), we are confident that most of the sediment volume comes from the Bonne Pierre torrent.

https://doi.org/10.5194/egusphere-2026-971
Preprint. Discussion started: 6 March 2026

Table 1. Sediment budget reconstructed using *pre* and *post*-event lidar surveys.

	Erosion (x1 000 m^3)	Deposition (x1 000 m^3)	Balance [x1 000 m^3]
Bonne Pierre torrent (I+II)	306*	26	-280*
Upper Étançons torrent (V)	89**	79**	-10**
Alluvial fan (III+IV)	34	233	+199

* *Due to the melting of the glacier between 2021 and 2024, an erosion rate was considered based on the DoD on the most upstream part of the channel (a 50-m swath corresponding to 8600 m^3).*

** *The post-event lidar does not cover the entire catchment and some part of the tributaries were under snow, so that the sediment budget is not complete (erosion underestimated).*

4 Drivers of the event

To understand the flood and its consequences, we need to characterize and quantify the sources of all water flowing downstream, entraining the large volumes of sediment and therefore responsible for the remodeling of the riverbed destroying the village. There are three main obvious water sources: 1) the rain which fell over a period of 48 h, 2) the melt resulting from an unusually thick snowpack, and 3) a supra-glacial lake drainage throughout the course of the event. Here we will provide estimates of the contribution of these three sources, and a more detailed explanation to the drivers leading to the individual hazards. A hydrological analysis and a seismic analysis comprising a larger region than the Étançons catchment provide a broader picture of the flood timing and the likely synchronicity of the flood drivers (Sect. 5).

4.1 Synoptic-scale weather and rain

On June 18, the jet stream pattern, in the upper part of the troposphere (500-250 hPa), was strongly meridian with a deep upper level trough oriented from Scotland to the southern part of Spain (Fig. 6 and A4). Over its eastern part, it generated a rapid northward flux picking moisture while crossing the Mediterranean Sea. It is to be noted that for the month of June 2024, the sea surface temperature anomaly between the Balearic Islands, Algeria, and Sardinia Island was about 1° C warmer than for the reference period June 1991-2020 (Fig. A5). The following day, June 19, this jet stream trough is bypassed in the north and a cold drop in the upper levels (*a.k.a* cut-off low) above Spain detached from the main jetstream. At the lower levels (close to the Earth surface), a low pressure located within the gulf of Biscay (Atlantic ocean off the French coast) combined with a high pressure system formed above Southern Italy and the Balkans (Fig. A4) enhanced the low-level convergence of the southern wind over the Mediterranean sea. This synoptic situation had multiple effects. The combination of the upper level trough, the associated rapid jet with the low level convergence enhanced the upward vertical speed and favored the formation of a perturbed area characterized by strong instability and moisture. The perturbed area advected moisture northward to the western Alps (Fig. A4). When encountering the high relief of the Écrins massif, the perturbed atmosphere underwent an orographic forcing, increasing further condensation and therefore precipitation. This synoptic situation was responsible for the heavy rains over Les Écrins massif for the 19-21 June, 2024 period. The synoptics over the whole month of June 2024 brought significantly

https://doi.org/10.5194/egusphere-2026-971
Preprint. Discussion started: 6 March 2026

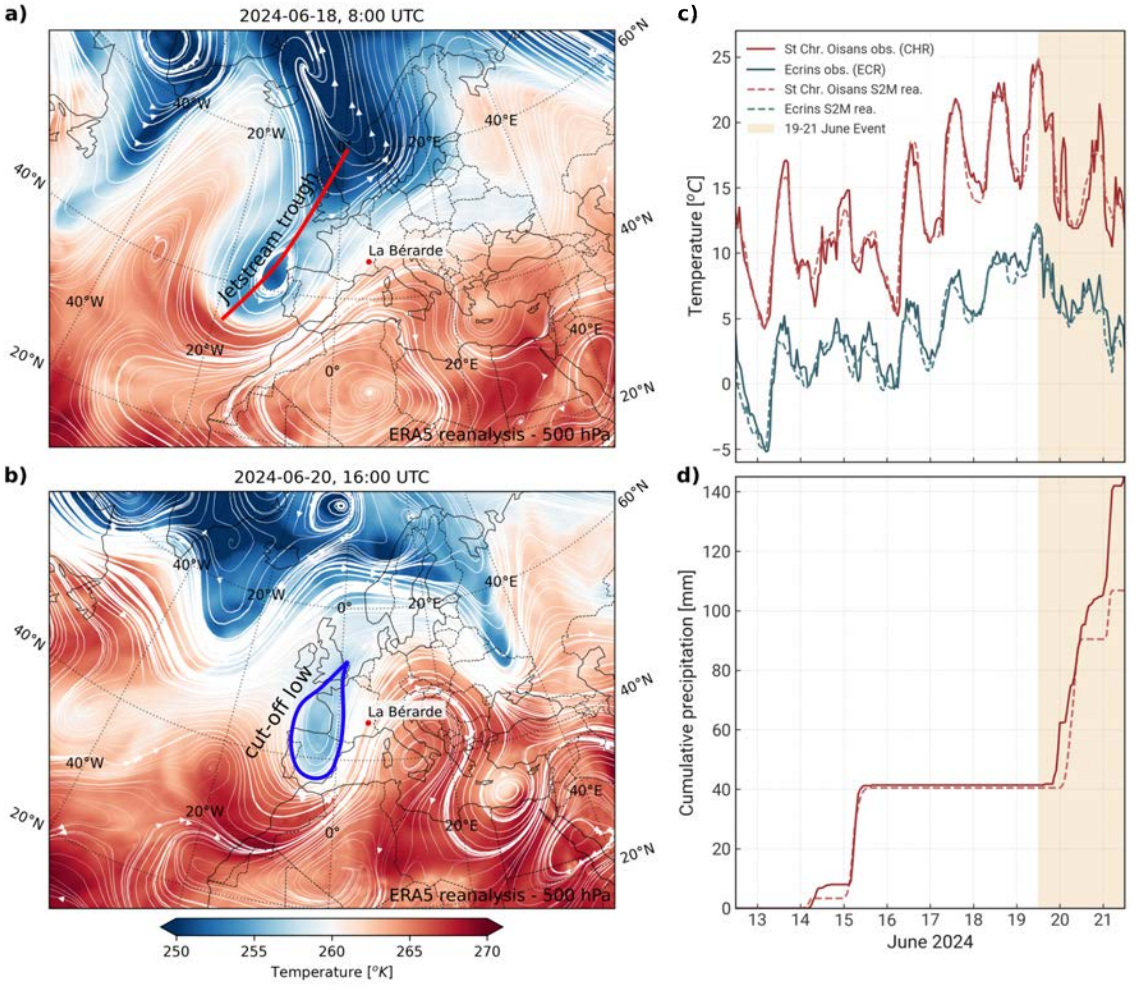

Figure 6. Synoptic (**a** and **b**) and meteorology (**c** and **d**) leading to the intense rain and snowmelt from June 19 to June 21, 2024. Data for the synoptic panels (**a** and **b**) are extracted from the ERA5 reanalysis (pressure level 500 hPa), and data for the meteorology panels (**c** and **d**) are extracted from Météo-France *in-situ* observations and the S2M reanalysis. **a)** Synoptic situation at 500 hPa (ERA5) on June 18 8:00 UTC above Europe shows the jet stream trough. **b)** Synoptic situation at 500 hPa (ERA5) on June 20 16:00 UTC shows the cut-off low pattern generating northward flux from the Mediterranean Sea towards the western Alps. For both synoptic panels, the color scale indicates the air temperature field, and the flow lines indicate wind direction (arrows) and speed (width). **c)** *In-situ* air temperature at the weather stations Les Écrins (ECR, 2970 m a.sl.) and Saint-Christophe-en-Oisans (CHR, 1564 m a.s.l.). Prior to the event starting late June 19, temperatures at ECR did not fall below 0^{o}C for the prior 5 days. **d)** Cumulative precipitation recorded at CHR. **c)** and **d)** show the corresponding S2M reanalysis air temperature and precipitation for the Oisans massif (dashed lines).

more precipitation over the Alps at large in comparison to the months of June in the reference period 1991-2020 (Fig. A5). This synoptic was also observed to repeat multiple times during the months of May and June (Kreitz, 2024).

https://doi.org/10.5194/egusphere-2026-971
Preprint. Discussion started: 6 March 2026

Locally, the precipitation over the 48 h period from June 19 to 21 (12:00 to 11:00 UTC respectively) formed a nodule right above the highest peaks of Les Écrins massif most likely due to the local convection and orographic effects. Temperature at the weather station of the Écrins (ECR, 2970 m a.s.l.) reached 12.5°C on the eve of June 19. Temperatures dropped to 5-7.5°C at the peak of the rainfall, meaning that the 0°C isotherm reached the 4000 m a.s.l. elevation peaks throughout the event. Lastly, estimates of precipitation by the mountain huts at the heart of the precipitation nodule are likely conservative as in the midst of the event, mountain hut hosts reported overflowing gauge and intense rain and wind (mean hourly speed peaking at 18.4 m s^{-1} at ECR).

From the network of observations (automated weather station, mountain huts reports, weather radar) and the ERA5 reanalysis (for the synoptic) and S2M (for the local weather), we could describe how the meteorological event unfolded itself locally. After three days of sunny weather and continuous above freezing temperatures at ECR (2970 m a.s.l.), clouds from the south started heavy rain at 21:00 (UTC) on June 19 almost continuously until June 21. In total, precipitation at CHR reached 104 mm in 48 h. Mountain huts in the surroundings recorded for the same period 112 mm on average (Tab. A3), with reports of instruments overfilling during the report. Radar observation were used, corrected by in-situ observation to estimate an hourly precipitation field over the Vénéon catchment (Fig. A1) for accurate hydrological modeling (Sect. 9).

4.2 Snowmelt

On June 17, the Sentinel-2 image shows a snowpack covering 59 % of the Étançons watershed (Fig. 5). Ten days later, on June 27, the snowpack cover extent retreated to 48 % of the watershed area, corresponding to a reduction of 3.23 km^2. Such snow cover extent in late June was typical during the years 1984-2003 (Fig. A6). Since then, the lower limit of the snowline has typically retreated on average 150 m higher in elevation for the period (2004-2023) (Fig. A6).

At the weather station ECR (2970 m a.s.l.) from November 2023 until June 2024, the snowpack was about twice as thick as for the median of the 1991-2020 reference period (Fig. 7a). On June 19, 2024, the snow was 2.91 m thick, corresponding to the percentile above 90 % for this day (ref. period 1991-2020). Since 1983, this is among the thickest snowpack observed at ECR (Fig. 7a). Therefore, at the onset of the event, the watershed had an unusual thick and extensive snowpack for the period of observation available.

To estimate the snowmelt water contribution to the flood, we simulated the snowpack over the Étançons watershed using the S2M workflow (Vernay et al., 2022) for the winter 2023-2024 based on the reanalysis downscaling scheme SAFRAN (Durand et al., 2009) followed by the land surface model Surfex (Masson et al., 2013; Vionnet et al., 2012). From this simulation, we aggregated the runoff at the base of the snowpack, from which the rain was withdrawn, assuming the snowpack was already saturated with liquid water and could not hold more. Because the downscaling of ERA-40/ARPEGE reanalysis is done at the mountain range scale, local effects, such as the localized rain of June 19-21 in the region of La Bérarde, can be smoothed over the larger region. Despite this method limitation, S2M succeeded in capturing an unusual rain for that event, with 95 mm w.eq. precipitation, corresponding to a 10-year return period rain within this dataset (estimated using a GEV, see Sect. A14). Moreover, S2M also captured well the seasonal evolution of the snowpack when compared to observation at ECR

https://doi.org/10.5194/egusphere-2026-971
Preprint. Discussion started: 6 March 2026

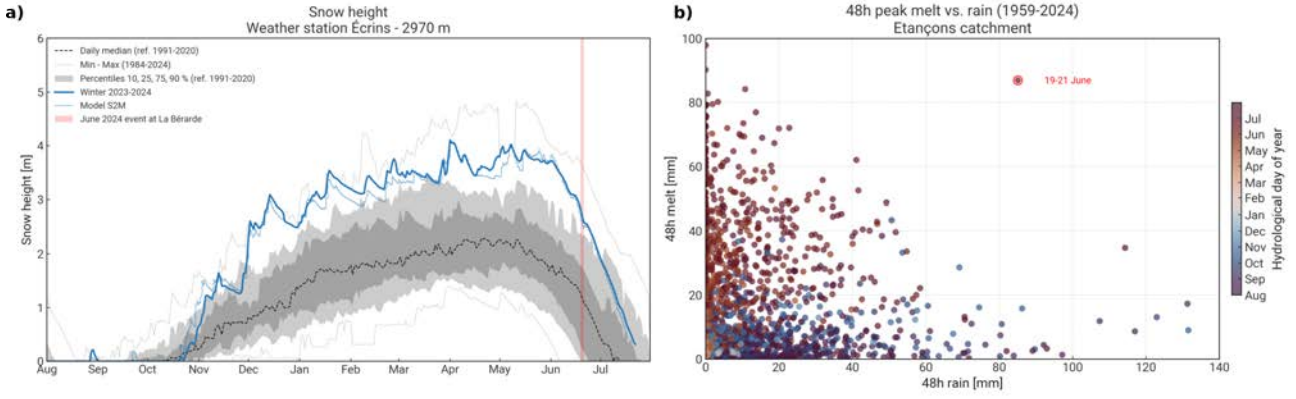

Figure 7. a) Snow climatology of winter 2023-2024 daily snow heights in respect to the 1991-2020 reference period and historical min and max since 1984. Data extracted from the Écrins (ECR, 2970 m a.s.l.) weather station observation. The corresponding modeled snow with S2M is shown in light blue for winter 2023-2024. **b)** Scatter plot of the 48 h melt *vs.* the 48 h rain averaged over the Étançons catchment since 1959 from the S2M reanalysis. Each point is colored by the day of year (hydrological year, starting on August 1) it occurred. We notice the intense melt in springtime, and the heavy precipitation during late summer early fall.

(Fig. 7a). From this double validation of the S2M model against local observations, we may interpret confidently the S2M rain precipitation and snowpack simulations.

The snowmelt runoff within the 48 h reference period from June 19 12:00 to June 21 12:00 UTC was estimated to be 75 mm w.eq. However, because melt and rain do not respond to the same physical processes, the timing of their respective peak contributions do not necessarily synchronize. For this event the snowmelt (M), the rain (R), and the contribution of both summed up (MR) do not coincide. Therefore, we searched independently for the three 48 h windows for the respective peaks. This is relevant in estimating return period and identifying the historical precedence of this event (Sect. 6.2). So, for the (M) peak, the 48 hr window is starting on the timestamps June 19 08:00 UTC, for (R) peak June 21 00:00 UTC, and for (MR) peak on June 20 05:00 UTC (Tab. A4). Respectively, the peak contributions are 94 mm w.eq. for (M)), 92 mm for (R) based on S2M (not corrected), and 172 mm w.eq. for (MR) corresponding to 85 mm and 87 mm w.eq. of (R) and (M) respectively. The peak contribution for (M) (92 mm w.eq.) was the 3rd most intense melt on record since 1959.

At the start of the event, the snowpack simulated at the Écrins station was isothermal from top to bottom since May 20. During the event, most energy came from sensible heat, short wave radiation, latent heat and to a limited extent from the rain's sensible heat (Fig. A8). As more rain fell during the event ($\geq$ 112 mm at the mountain huts), we tested the sensitivity of our results to an increase in the forcing of the rain precipitation to match the observation (Sect. A6.1). Given that rain brought little energy to the snowpack (481 W h m^{-2} in 48 h), this sensitivity analysis concluded that correcting precipitation had little impact on the final estimates of snowmelt runoff with only 1.4 mm additional melt.

From the S2M dataset, we estimated the snowmelt runoff history from 1959 to 2024 averaged over the entire catchment of Les Étançons. Figure 7b shows the respective contribution of snowmelt and rain for any given 48 h rolling window for

https://doi.org/10.5194/egusphere-2026-971
Preprint. Discussion started: 6 March 2026

MR. We can observe two main regimes, a dominance of the snowmelt contribution to MR in spring, and a dominance of the rain contribution to MR in summer and fall. An MR water contribution in the Étançons catchment from snowmelt and rain simultaneously is either of small intensity (<80 mm) or rare. This will be discussed further in section 6.2.

4.3 Glacial Lake Outburst Flood (GLOF)

The third driver of the debris flood corresponds to a transient storage and release of water from a supra-glacial lake over the Bonne Pierre glacier. Bonne Pierre glacier has relatively shallow mean slope (16°) and slow flow velocity (averaging 3-5 m yr $^{-1}$). The glacier surface is extensively debris covered (about 60 % of its surface). The debris cover acts as an insulator, generating differential ablation in between zones of different debris thickness (Benn et al., 2012), and mitigating the general negative glacier mass balance of the region's glaciers. Accordingly, the Bonne Pierre glacier lost -0.54 m of water equivalent per year (m w.eq. yr^{-1}) for 2014-2018 and -0.82 m w. eq. yr^{-1} for 2018-2023 (Fig. A9, estimated from Pléiades satellite imagery). In comparison, the Glacier Blanc, a nearby non debris-covered glacier just across the ridge toward the East (Fig. A9, experienced an enhance negative mass balance of about -0.98 and -1.18 m w. eq. yr^{-1} over the same time spans respectively. Consistent with this contrast, the Bonne Pierre glacier front retreated at a rate of ≈5.5 m yr^{-1}, about one-third of the front retreat rate of Glacier Blanc (≈14 m yr^{-1}) (WGMS-front-variation). The debris cover is primarily formed by rockfalls and rock avalanches from the cirque's north and west walls. For instance, a major rockfall occurred on July 17, 2016, with approximately 400 000 m^3 of debris deposited on the glacier surface, as estimated from differentiated co-registered Pléiades DEMs (Fig. A9; A2; Berthier et al. (2014)).

Since 1990, numerous circular thermokarst-like sinkholes (Kääb and and, 2001, hereafter called ponds) have expanded (Fig. A10) due to the heterogeneous debris thickness. The pond corresponding to the supra-glacial lake that drained in June 2024 initiated its formation in 2009. It grew in area at an average rate of 30 % yr^{-1}. By 2024, at least three ponds had coalesced (Fig. 8a) into a 14 000 m^2 larger pond. This newly formed pond reached a maximum storage volume of about 90-100 000 m^3 as measured from a DEM derived by photogrammetry from a dedicated UAV survey conducted a few days after the drainage. The lake probably reach a depth of 25 m based on the DEM and the snow markings on the lake shore.

A detailed analysis of Sentinel-2, Landsat 7-9, and PlanetScope images since 2016 indicates that the pond was systematically filled with water in late spring and early summer (usually in June). For most years (excluding 2024), the lake drainage had never been notified by residents of La Bérarde, indicating a gradual discharge —over days to weeks— via an outlet on the glacier's left bank, with no evidence of surface overflow. In 2024, water in the lake can be first observed on June 10 from a Landsat 9 image (Fig. A11). Then, the lake grew in size, observed on the Sentinel-2 image from June 17 (Fig. 5). On June 18 the lake was visible in the background of a picture posted on the climbing forum https://www.camptocamp.org/outings/1656229/fr/dome-de-neige-des-ecrins-voie-mayer-dibona (Fig. A12). The following observation of the lake was on June 22 from a helicopter overflight, post-flood, where it appeared empty without any supra-glacial channel.

Figure A2g shows the drainage outlet, funneling the water into the intra/sub-glacial channel system. The morphology of the Bonne Pierre glacier, being of low angle, with an increasing number of ponds at its surface due to differential melting, promotes drainage of the seasonal water-filled ponds by a hydraulically connected intra- and subglacial network (Cusicanqui et al., 2023;

https://doi.org/10.5194/egusphere-2026-971
Preprint. Discussion started: 6 March 2026

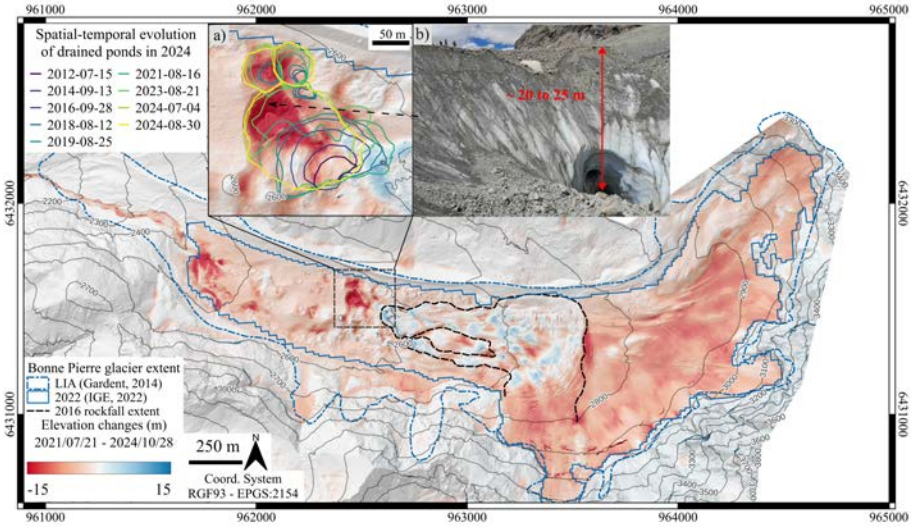

Figure 8. Map of elevation changes of Bonne Pierre glacier between 2021-2024 using two aerial Lidar acquisitions. Inset map a) shows a zoom of the supra-glacial ponds drained on June 21, 2024 as well as their spatiotemporal extent from 2009 (Fig. A10). Inset b) shows a field photograph a few days after the lake drainage. Photo credits to RTM.

Gulley et al., 2009). Such network is prone to exhibit hydraulic barriers down to the glacier base (Ogier et al., 2025), leading to potential water retention not visible at the glacier surface. For instance, a cavity of 5 000 to 10 000 m^3 close to the glacier front was found after the flood. In the twin study (Ogier et al., 2026) to this work, about the subglacial hydrology concluded from a modeling exercise that the Bonne Pierre glacier would have a maximal potential storage capacity of 150 000 m^3. This value is a maximum theoretical intra-glacial volume estimate. In practice, it is unlikely such volume of water was reached, but ground penetrating radar transects flown by helicopter during summer 2024 suggest a number of cavities along two main subglacial channels. It is therefore likely that an additional substantial volume of water stored intra-glacier to the supra-glacial lake contributed to the flood. Similar disaster related to combined effects of supra-glacial ponds (*e.g.* Cusicanqui et al., 2023) and intra-glacial water-cavities (*e.g.* Vincent et al., 2010) have been documented in the French Alps and elsewhere in the European Alps (*e.g.* Lützow et al., 2023), underscoring the difficulty of constraining potential sub/supra-glacial water storage.

While the total volume retained and released from the glacier during the debris flood may appear important, though its actual contribution to the flood depends on the drainage rate. Glaciological observations are not sufficient to conclude neither the rate of discharge nor the timing and water release dynamic in between June 18 and 22. Additional observations and approach are needed to decipher the potential role of the GLOF during this event.

https://doi.org/10.5194/egusphere-2026-971
Preprint. Discussion started: 6 March 2026

5 Rivers' response

In this section, hydrometric observation and hydrological modeling supported by seismic observation bring further elements to the timing of water discharge in the Vénéon river, an essential key in deciphering the event dynamic and chronology.

5.1 Hydrometric observations

The discharge gauging station Les Étages (ETA), in operation since the late 1950s on the Vénéon river (since 1983 at an hourly resolution), is located approximately 3.5 km downstream of La Bérarde and drains a catchment area of 104 km^2. (Fig. 3). The sensor recorded the river water level until June 21, 03:00 (UTC), reaching a maximum hourly water level close to 2.80 m (eq. 80 m^3 s^{-1}), the highest observation on record since 1983. After that, the station got destroyed during the event by unidentified floating objects and therefore stopped recording. The rating curve of this station is based on dilution measurements to about 30 m^3 s^{-1}. The rating curve was extended using the hydraulic model Telemac-1D (Hervouet and Haren, 1996) to about 3.25 m (eq. 100 m^3 s^{-1}). Since 1983, the station recorded four floods reaching 2.4 m.

Figure 9a shows the hourly discharge timeseries at ETA station (104 km^2). We compare it to the downstream gauging station at Pont Rouge 33 km downstream on the Romanche river (ROU, 804 km^2) of which the Vénéon is a tributary (Fig. 3b). To give a sense of the general timing of the flood at multiple scales, ROU hourly observations are transposed to ETA, using a scaling correction based on the mean runoff values (0.18), and an appropriate time shift (-3h). Because the ROU station integrates a much larger catchment of similar configuration than ETA (*i.e.* high mountains, multiple glaciers), ROU reacts to the hydrological event (rain and snowmelt), providing a reliable comparison to the possible GLOF influence that would have affected ETA.

The debris brought and deposited by the flood formed a line around the ETA station. Combined with lidar surveys and the 2D hydraulic model Telemac-2D (Hervouet and Haren, 1996), we estimated the instantaneous peak discharge reached during the event. Lidar surveys show a rise of the riverbed around the ETA station ranging from 1 m at the station to 2 m upstream. Because of large uncertainties due to this morphogenic event (though constrained by the flood marks), we estimated a range of possible instantaneous discharge peak from 85 to 110 m^3 s^{-1} depending on the Strickler coefficient value (8 to 12 $m^{1/3}$ s^{-1} respectively) (Fig. A15).

Given the historical flood events at ETA (four reaching 2.4 m), the rating curve being validated to 2.4 m (eq. 50 m^3 s^{-1}), we are confident in the observation up to 60 m^3 s^{-1} (solid black line in Fig. 9a). Beyond this discharge value, as the station got eventually destroyed (without knowledge of the time), our confidence in the measurements and the associated discharge dynamic passed June 20 22:00 UTC (dashed black line in Fig. 9a) decreases. Though, based on the hydrodynamic modeling, we are confident that the peak discharge reached at least 85 m^3 s^{-1}. We have no knowledge of when it exactly occurred.

5.2 Hydrological modeling

Runoff modeling was performed with the MORDOR-SD hydrological model (Garavaglia et al., 2017), a semi-distributed conceptual rainfall-runoff model aiming at representing the main hydrological processes of a catchment. The model is driven

https://doi.org/10.5194/egusphere-2026-971
Preprint. Discussion started: 6 March 2026

with hourly rainfall and mean air temperature of the catchment. The model simulates five output water fluxes (snow and ice melts, surface, subsurface and baseflows) based on nonlinear relationships of five water storage (snowpack S, surface storage U, hillslope storage L, capillarity storage Z and ground storage N). To capture the elevation gradient, the Vénéon catchment is split into 10 elevation bands. Apart from ground storage N, all storage and input fluxes are represented independently within each elevation band. The model runs at an hourly timestep.

To calibrate the model, we used the 2019-2023 discharge observation at ETA gauging station. The calibration produced a reliable parameterization of the model (Nash–Sutcliffe Efficiency of 0.86 for the calibration period) with a good representation of both seasonal regime and high discharge distribution. Once the set of parameters calibrated, the model is run starting from September 2023 (which ensures a proper initialization) and forced during the event (June 19-21) with 1) catchment-averaged values of an adjusted version of the precipitation fields observed by the meteorological radar, and 2) an elevation compensated temperature timeseries. The precipitation fields from the radar product ANTILOPE (Champeaux et al., 2009) are corrected based on local *in-situ* precipitation observation at St Christophe en Oisans (CHR), Villar d'Arène (ARE) and Pelvoux (PEL) (Fig. 3b, Table A4). The air temperature timeseries were constructed based on the observed air temperature at the weather station Écrins (ECR, 2970 m a.s.l.), extrapolated to the entire catchment by applying an altitudinal lapse-rate of -0.6°C/100 m. Further details on the method can be found in the supplemental materials (Sect. A10).

After the careful calibration and corrections of the forcing inputs (*i.e.* precipitation and temperature), the modeled discharge at ETA for the event (June 19-21) period shows interesting findings when compared to the ETA discharge observations (Fig. 9a). First, as can be seen in the figure, the model is able to well reproduce the discharge prior to the event. Second, the maximum modeled hourly peak discharge reaches 66 m^3 s^{-1} on June 21, 6:00 (UTC). This modeled peak includes all water sources, except the GLOF contribution. Third, based on observation, a peak at about 60 m^3 s^{-1} was already reached on June 20 21:00 (UTC) (solid line Fig. 9a). And fourth, the hydrological modeled response of the Vénéon river follows closely the hydrological response of the Romanche river observed at ROU, located 33 km downstream (with a negligible influence from the GLOF). Therefore, based on these findings from observation and hydrological modeling only, we think likely that the glacial lake contributed significantly to the river discharge ahead of the hydrological peak (which includes only rain, snow and water storage). Because the gauging station at ETA got destroyed during the event, it is impossible to estimate precisely the volume of water missing to explain the peak that would have been observed at ETA. Hydrometric observations and modeling (Sect. 5.1) indicates a peak reaching somewhere between 85 and 110 m^3 s^{-1} occurring in between June 20 21:00 (UTC) and June 21 06:00 (UTC) (Sect. 5.1). However, even with early observation and hydrological models, including rain and snow melt, the actual river discharge behavior remains uncertain after June 20 21:00. All together, these observations support the hypothesis of an additional discharge source.

5.3 Seismic analysis

To further investigate the discharge observations made at the ETA station, three seismic stations located in the region of La Bérarde were analyzed to determine whether the event could be detected by seismology. These stations - OGSA, OGVG, and

https://doi.org/10.5194/egusphere-2026-971
Preprint. Discussion started: 6 March 2026

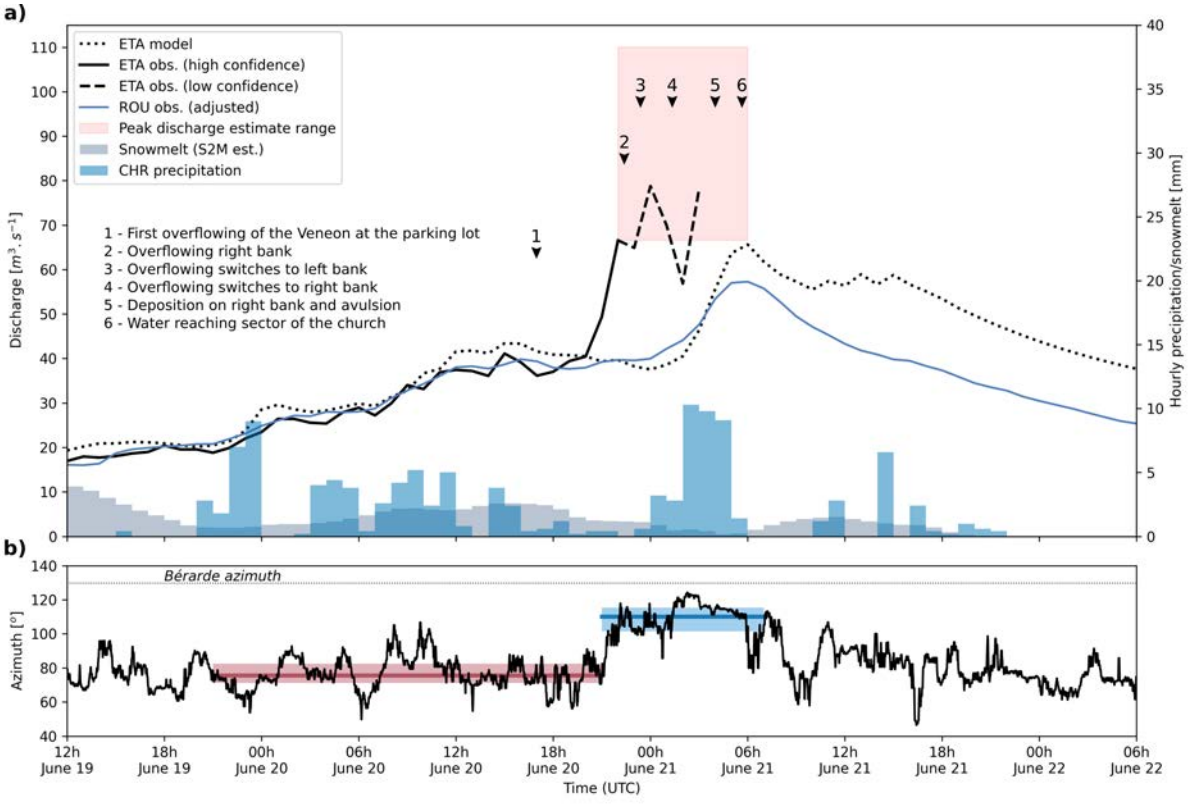

Figure 9. River discharge and seismic azimuth. **a)** Hourly discharge of the Vénéon river at ETA and ROU. ROU being downstream of ETA, it has been adjusted in time and absolute value to be comparable to ETA. The dashed line represents the discharge at ETA given a lower confidence in the measurement as the discharge station was eventually destroyed. The dotted line represents the modeled discharge using the MORDOR rainfall-runoff model based on rain and snowmelt inputs only. The peak discharge range was estimated using both landmarks and numerical modeling (Telemac-2D model), between 85 and 110 $m^3\ s^{-1}$. Hourly observed precipitation at CHR, and mean snowmelt (estimated with S2M for the whole Étançons catchment) are shown in panel **a** as barplot on the right y-axis. Numbering shows six important observations from local residents during the event (see the complementary Figure A24). **b)** Orientation of the particle motion obtained from the seismic station OGAG located in Argentière la Bessée. La Bérarde is located at azimuth 129.7° compared to the seismic station, which is represented by the dotted black line. Median azimuths with the 25th-75th percentiles, for the two periods before and during the rapid discharge increase are represented by the red and blue lines/areas. Figures in appendix A20 show a map of these azimuths.

OGAG — belong to the permanent seismic network in metropolitan France (FR) and are located approximately 13 km, 19 km and 25 km away from La Bérarde, respectively (Fig. 3).

Multiple studies have shown that turbulent water flow and sediment transport generate observable seismic power, especially at high (>1 Hz) frequencies (e.g., Tsai et al., 2012; Gimbert et al., 2014; Schmandt et al., 2013; Burtin et al., 2008). The station spectrograms show that the three stations do not respond similarly in the 2-10 Hz frequency band (Fig. A16). While OGSA does not exhibit a significant signal in this frequency band during the event, OGAG and OGVG displayed a clear

https://doi.org/10.5194/egusphere-2026-971
Preprint. Discussion started: 6 March 2026

increase in energy. For OGAG, this is likely related to the Durance river, which flows approximately 1.5 km from the station. Indeed the energy between 2-10 Hz and the river flow increase simultaneously (Fig. A18). OGVG, located about 500 m from the Séveraisse river, shows a similar frequency content, likely due to an increase in the river flow as well. Nevertheless, the absence of hydrological data for this river hampers direct validation of its influence. All three stations, however, show a distinct and temporally coincident signal in the 0.4–0.5 Hz frequency band during the event of la Bérarde (Fig. A19).

To characterize this common signal, we performed a polarization analysis using the $particle\_motion\_odr$ function from the ObsPy library (Krischer et al., 2015), applying first a 1-minute sliding window and then smoothing the results with a 60-sample moving median filter. Because linear polarization analysis is subject to a 180° ambiguity, the resulting directions represent only the axis of motion, not the sense of propagation. Consequently, azimuths must be interpreted modulo 180°. For example, the direction from the stations toward La Bérarde can be expressed as 129.7° or, equivalently, 309.7° from North, even though the polarization analysis returns values only within 0–180°.

Before the June 2024 flood, the polarization directions at the three stations ranged between 50° and 90° (Fig. 9b, Fig. A19 and Fig. A20). A distinct change in polarization was observed at OGAG, oriented towards the mountain range of the Écrins, beginning around 21:00 UTC on June 20 and persisting until approximately 06:00–08:00 UTC on June 21. In contrast, the polarization angles at OGSA and OGVG remained relatively stable, consistent with the fact that their pre-event polarization directions were already aligned with the broader region of Les Écrins massif and thus La Bérarde (Fig. A20 in Appendix). Because of the steep topography and complex geology, seismic waves are unlikely to travel along straight-line paths (e.g., Imperatori and Mai, 2015; Baron et al., 2022). This can partially explain the discrepancy between the expected azimuth toward La Bérarde (assuming straight-line propagation) and the azimuths measured at the seismic stations.

Although the 0.4-0.5 Hz frequency band is typically dominated by oceanic microseisms, we verify that background noise alone cannot explain the characteristics of the identified signal. For that, we modeled the expected ambient noise that would have been generated by secondary microseism between 0.1 and 0.5 Hz at this time period using the WMSAN package (Tomasetto et al., 2024). Although the model reproduced the long-term variability in the 0.4–0.5 Hz band, it failed to capture the energy increase observed during the event. This discrepancy indicates that the signal is not of oceanic origin.

While high-frequency (> 1 Hz) signals are dominated by turbulence (Gimbert et al., 2014) and sediment transport (Tsai et al., 2012), low-frequency observations have also been documented. For debris flows, this can be attributed to the bulk displacement force of the viscous mass (*e.g.*, Ekström and Stark, 2013), whereas in large floods, such signals can arise from large-scale turbulence (Schmandt et al., 2013; Goodling et al., 2018). Given these observations, the signal detected across the three stations — particularly the strong azimuthal response at OGAG — is consistent with flow-related activity in the Vénéon valley during the La Bérarde event. Such events generate low-frequency seismic energy capable of propagating over long distances (Cook et al., 2021), and the timing and characteristics of the signal align well with the rapid increase in river discharge observed at ETA.

https://doi.org/10.5194/egusphere-2026-971
Preprint. Discussion started: 6 March 2026

5.4 Reconstructing the event's chronology

The chronology of the event could be reconstructed based on observed data, but also on the testimonies of people who endured the event. On June 20, water started to rise in the Vénéon, following the rain initiated the day before and the important melt due to favorable energy fluxes (*e.g.* increased turbulent fluxes). By 09:15 (UTC), the valley road closed due to overflows of the Vénéon. Figure 9a shows some key testimonies (numbered 1-6) with their timing placed along to the hydrographs. The corresponding estimated evolution of material deposition/erosion and water flows can be seen in Figure A24. Timing and spatial accuracy are approximate given the limited amount of testimonies, photos and videos available. So at 17:00 (UTC), the first overflowing of Les Étançons occurred around the parking which used to be located NW of the village (1). At 22:15 (UTC), the Les Étançons broke off the right bank (2). It later (23:15 (UTC)) broke off the left bank (3). Just an hour later, at 01:15 (UTC) on June 21, the river overflew back again on the right bank depositing materials (4). Around 04:00 - 05:30 (UTC), massive deposition had occurred on the right bank triggering an avulsion to the left bank (5). At 05:40 (UTC), the water started reaching the SE part of the village, the older part of the village (6). From this moment onward, most of the water kept flowing on the left bank of the original river bed with little material being deposited anymore. The river later deeply incised the bed on a track going through the SE part of the village destroying the 132-year old church among many other buildings (Fig. A2c). Observation on June 22 indicated that the supra-glacial lake of Bonne Pierre had fully drained (Fig. A2f-g). Most material was deposited in the north west of the village (Fig. 4). By deduction with the timing and spatial extent of the event unfolding (Fig. A24), we estimate that most of the material deposition may have occurred in between stages (3)-(5), the missing 100 000 m^3 have probably been transported to the receiving Vénéon river before or during these stages.

So, to summarize, over the period June 19, 12:00 - June 21, 11:00 UTC, we estimate a contribution of least 114 mm from the rain, of 75 mm w. eq. from snowmelt averaged over the entire catchment. The peak 48 h snowmelt reached within this time frame is 95 mm w.eq. on the morning of June 19 prior to the debris flood event. Rain reached at least 104 mm (CHR) in 48 h with a peak reached of precipitation intensity during the night of June 20 to June 21 (Fig. 6). When aggregated over the two catchments, of 1) Bonne Pierre (3.3 km^2) and of 2) Etançons (8.7 km^2 - including Bonne Pierre), the instantaneous volumes of water (estimated from S2M) from rain plus snow vary from $1.19 - 1.43 \times 10^6$ m^3 and $4.42 - 5.42 \times 10^6$ m^3, respectively depending on precipitation estimates (Tab. 2). On top of that, the supraglacial lake represents another 0.1×10^6 m^3 of water, with a potential additional internal storage of up to 0.15×10^6 m^3 of water.

6 Qualifying the rarity of the event

6.1 Historical events

The village of La Bérarde, built on the alluvial fan, hosted more than 100 people seasonally prior to the event. The first evidence of human settlements at La Bérarde and its neighboring village (Les Étages) dates back to at least 1339, with most likely some anterior habitations downstream of its current location. The position of the torrential channel along the right edge of the fan, as well as the location of the village in the middle of the fan are testified since the mid 18th Century on old maps. Despite

https://doi.org/10.5194/egusphere-2026-971
Preprint. Discussion started: 6 March 2026

Table 2. Total volume of water estimates contributing to the flood for the period of reference of 48 h (June 19 12:00 - June 21 11:00 UTC) and the period during which material transport is witnessed at the village (June 20 20:00 - June 21 12:00 UTC). Volumes are computed for the Bonne Pierre catchment (8.7 km^2), and for entire Étançons catchment (33.8 km^2). No hydrological routing was applied.

Water source	**Total volume of water [x1 000 m^3]**			
	Bonne Pierre		Étançons (at La Bérarde)	
	48 h period	16 h period (solid transport)	48 h period	16 h period (solid transport)
Rain	610* - 850**	130* - 300**	2500* - 3500**	530* - 1 240**
Snowmelt	580	100	1920	300
Supra-glacial lake	100		-	-
Potential intra-glacial storage	≤150***		-	-

* *Estimates based on S2M (Sect. 4.2).*

** *Estimates based on S2M adjusted (Sect. A6.1).*

*** *Estimates based on DEM and modeling (Sect. 4.3) (Ogier et al., 2026).*

poor quality soils, a rugged topography, a harsh climate and and prevalent natural hazards (Fig. A3), the inhabitants shaped and adapted to the surrounding landscape for agriculture, with the most favorable place found on the alluvial fan. Permanent settlements are reported since at least 1830 (and likely since medieval period based on birth and death records) despite the typical 7-month snow season (de Beaumont, 1834). In 1911, a total of 58 inhabitants resided annually at La Bérarde. Natural hazards, snow avalanches, rockfalls, and floods have been an integral part of shaping the village history and development, though few records of natural hazards events exist prior to the 17th Century. The first flood event known to produce significant damage on record occurred on August 3-4, 1785 (based on local archive records), during which a flood of the Vénéon river due to rain and glacial melt led to damages to crops, forest, bridges and a building. Then a series of floods occurred during the mid-summer of the years 1877, 1878, 1879, and 1888 for which no casualties have been reported, but some damages to infrastructure were recorded and in 1877 some material deposited on the northeastern part of the alluvial fan (Archives Départementales de l'Isère, 1785). This event triggered the construction of an embankment to guide the torrent. In September 1956, the Étançons torrent suddenly flooded, destroyed a dike, deposited material on the northern part of the fan, thus threatening the village. Since 1956, no significant flooding event in the village had been reported previously to the event described herein (ONF-RTM, 2025).

6.2 Event probability

The 2024 event being rooted in multiple drivers not necessarily independent, we attempted to estimate the probability of occurrence for each component of the event when data were available. Precipitation records and reanalysis products (*e.g.* S2M) provide estimates for rain and snowmelt return periods computation. For sediment transport, we compared this event to

https://doi.org/10.5194/egusphere-2026-971
Preprint. Discussion started: 6 March 2026

analogous transport events in the literature. Concerning the GLOF, we could not estimate precisely the actual intensity of its role during the event. We lack too historical precedent of any GLOF from Bonne Pierre glacier.

Based on the precipitation records at CHR since 1964 as well as the S2M reanalysis, we could approximate the return period of the June 2024 rain event using a Generalized Extreme Value distribution (GEV) (Coles et al., 2001) fitted against the observed annual maxima of 48 h precipitation using a Bayesian approach (Abril-Pla et al., 2023). Details about the method are described in section A14. The return period for a 48 h event of 104 mm at CHR is ranging from 9.8 to 15 years based on observation (Fig. A25). While this may not be characterized as an extreme precipitation, we observe that such rain is unusual in springtime. Intense precipitation tends to occur from mid-July to October (Fig. 7b).

Given that estimates from the S2M (Vernay et al., 2022) reanalysis of precipitation extremes are statistically equivalent to observation at CHR, and that S2M has already been used to study extreme snowfall (Le Roux et al., 2021), we are confident to analyze extreme event based on the S2M dataset (1959-2024). S2M provides data on precipitation (partitioned liquid *vs.* solid) and on the snowpack in an abstract geometry (Sect. 2.3). To perform the return period analysis, we first projected the S2M data onto the Étançons catchment and computed average values for rain, snowmelt, and the combined total of rain plus snowmelt (Sect. 4.2 and A6, Fig. 7b). We fitted three independent GEV models to the rain, melt, and total runoff respectively. We found that for the 48-h centered on the peak of total runoffs (rain plus snow, 172 mm, June 19-21 from 05:00 to 05:00 (UTC)) the median return periods are 7, 22 and 153 years for the rain, snow melt, and the sum of rain and melt respectively. These return periods correspond to return levels of 85.1, 86.9, and 172 mm respectively (Table A4). The Bayesian approach provides an estimate of the uncertainty associated with the return period estimates, which can be substantial (Fig. A26, appendix A14). For instance, the snowmelt runoff return period ranges from 14-25 years for the 48-h period starting on June 19 at 05:00 (Fig. A26, Appendix A14).

However, snowmelt and liquid precipitation did not remain constant over the june flooding event (Fig. 9), so we evaluated the return periods for each of the components (rain and snowmelt) at their peak. The maximum 48-h melt rate during this event (93.8 mm) is the third most intense since the start of our reanalysis record (1959). Such a melt rate corresponds to a median return period of 57 years. As demonstrated in Figure 7b, the co-occurrence of such a high melt rate with a 10-year return period rain is, to our record, unique. The return period estimate for total runoff (summing rain and melt) of 157 years, in its current mathematical formulation, does not account for precipitation seasonality, while we know that such intense rain is scarce at this season. Spring and early summer are mostly under the influence of westerly circulation patterns while Mediterranean circulation (Sect. 4.1) tend to typically occur in fall (Tramblay et al., 2023), leading the most extreme precipitation events (Blanchet et al., 2021). Given the timing (late spring) of the Mediterranean circulation, we, therefore, think this return period estimate to be conservative.

Assigning a return period to the sediment production of the catchment cannot be done for several reasons: (i) it would require to have records of past events to adjust a suitable statistical law (*e.g.* Morel et al., 2023, as based on debris basin data) but the 2024 event is the only quantified event of this catchment. (ii) Assuming that further geo-historical works would enable to reconstruct a few past event (which is doubtful), it would also require to assume a stationarity of the debris flow and debris flood activity, *i.e.* of meteorological- and glacier-related triggering factors and of sediment availability and propagation potential. Due

https://doi.org/10.5194/egusphere-2026-971
Preprint. Discussion started: 6 March 2026

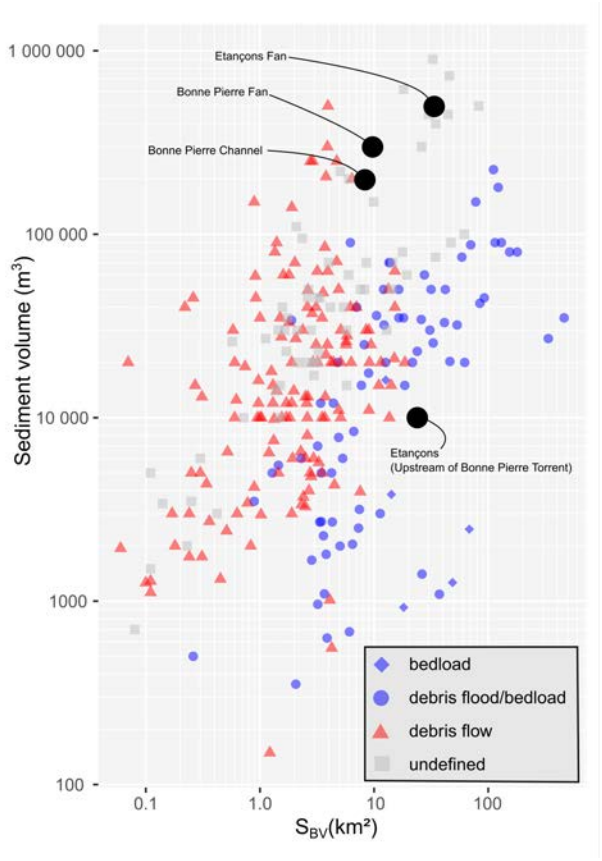

Figure 10. Sediment production as a function of catchment area for the studied event and comparison with other debris floods in Alpine catchments. Values for the sub-catchments of the Étançons are indicated with black points. The type of sediment transport ("bedload", "debris flood/bedload", "debris flow" and "undefined" is based on details available in the published data from Morel et al. (2023); Rickenmann and Koschni (2010); Gertsch (2009); D'Agostino et al. (1996)

to climate change and recent glacier retreat, this assumption is unreasonable and prevents any coarse or precise estimation of a geomorphological return period (see also discussion Sect. 7.5). Nonetheless, to give a sense of the event extreme character in terms of sediment transport and morphological changes, we conducted several comparisons with other high magnitude events. First, comparing the volume of sediment exported from the catchment as a function of the catchment area shows that the event of June 2024 on the Étançons is in the upper range of data published for Alpine catchments (Fig. 10). This is true for the Bonne Pierre torrent (part I and II, Fig. 4) and the Étançons torrent downstream the confluence with Bonne Pierre. On the upstream part of the Étançons torrent (part V, Fig. 4),the sediment production is one order of magnitude lower and corresponds to the lower part of published data (Fig. 10). The comparison with the published data of Marchi et al. (2019) of 590 debris flows in the Italian Alps shows that the volume exported on the Bonne Pierre torrent and lower Étançon is near the 98 % percentile of this dataset. A comparison with statistical models obtained in the French Alps by Morel et al. (2023) suggests that the sediment

https://doi.org/10.5194/egusphere-2026-971
Preprint. Discussion started: 6 March 2026

export is 4 to 6 times higher than the 100-year return period for the Bonne Pierre torrent, while the upper Étançons branch produced a lot less than its theoretical 10-year return potential.

A second comparison with published erosion rates was undertaken on the Bonne Pierre torrent which experienced a large channel incision/erosion. The median erosion rate (part I in fig. 4) is around 150 m^3 m^{-1}, while it reaches 300 m^3 m^{-1} at some locations (erosion rate calculated considering 30-m long reaches). On the Bonne Pierre fan (part II in fig. 4), its median value is around 230 m^3 m^{-1} and it reaches 350 m^3 m^{-1}. These values are quite high in comparison to the erosion rates found in the literature. Erosion rates synthesized by Marchi and D'Agostino (2004) rarely exceeded 100 m^3 m^{-1}. Those proposed by Hungr et al. (1984) are generally lower than 200 m^3 m^{-1}. Even during Storm Alex (October 2020, southeastern France), when rainfall higher than 1000-yr return period impacted steep catchments triggering dozens of debris flows and debris floods, erosion yields higher than 200 m^3 m^{-1} were reached in only one debris flow catchment, although the debris floods that devastated the valley bottom reached higher values (Martini et al., 2025, values higher than 380 m^3 m^{-1} where measured on about 2 km). In some steep torrents too, we can find a few example of higher values, for instance during the 1987 events in Switzerland with erosion rate reaching 500 to 650 m^3 m^{-1} (Rickenmann and Zimmermann, 1993) or for GLOF events with much higher values reaching 2000 m^3 m^{-1} in the Andes or in Himalaya (Mool et al., 2001).

Considering that it is impossible to assign a probability to the GLOF, and the sediment production, the occurrence probability of this event cannot rely on rain and snowmelt contribution only to be precisely quantified.

7 Discussion

7.1 Role of the GLOF

Intersecting the independent facts enumerated here-above about 1) the about the Bonne Pierre glacier and its supraglacial lake (Sect. 4.3, 2) the hydrological modeling of the peak discharge at ETA (Sect. 5.2), 3) the coincidental seismic signal (Sect. 5.3), 4) the sediment transport (Sect. 3.2), and 5) the testimonies (Sect. 5.4, we may incriminate the role of the GLOF in the unfolding of events. From Figure 9a), we see that the peak discharge at ETA cannot be explained by the hydrological model (forced by rain and snowmelt only). The model reacts similarly to the discharge observed for the larger catchment at ROU (sensitive to rain and snowmelt). The hydrodynamic analysis at ETA from the *in-situ* observations and the modeling effort does confirm a peak discharge of at least 60 m^3 s^{-1} occurring at 22:00 UTC on June 20 (Sect. 5.1). Historically, there are four records of the Vénéon reaching discharge of 40 m^3 s^{-1} without any equivalent observation of sediment transport from the Étançons. This minimal peak discharge coincides with the testimonies of the first material deposition on the alluvial fan of La Bérarde (Sect. 5.4), and a shift in seismic signal source towards the center of the Écrins mountain range (Sect. 5.3, fig. 9b). *A posteriori*, the presence of debris flow lobes were observed on the Bonne Pierre fan, indicating the possible initiation of the erosion. Most material are in provenance from the Bonne Pierre torrent, starting the erosion scarce from the glacier front (Sect. 3.2, fig. 4).

Despite the very likely influence of the lake drainage on the flood magnitude, we think that a scenario of a sudden drainage, within less than half hour, should be excluded. Assuming a volume of 100 000 m^3 of water stored in the lake, the sudden release of water in the steep channel downstream of the glacier (slope ranging 0.3-0.4 m m^{-1}), containing large stocks of sediments

https://doi.org/10.5194/egusphere-2026-971
Preprint. Discussion started: 6 March 2026

would have triggered a debris flow. Based on the Takahashi criteria (Takahashi, 1978) or flume measurements (Lanzoni et al., 2017), this debris flow would have reached a sediment *vs.* water volume fraction of about 50 %, that would have transported a global volume of 200 000 m^3. Using the empirical equations (Sect. A12) relating debris flow propagation to total volume and peak discharge to total volume for granular debris flow (*i.e.* consistent with the type of material and the shape of deposits observed on site), this hypothetical debris flow would have reached the Bérarde village, with a peak discharge in somewhere in between 1800 to 3000 m^3 s^{-1}) (Mizuyama et al., 1992; Bovis and Jakob, 1999; Rickenmann, 1999).

From the simplified friction law proposed by Rickenmann (1999), we could expect a debris flow height for the main surge in the range of 10 to 13 m inside the canyon downstream of the Bonne Pierre Torrent (part III in Figure 4), and of 12 to 17 m at the Bérarde fan (part IV in Figure 4). These estimates are not consistent with observations made at these two locations. The maximum height measured is in the range of 3-3.5 m in the canyon. No sudden overflowing was witnessed on the main bridge during the event. Simplified non-Newtonian modeling of granular debris flow propagation on the alluvial fan (Sect. A12) confirms that a debris flow with such large peak discharge would have reached the fan, generated much greater damages and therefore been witnessed during the event. In conclusion, this simple analysis excludes an hypothetical sudden drainage of the lake ($\leq$30 min). Further methodological details about this analysis are provided in the Sect. A12.

So, for all these intersecting evidences, we think that:

- the GLOF probably started around 19-21 h UTC, that corresponds to start of the discharge diverging from rain and snowmelt water explained contribution
- the GLOF likely initiated the erosion
- no possible reconstruction of the GLOF drainage dynamic after its initiation
- The GLOF was not a sudden release
- the hydrological system of the Étançons catchment was already fully saturated by water due to snowmelt and rain (Sect. 4.1 and 4.2).
- the role of the GLOF is deduced from a number of independent evidences but is still missing a hard proof of its role.

It now remains to zoom out and contextualize the nature of this event within a broader scientific scope related to 1) the role of the specific geography and geomorphological history at La Bérarde, 2) the paradigm of compound events and, 3) the potential role of climate change.

7.2 Paraglacial adjustment

The nature of the 2024 event can be related to the concept of paraglacial adjustment paradigm, developed by Ballantyne (2002). It postulates that retreating glaciers leave large amounts of unconsolidated and easily re-workable sediments at the glacial margins, and on steep and potentially unstable valley slopes. Glacier retreat is therefore followed by a geomorphological adjustment phase of the system, characterized by a high rate of sediment transport and gravitational slope movements. In

https://doi.org/10.5194/egusphere-2026-971
Preprint. Discussion started: 6 March 2026

case of rapid glacier retreat and/or high amounts of sediments release, this adjustment phase may become a geomorphological crisis. The paraglacial concept was developed for interpreting past landscape evolutions. For instance, the building of the largest torrential cones in the Alps occurred during the Early Holocene, a paraglacial phase consecutive to the rapid retreat of glaciers from their Lateglacial positions of the Younger Dryas / Egesen stadial (Ballandras, 1997). The recent retreat from the LIA glacier positions since *c.a.* 1850 induces a new paraglacial phase of much smaller intensity, that nevertheless can be significant at local scale (*e.g.* Curry et al., 2006).

The paraglacial paradigm provides an interesting conceptual framework for analyzing the present day dynamics of mountain ranges deglaciation due to climate change, and therefore for interpreting events like the one discussed here (proglacial debris supply). Applied to the case of the Bonne Pierre catchment, the paraglacial paradigm induces several consequences. First, the supply of sediments is bounded. This is due to i) a glacier retreat similar to the present one has not occurred since at least the beginning of the Medieval Warm Period, *i.e.* some thousand years ago, or even earlier (see datings of the moraine, Sect. 2.1), ii) we are in a crisis situation, similar events may occur again at possibly short intervals, as long as sediments are available. As a consequence, statistical approaches based on extreme laws are not applicable to estimate return periods for the sediment transport event (breaking the stationarity hypothesis). To do so, we instead use a comparative approach to other events across the Alps (Sect. 6.2). Second, the paraglacial paradigm relies on an "exhaustion model", postulating that the intensity of reworking decreases with time along with the exhaustion of the available sediment stock. Accordingly, one could postulate that the intensity of forthcoming events should decrease. However the current stock of sediments mobilizable from the Bonne Pierre fan has not been estimated and as long as the glacier will continue its retreat, it will release new sediment volumes and renew the sediment stock. Moreover, thick debris resulting from a rockfall of the early 1930's, currently covering the glacier front may be released in the near future. Finally, despite of the reworking of the Bonne Pierre proglacial sediments on June 2024 by fluvial processes is the first to occur in centuries, erosion of the inner flank of lateral moraines is releasing greater amount of sediments. This is already occurring on the prominent right lateral moraine of the Bonne Pierre glacier, contributing soon to the sediment supply. Regarding the compound event concept, the glacier retreat and the corresponding sediment supply and reworking appear as necessary pre-conditioning factors that made the event possible. Though, one can suppose that in a non-glacial context, an event of such magnitude would be hardly possible.

7.3 Spatial connectivity

Loose materials within the Étançons catchment are sensitive to gravity-driven mass wasting processes. In this respect, the spatial configuration, a product the paraglacial adjusmtents, should be quantified for understanding the severity of the event and the geographical arrangement of its different elements (e.g., bringing materials from high elevation to lower elevation). This event stresses how the spatial configuration of sediment sources and their connectivity is a prerequisite to generate a dramatic torrential compound event. Analyzing this precondition on this specific case could help, in the future, better define sites potentially subject to such compound scenarios. In particular, the geological map shows that large areas in the catchment are covered by loose material easily erodible, in particular in the upper Étançon catchment (Fig. 11a). The analysis of structural connectivity using the Cavalli et al. (2013) index can help to localize areas that are highly connected to the outlet of the basin

https://doi.org/10.5194/egusphere-2026-971
Preprint. Discussion started: 6 March 2026

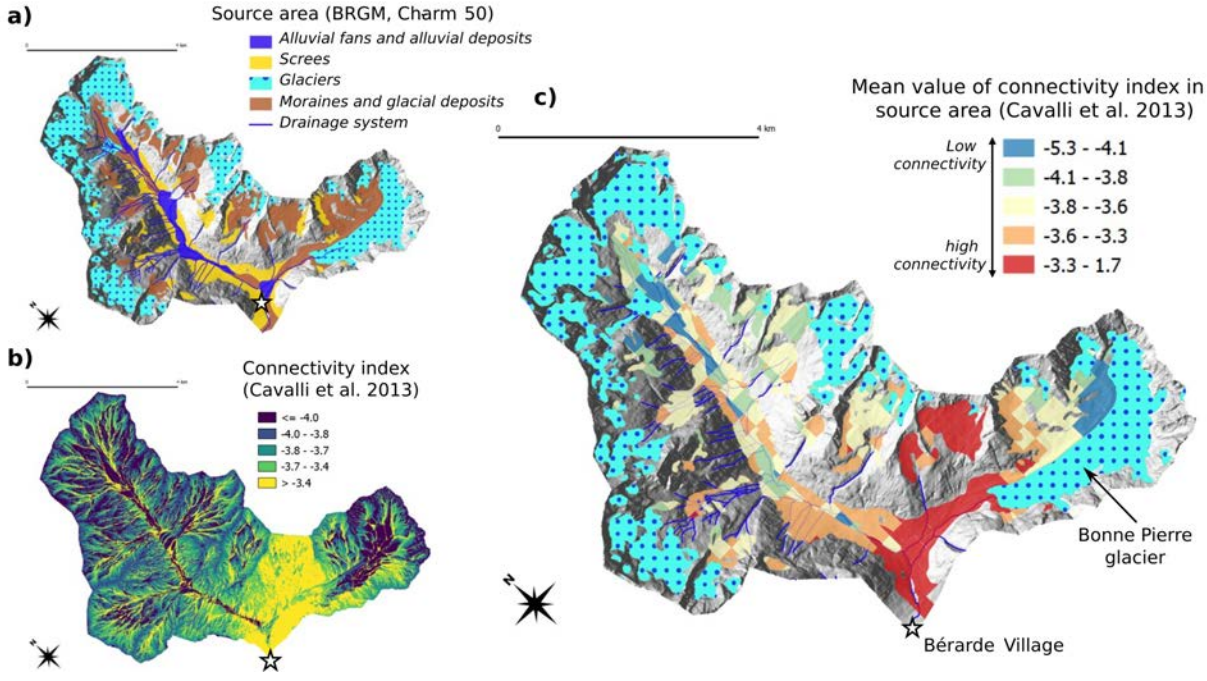

Figure 11. a) Available loose material in the Étançons catchment and glacier cover based on the French geological map, **b)** connectivity map using the connectivity index developed by Cavalli et al. (2013). **c)** Mean values of connectivity index extracted in sediment sources on a grid of 250 m.

(here defined as the fan of La Bérarde) and areas that are less connected or fully disconnected (Fig. 11b). This connectivity map shows in particular how the Bonne Pierre torrent downstream of the glacier front (part I and II, Fig. 4) is connected to the village, as the torrent slopes are steep (20-40 %) with no alluvial reaches in between. By contrast, the upper Étançon catchment (part V, Fig. 4) is partly disconnected from the village due to long and large braiding reaches with mild slopes (4-9 %), that are consistent with the alluvial fan channel slope (7-9 %).

By coupling the source areas and the connectivity map it is possible to stress the areas where loose materials are highly connected or disconnected to the outlet (Fig. 11c). This approach is in good agreement with the observed dynamics during the June 2024 event: despite the presence of large areas of unstable moraines located on the upstream part of the Étançons catchment, the long braiding reaches have buffered these potential inputs. These areas are of low connectivity on Fig. 11c). In comparison, the most active area during the June 2024 event on the Bonne Pierre torrent appears highly connected to the village so that no buffering of sediment transport can be expected: the very steep slope of the Bonne Pierre torrent (part II) directly delivered large amount of sediments directly into the steep canyon (part III, slope : 12-25 %) located upstream of Bérarde fan apex (part IV, Fig. 4). The large volume of water coming from the larger upper Étançons catchment (part V) was then able to remobilize the loose sediments down onto the fan of La Bérarde. There, the slopes are shallower. The Vénéon river (slope : 3-4 %) was subsequently not able to convey all of the sediments further downstream. This shows how both, sediment sources

https://doi.org/10.5194/egusphere-2026-971
Preprint. Discussion started: 6 March 2026

and connectivity mapping, can help practitioners to better define areas subjected to torrential compound hazards, as both are preconditions to such an event becoming damaging.

7.4 Compound nature of the event

Driven by excess water originating from rain, snow melt, and the drainage of the supra-glacial lake and potential intraglacial storage, the debris flood reaching its peak during the night of June 20-21 entrained large volumes of sediment downstream ($\approx 300\,000$ m^3). The relative contribution, intensity, and timing of these key drivers are now better understood (Sect. 4 and 5.4). Though it remains difficult to isolate and attribute the magnitude and severity of the event to one specific driver. Our analysis on return periods of the rain and snowmelt water inputs shows that, independently, none of them may be qualified as extreme (Sect. 6.2). The intersection and timing of both (rain and snowmelt) starts highlighting a unique event, not observed for the past 60 years according to the S2M reanalysis data (Fig. 7b). Once adding the drainage of the supra-glacial lake (Sect. 4.3 and 7.1), we now have a number of independent components of a compound event according to the definition given by Zscheischler et al. (2018) and AghaKouchak et al. (2020) (Sect. 1).

To capture the spatial and temporal intricacy of the event, we represented each key element of the event into a conceptual diagram *timescale vs. elevation* (Fig. 12). The *timescale* axis, ranging from millennia to minute, reflects the time each of the event component needed to built up and play a role into the event. Those building up on the long term (*e.g.* sediment deposits, glacier topography) can be considered as *preconditions* to the event. The *elevation* axis provides a proxy for the geography, particularly marked by the elevation gradient (1700 - 4000 m) in the Étançons catchment. This representation (Fig. 12) depicts how the event occurring in June 2024 is the result of preconditions (*i.e.* glacier retreat, sediment deposit formation, and supra-glacial lake formation, snowpack) that range from the millennial to the seasonal timescale in the upper part of the valley. The warm air spell then comes within days to hours to melt snow and generate heavy rain, saturating the entire hydrological system and filling all glacial cavities offered by the vanishing shallow angle debris-covered glacier. The likely GLOF co-occurring with the rain and snowmelt, in a watershed where large volumes of sediments highly connected to downstream human infrastructure (Sect. 7.3) demonstrates the intertwined and complex interactions of this event.

In the hypothetical situation that one element constituting of this event is withdrawn, we understand that as a consequence, the severity would drop drastically. For instance, the runoff generated from the rain and the snowmelt combined exceed a 100-year return period, while considered individually, snowmelt and rain are both 5 to 10 times more likely, respectively. A number of evidences (Sect. 7.1) points to the role of the GLOF during the most intense period of the debris flood. The intensity and severity of this event cannot be explained by one main factor, and can therefore be identified as *compound*.

This classification as a compound event is important 1) to appreciate the uniqueness of this event, 2) to understand the difficulty of estimating an overall occurrence probability, 3) to better understand the causality of hazards and processes at play, 4) to realize that low to medium magnitude hazards, if co-occurring, may generate extreme consequences, and 5) to guide our search for analogous events in the past and future in response to climate change (Zscheischler et al., 2018; Pörtner et al., 2019). Zscheischler et al. (2018) introduce the concept of *bottom-up approaches* to compound events. By identifying first a system point of failure (i.*e.* impact on life or critical infrastructure), the bottom-up approach then leads to find scenarios of compound

https://doi.org/10.5194/egusphere-2026-971
Preprint. Discussion started: 6 March 2026

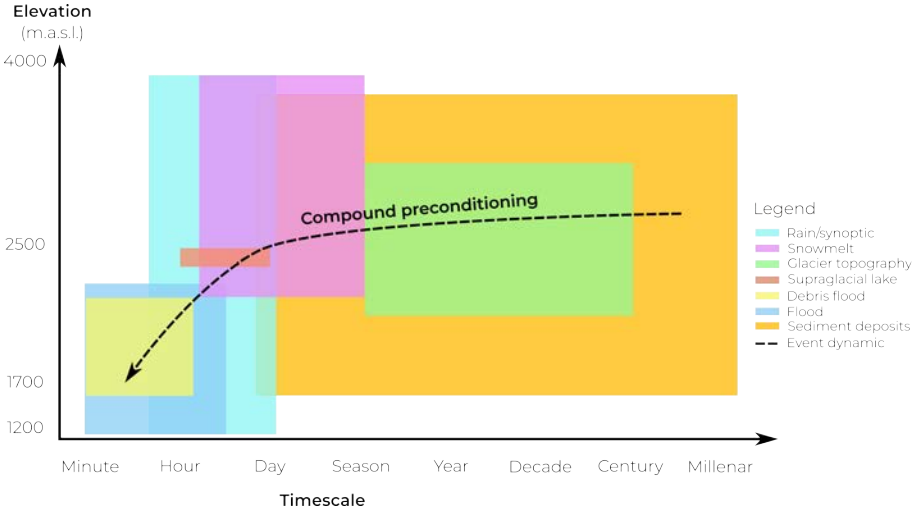

Figure 12. Timescale and elevation dependencies of the components playing a role in the June 2024 event and the following cascading hazards. The village of La Bérarde is located at 1700 m a.s.l.

events that may increase risks for that system, and *in fine* to hazards and/or drivers of greatest impacts. This is in opposition to the *top-down approach* that first focuses on identifying extreme hazards and/or drivers objectively without consideration of their connection to impacts (*e.g.* an extreme precipitation analysis based on climate emission scenarios), or of the possible co-occurrence with other processes amplifying an event intensity. The compound event paradigm would be beneficial in a situation like La Bérarde as it helps analyzing the chain of events and attempting to identify the "*drivers or hazards that may fail the system*". In our situation we can point to a combination of three factors: 1) the high connectivity between the sediment source and deposition on a village, 2) the co-occurrence of rain and snowmelt in June, and 3) the GLOF propensity of the Bonne Pierre glacier. Without any of these three factors, the event would likely have been of much lesser magnitude, as witnessed in the adjacent valleys, exposed to similar weather and snow conditions but without GLOF or the high connectivity.

Bringing this event in light of the *compound event* paradigm will hopefully raise attention in how extreme events may arise, and therefore expand adaptation and mitigation strategies for communities and/or infrastructure identified as vulnerable. The event of La Bérarde is demonstrating how extreme consequences may not arise necessarily from one extreme driver, but rather from a combination of drivers of low to moderate magnitude with given geographical specificities. While it would practically be impossible to analyze every alpine communities or infrastructures from the perspective of compound events, it may be thought a strategy to identify critical and/or the most vulnerable communities/infrastructures within that scope. This will become even more relevant with the underlying constrain over-imposed by climate change on almost all of the event components listed here-above.

https://doi.org/10.5194/egusphere-2026-971
Preprint. Discussion started: 6 March 2026

7.5 Climate change

La Bérarde is located at the core of Les Écrins massif, among the highest mountain ranges of the French Alps, which are prone to rapid changes under the constraint of climate change. The European Alps are undergoing an increase in temperature of already +2°C since 1850-1900 (Kuhn and Olefs, 2020; Dumont et al., 2025), and a modification in precipitation regime (Scherrer et al., 2016; Brönnimann et al., 2018; Kuhn and Olefs, 2020; Peleg et al., 2025). These changes are complex and heterogeneous across the Alps, with non-uniform responses throughout seasons and elevations (Kuhn and Olefs, 2020; Dumont et al., 2025). To date, we witness major impacts on glaciers losing 2 ± 0.1 Gt y^{-1} (2000–2023) of their mass across the Alps (Sommer et al., 2020; Zemp et al., 2025), with a major retreat of glaciers since the Little Ice Age (Reinthaler and Paul, 2025) (Sect. 3.2 and 7.2). Mountain permafrost is also impacted by warming at an alarming rate, leading to slope instability (Noetzli et al., 2024; Magnin et al., 2024; Jacquemart et al., 2024). Meanwhile, synoptic weather patterns generating intense precipitation are becoming more frequent in the western southern Alps (Blanchet et al., 2021; Blanc et al., 2022b, a). Consequential hazards due to change in air temperature and precipitation regime can be spring or summer low flows due to the lack of snow melt and glacial melt (Colombo et al., 2023; Gascoin et al., 2024; Sauquet et al., 2025), glacier collapse (Bondesan and Francese, 2023; Chiarle et al., 2023), permafrost slope instability (Legay et al., 2021), GLOF (Lützow et al., 2023), and floods due to intense precipitation or rain on snow (Wilhelm et al., 2022). Two questions arise in respect to climate change: 1) what may have been the contribution of climate change in terms of occurrence probability and intensity, and 2) how may we better predict extreme events in alpine regions under the non-stationarity associated to a changing climate?

The catchment of Les Étançons, like the rest of the Alps, has seen its glaciers retreating (Sect. 4.3 and 7.2). The glacier of Bonne Pierre, being debris covered in its main part, has a growing number of supra-glacial lakes in recent decades (Fig. 8). Moraines and rock walls above 2700 m a.s.l. where permafrost is degrading (Magnin et al., 2024) may experience deeper active layers (*i.e.* summer thawing depth). This may be altering the mechanical properties, therefore leading to an increased probability of rock wall destabilization events like the 2016 rockfall onto the Bonne Pierre glacier (Sect. 4.3). As a consequence, we observe an increasing amount of materials covering the glacier responsible for the uneven melt of the glacier surface (differential melting of the ice due to heterogeneous insulation by the debris, Sect. 4.3) leading to the formation of ponds (*c.f.* the supraglacial lake). *In fine* these loose materials may also add to the initial erodible stock (*i.e.* paraglacial adjustment and susceptibility) (Ballantyne, 2002; Jacquemart et al., 2024). From a historical reconstruction of debris flows of about 500 years in the Swiss Alps, Stoffel and Beniston (2006) showed an increased debris flow activity during the Little Ice Age (1864-1895), coincidental to the flooding activities in historical records for La Bérarde (years 1877, 1878, 1879, and 1888, Sect. 6.1). Such local knowledge does not exist at La Bérarde, where dendrochronology, or soil pit stratigraphy would be beneficial to study the genesis history of the alluvial fan (Baumann and Kaiser, 1999; Stoffel et al., 2005; Schneuwly-Bollschweiler and Stoffel, 2012).

For the event of June 2024 at La Bérarde, Kreitz (2024) noticed that Spring 2024 in France had an unusual number of "cold drop" synoptic in the region (Sect. 4.1). Just a week later a similar synoptic pattern, shifted by couple hundred kilometers to the east, produced floods and landslides in the Valley of Aosta (Italy), and Ticino and upper Valais cantons (Switzerland). There,

https://doi.org/10.5194/egusphere-2026-971
Preprint. Discussion started: 6 March 2026

precipitation were of similar magnitude to the La Bérarde event. However, such synoptic was showed to not be untypical in spring and without clear response to climate change (Garavaglia et al., 2017; Tramblay et al., 2023). Perhaps in the case of June 2024, the precipitation phase was a key factor to explain some of the impact of climate. Nevertheless, without performing a full climate change attribution study (Ginesta et al., 2023, e.g.), it is complex to decipher the actual role of climate change for a single weather event such as the event of June 2024 at La Bérarde.

In the future, given the effect of warming air on the carrying capacity of moisture, extreme precipitations are expected to intensify, glacier-related lakes are also growing in number, so are the consequential debris flood/flows for catchment with sufficiently high susceptibility (Stoffel et al., 2024) undergoing paraglacial adjustment. In the Ubaye valley located 60 km SE of La Bérarde, Turkington et al. (2016) found an increasing probability of debris flows by 2080 based on increased intense precipitation in climate scenario (ref. period 1980-2009). Currently, most intense precipitations occur in summer. These are expected to shift into spring and fall and possibly winter as well (Beniston, 2006; Stoffel and Beniston, 2006; Stoffel et al., 2024). But given the warming trend, leading to a snowpack melting earlier in spring, the likelihood of rain-on-snow events impacting hydrology in the french Alps is expected to decrease (Tramblay et al., 2025). Though, Beniston and Stoffel (2016) found that for a smaller Swiss alpine catchment, there might be a phase during the warming when late spring rain-on-snow events may become more frequent. With an increasing susceptibility due to the receding cryosphere and the phase of intensification of rain during the snow season for small high elevation catchment, one may foresee an increased probability of an event like the June 2024 debris flood in the future. As such, in 2010, Keiler et al. had concluded that communities and infrastructure as of now (*i.e.* in Austria) would not be ready to sustain the intensification of such extreme events.

As discussed in section 7.4, the paradigm of compound events showed that the long term build-up and co-occurrence of low to moderate magnitude hazards combined to geomorphological specificities can lead to a local extreme event. Assessing communities' vulnerability will require to consider such intricate situations. Zscheischler et al. (2018) argue that risk assessment of extremes based on climate scenario and univariate statistics is not sufficient as it may not reflect and capture the intricacies of an event like the one described here. They argue that the storyline approach (Hazeleger et al., 2015; Moezzi et al., 2017), may become an appropriate and complementary approach to identifying critical situations in a non stationary climate. For that purpose, historical records and hindcast analysis of events may become crucial starting steps for identifying the range of "*lines of evidence*" to build a portfolio of storyline about compound events (Zscheischler et al., 2018). While our work was not focused on characterizing the role of climate change, we suggest here a new approach that may help our community more finely assess natural hazards in a non-stationary climate.

8 Conclusions

In June 2024, during the night of June 20 to the 21, the small village of La Bérarde (Les Écrins massif, south eastern French Alps), constructed on an alluvial fan, was hit by a debris flood. The work presented here aims to describe as accurately as possible the drivers responsible for triggering the debris flood, reconstruct the chain of events leading to the catastrophe, characterize its occurrence probability, and discuss what makes this event of particular interest to the scientific community.

https://doi.org/10.5194/egusphere-2026-971
Preprint. Discussion started: 6 March 2026

During the event, 300 000 m^3 of material have been eroded from the Bonne Pierre branch of the Étançons catchment, from which about 200 000 m^3 have been deposited where the village stood. The river also changed course, moving from the NW to SE on the fan, ultimately scouring the older part of the village. No casualties were recorded but 66 buildings got partially to fully destroyed or buried.

This event was the result of a number of components and could be characterized as a *compound event*. On June 19, the meteorological synoptic led warm air charged with moisture from the Mediterranean sea towards the Alps, triggering heavy rain for the next 48 h, dropping up to 120 mm of water. The Étançons catchment (34 km^2), upstream of La Bérarde, was at the time, covered at 59 % by an unusually thick snowpack, fully isothermal and already melting at the start of the event. In total, we estimated that during these 48 h, 75 mm of equivalent water melted on average over the catchment. The glacier of Bonne Pierre with its long and shallow angle debris covered ablation area had a supra-glacial lake of about 100 000 m^3 with up to 150 000 m^3 of additional internal storage that drained during the event. Hydrological modeling suggests that rain and snowmelt were not sufficient to explain the observed discharge dynamic on the Vénéon river just 3.5 km downstream of La Bérarde. An analysis of seismic activities corroborates a high activity of the river coincidentally with the rapid rise of discharge with signals originating from Les Écrins massif.

While we found the supra-glacial lake to have filled and drained on a yearly basis since at least 2016 without being noticed, this rain-on-snow and GLOF event is one of a kind with respect to the period 1960 to today for which we have meteorological data. This event is already unique with a rain having a 7-year return period and a snowmelt having a 22-year return period, both simultaneously occurring in spring. While our analysis did not focus on specifically quantifying the role of climate change for this meteorological event, the literature tends to suggest that extreme precipitation events in this region are likely to have intensified and would continue to do so. It is also suggested that the seasonality of extreme precipitation may change, increasing the chances of analogous rain-on-snow events in a catchment with strong altitudinal gradient (*i.e.* with a capacity to store snow late in the season). The huge amount of sediments mobilized by the flood has also to be considered in relation with the glacier retreat and the concept of paraglacial adjustment. The context of rapid glacier retreat of a heavily debris covered glacier produces large volumes of sediments available for reworking by torrential processes.

In conclusion, neither the precipitation, the snowmelt, nor the GLOF separately can explain the magnitude of this event. It is the combination and concomitance of the three that saturated the hydrological system. Nevertheless, the water flow is not sufficient to explain why the village was destroyed. The susceptibility and connectivity of the sediments from source to deposition are other key aspects of this event. The location of the village, constrained by rugged terrain and a minimization of acceptable natural hazards, led the inhabitants to build on the alluvial fan, which remained ultimately a vulnerable place. All these elements taken together led us to associate this event with the paradigm of *compound event* as it provides a framework of analysis that may be complementary to established technics for identifying extreme events.

https://doi.org/10.5194/egusphere-2026-971
Preprint. Discussion started: 6 March 2026

Author contributions. SF with the core team CM, DC, NB and EP conceptualized, structured and wrote the manuscript. Everyone participated in the final version of the manuscript. This work builds on the hind-cast study led by AB commissioned by the French government (Blanc et al., 2024), and including the majority of co-authors for their specific expertise.

Competing interests. No competing interest to declare.

Acknowledgements. To this date, the village reconstruction is yet to be determined. Local residents have lost their homes and, for some, their livelihood. La Bérarde also being an iconic place of the Alps, we would like to express our compassion for the people who suffered irreparable losses due to this event. We would like to thanks local residents and mountain huts wardens for their testimony and sharing of pictures, videos and observations that helped to the reconstruction of the event chronology.

SF received support from the French Ministry of Ecological Transition through its PAPROG program (convention 261168), and works at CEN, a member of the Labex OSUG. MD has received funding from the European Research Council (ERC) under the European Union's Horizon 2020 research and innovation program (grant agreement no. 949516, IVORI). SG received support by the Centre National d'Etudes Spatiales and the ANR TOP project (grant no. ANR-20-CE32-0002) of the French Agence Nationale de la Recherche. FK and GJ acknowledge the financial support provided by the Direction Générale de la Prévention des Risques (DGPR) through the PAPROG (Action Plan for the Prevention of Glacial and Periglacial Risks) initiative and by the Centre National d'Etudes Spatiales (CNES) through the APR SHARE and SNOBELT projects. JB received support from the French ministry for Ecological Transition and Territorial Cohesion (Ministère de la Transition écologique et de la Cohésion des territoires) through its PAPROG program. PF received support from the French Ministry of Ecological Transition (convention 2104326877) and from IGE, a member of the Labex OSUG and Labex Tec21 (Investissements d'Avenir Grant No. ANR-10-LABX-0056 and ANR-11-LABX-0030). FdM received funding through the postdoctoral fellowship Labex ITTEM in 2022-2023.

https://doi.org/10.5194/egusphere-2026-971
Preprint. Discussion started: 6 March 2026

References

Aaron, J. and McDougall, S.: Rock avalanche mobility: The role of path material, Engineering Geology, 257, 105 126, https://doi.org/https://doi.org/10.1016/j.enggeo.2019.05.003, 2019.

Abril-Pla, O., Andreani, V., Carroll, C., Dong, L., Fonnesbeck, C. J., Kochurov, M., Kumar, R., Lao, J., Luhmann, C. C., Martin, O. A., et al.: PyMC: a modern, and comprehensive probabilistic programming framework in Python, PeerJ Computer Science, 9, e1516, https://doi.org/10.7717/peerj-cs.1516, 2023.

AghaKouchak, A., Chiang, F., Huning, L. S., Love, C. A., Mallakpour, I., Mazdiyasni, O., Moftakhari, H., Papalexiou, S. M., Ragno, E., and Sadegh, M.: Climate Extremes and Compound Hazards in a Warming World, Annual Review of Earth and Planetary Sciences, 48, 519–548, https://doi.org/10.1146/annurev-earth-071719-055228, 2020.

Ahmed, R.: From Vulnerability to Resilience: Community-Based Approaches in Glacial Lake Outburst Flood (GLOF) Risk Mitigation, Discover Sustainability, 6, 335, https://doi.org/10.1007/s43621-025-00967-7, 2025.

Archives Départementales de l'Isère: Etat Estimatif des fonds que la Rivière de veneon a Emporté aux habitants de la bérarde hameau de St Christophle Les 3 et 4 aout 1785, 1785.

Ballandras, S.: Contribution à l'étude de la torrentialité alpine: stratigraphies, morphodynamique, paléoenvironnements, Ph.D. thesis, Chambéry, http://www.theses.fr/1997CHAMLA01, 1997.

Ballantyne, C. K.: Paraglacial geomorphology, Quaternary Science Reviews, 21, 1935–2017, https://doi.org/https://doi.org/10.1016/S0277-3791(02)00005-7, 2002.

Baron, J., Primofiore, I., Klin, P., Vessia, G., and Laurenzano, G.: Investigation of topographic site effects using 3D waveform modelling: amplification, polarization and torsional motions in the case study of Arquata del Tronto (Italy), Bulletin of Earthquake Engineering, 20, 677–710, https://doi.org/10.1007/s10518-021-01270-2, 2022.

Barrou Dumont, Z., Gascoin, S., Inglada, J., Dietz, A., Köhler, J., Lafaysse, M., Monteiro, D., Carmagnola, C., Bayle, A., Dedieu, J.-P., Hagolle, O., and Choler, P.: Trends in the annual snow melt-out day over the French Alps and the Pyrenees from 38 years of high resolution satellite data (1986–2023), EGUsphere, 2024, 1–41, https://doi.org/10.5194/egusphere-2024-3505, 2024.

Baumann, F. and Kaiser, K. F.: The Multetta Debris Fan, Eastern Swiss Alps: A 500-year Debris Flow Chronology, Arctic, Antarctic, and Alpine Research, 31, 128–134, https://doi.org/10.1080/15230430.1999.12003290, 1999.

Beniston, M.: August 2005 intense rainfall event in Switzerland: Not necessarily an analog for strong convective events in a greenhouse climate, Geophysical Research Letters, 33, 2005GL025 573, https://doi.org/10.1029/2005GL025573, 2006.

Beniston, M. and Stoffel, M.: Rain-on-snow events, floods and climate change in the Alps: Events may increase with warming up to 4 °C and decrease thereafter, Science of The Total Environment, 571, 228–236, https://doi.org/10.1016/j.scitotenv.2016.07.146, 2016.

Benn, D. I., Bolch, T., Hands, K., Gulley, J., Luckman, A., Nicholson, L. I., Quincey, D., Thompson, S., Toumi, R., and Wiseman, S.: Response of Debris-Covered Glaciers in the Mount Everest Region to Recent Warming, and Implications for Outburst Flood Hazards, Earth-Science Reviews, 114, 156–174, https://doi.org/10.1016/j.earscirev.2012.03.008, 2012.

Berthier, E., Vincent, C., Magnússon, E., Gunnlaugsson, Á. Þ., Pitte, P., Le Meur, E., Masiokas, M., Ruiz, L., Pálsson, F., Belart, J. M. C., and Wagnon, P.: Glacier Topography and Elevation Changes Derived from Pléiades Sub-Meter Stereo Images, The Cryosphere, 8, 2275–2291, https://doi.org/10.5194/tc-8-2275-2014, 2014.

Blanc, A., Blanchet, J., and Creutin, J.-D.: Characterizing large-scale circulations driving extreme precipitation in the Northern French Alps, International Journal of Climatology, 42, 465–480, https://doi.org/10.1002/joc.7254, 2022a.

https://doi.org/10.5194/egusphere-2026-971
Preprint. Discussion started: 6 March 2026

Blanc, A., Blanchet, J., and Creutin, J.-D.: Past evolution of western Europe large-scale circulation and link to precipitation trend in the northern French Alps, Weather and Climate Dynamics, 3, 231–250, https://doi.org/10.5194/wcd-3-231-2022, 2022b.

Blanc, A., Misset, C., Mainieri, R., and Llamas, B.: Rétro-analyse de la crue du torrent des Etançons du 21 juin 2024, Tech. rep., ONF-RTM, https://hal.science/hal-04865442, 2024.

Blanchet, J., Creutin, J.-D., and Blanc, A.: Retreating winter and strengthening autumn Mediterranean influence on extreme precipitation in the Southwestern Alps over the last 60 years, Environmental Research Letters, 16, 034 056, https://doi.org/10.1088/1748-9326/abb5cd, 2021.

Bondesan, A. and Francese, R. G.: The climate-driven disaster of the Marmolada Glacier (Italy), Geomorphology, 431, 108 687, https://doi.org/10.1016/j.geomorph.2023.108687, 2023.

Bovis, M. J. and Jakob, M.: The role of debris supply conditions in predicting debris flow activity, Earth Surface Processes and Landforms, 24, 1039–1054, https://doi.org/https://doi.org/10.1002/(SICI)1096-9837(199910)24:11<1039::AID-ESP29>3.0.CO;2-U, 1999.

Bromirski, P. D., Duennebier, F. K., and Stephen, R. A.: Mid-ocean microseisms, Geochemistry, Geophysics, Geosystems, 6, 2005.

Brönnimann, S., Rajczak, J., Fischer, E. M., Raible, C. C., Rohrer, M., and Schär, C.: Changing seasonality of moderate and extreme precipitation events in the Alps, Natural Hazards and Earth System Sciences, 18, 2047–2056, https://doi.org/10.5194/nhess-18-2047-2018, 2018.

Burtin, A., Bollinger, L., Vergne, J., Cattin, R., and Nábělek, J. L.: Spectral analysis of seismic noise induced by rivers: A new tool to monitor spatiotemporal changes in stream hydrodynamics, Journal of Geophysical Research: Solid Earth, 113, https://doi.org/https://doi.org/10.1029/2007JB005034, 2008.

Cavalli, M., Trevisani, S., Comiti, F., and Marchi, L.: Geomorphometric assessment of spatial sediment connectivity in small Alpine catchments, Geomorphology, 188, 31–41, https://doi.org/10.1016/j.geomorph.2012.05.007, sediment sources, source-to-sink fluxes and sedimentary budgets, 2013.

Champeaux, J., Laurantin, O., Mercier, B., Mounier, F., Lassegues, P., and Tabary, P.: Quantitative precipitation estimations using rain gauges and radar networks: inventory and prospects at Meteo-France, in: WMO Joint Meeting of CGS Expert Team on Surface-based Remotely-sensed Observations and CIMO Expert Team on Operational Remote Sensing, vol. 5, pp. 1–11, 2011.

Champeaux, J.-L., Dupuy, P., Laurantin, O., Soulan, I., Tabary, P., and Soubeyroux, J.-M.: Les mesures de précipitations et l'estimation des lames d'eau à Météo-France : état de l'art et perspectives, La Houille Blanche, 95, 28–34, https://doi.org/10.1051/lhb/2009052, 2009.

Chiarle, M., Viani, C., Mortara, G., Deline, P., Tamburini, A., and Nigrelli, G.: Large glacier failures in the Italian Alps over the last 90 years, Geografia Fisica e Dinamica Quaternaria, pp. 19–40, https://doi.org/10.4461/GFDQ.2022.45.2., 2023.

Chmiel, M., Godano, M., Piantini, M., Brigode, P., Gimbert, F., Bakker, M., Courboulex, F., Ampuero, J.-P., Rivet, D., Sladen, A., et al.: Brief communication: Seismological analysis of flood dynamics and hydrologically triggered earthquake swarms associated with Storm Alex, Natural Hazards and Earth System Sciences, 22, 1541–1558, 2022.

Choi, S.-K., Park, J.-Y., Lee, D.-H., Lee, S.-R., Kim, Y.-T., and Kwon, T.-H.: Assessment of barrier location effect on debris flow based on smoothed particle hydrodynamics (SPH) simulation on 3D terrains, Landslides, 18, 217–234, https://doi.org/10.1007/s10346-020-01477-5, 2021.

Church, M. and Jakob, M.: What Is a Debris Flood?, Water Resources Research, 56, e2020WR027 144, https://doi.org/https://doi.org/10.1029/2020WR027144, e2020WR027144 2020WR027144, 2020.

Coles, S., Bawa, J., Trenner, L., and Dorazio, P.: An introduction to statistical modeling of extreme values, vol. 208, Springer, https://doi.org/10.1007/978-1-4471-3675-0, 2001.

https://doi.org/10.5194/egusphere-2026-971
Preprint. Discussion started: 6 March 2026

Colombo, N., Guyennon, N., Valt, M., Salerno, F., Godone, D., Cianfarra, P., Freppaz, M., Maugeri, M., Manara, V., Acquaotta, F., Petrangeli, A. B., and Romano, E.: Unprecedented snow-drought conditions in the Italian Alps during the early 2020s, Environmental Research Letters, 18, 074 014, https://doi.org/10.1088/1748-9326/acdb88, 2023.

Cook, K. L., Andermann, C., Gimbert, F., Adhikari, B. R., and Hovius, N.: Glacial Lake Outburst Floods as Drivers of Fluvial Erosion in the Himalaya, Science, 362, 53–57, https://doi.org/10.1126/science.aat4981, 2018.

Cook, K. L., Rekapalli, R., Dietze, M., Pilz, M., Cesca, S., Rao, N. P., Srinagesh, D., Paul, H., Metz, M., Mandal, P., et al.: Detection and potential early warning of catastrophic flow events with regional seismic networks, Science, 374, 87–92, 2021.

Coron, L., Thirel, G., Delaigue, O., Perrin, C., and Andréassian, V.: The Suite of Lumped GR Hydrological Models in an R package, Environmental Modelling and Software, 94, 166–171, https://doi.org/10.1016/j.envsoft.2017.05.002, 2017.

Coron, L., Delaigue, O., Thirel, G., Dorchies, D., Perrin, C., and Michel, C.: airGR: Suite of GR Hydrological Models for Precipitation-Runoff Modelling, https://doi.org/10.15454/EX11NA, r package version 1.7.6.9000, 2023.

Curry, A. M., Cleasby, V., and Zukowskyj, P.: Paraglacial response of steep, sediment-mantled slopes to post-'Little Ice Age' glacier recession in the central Swiss Alps, Journal of Quaternary Science, 21, 211–225, https://doi.org/https://doi.org/10.1002/jqs.954, 2006.

Cusicanqui, D.: Cusicand/Lidarhd_ign_downloader: Lidar_ign_downloader v1.0, Zenodo, https://doi.org/10.5281/zenodo.10697627, 2024.

Cusicanqui, D., Bodin, X., Duvillard, P.-A., Schoeneich, P., Revil, A., Assier, A., Berthet, J., Peyron, M., Roudnitska, S., and Rabatel, A.: Glacier, permafrost and thermokarst interactions in Alpine terrain: Insights from seven decades of reconstructed dynamics of the Chauvet glacial and periglacial system (Southern French Alps), Earth Surface Processes and Landforms, 48, 2595–2612, https://doi.org/10.1002/esp.5650, 2023.

de Beaumont, E.: « Faits pour servir à l'histoire des Montagnes de l'Oisans », in Mémoires pour servir à une description géologique de la France, Levrault, 1834.

Deschamps-Berger, C., Gascoin, S., Berthier, E., Deems, J., Gutmann, E., Dehecq, A., Shean, D., and Dumont, M.: Snow Depth Mapping from Stereo Satellite Imagery in Mountainous Terrain: Evaluation Using Airborne Laser-Scanning Data, The Cryosphere, 14, 2925–2940, https://doi.org/10.5194/tc-14-2925-2020, 2020.

Dumont, M., Monteiro, D., Filhol, S., Gascoin, S., Marty, C., Hagenmuller, P., Morin, S., Choler, P., and Thuiller, W.: The European Alps in a changing climate: physical trends and impacts, Comptes Rendus. Géoscience, 357, 25–42, https://doi.org/10.5802/crgeos.288, 2025.

Durand, Y., Giraud, G., Laternser, M., Etchevers, P., Mérindol, L., and Lesaffre, B.: Reanalysis of 47 Years of Climate in the French Alps (1958–2005): Climatology and Trends for Snow Cover, Journal of Applied Meteorology and Climatology, 48, 2487 – 2512, https://doi.org/10.1175/2009JAMC1810.1, 2009.

D'Agostino, V., Cerato, M., and Coali, R.: Extreme events of sediment transport in the eastern Trentino torrents, Atti del Convegno Interpraevent, 1, 377–386, 1996.

Ekström, G. and Stark, C. P.: Simple Scaling of Catastrophic Landslide Dynamics, Science, 339, 1416–1419, https://doi.org/10.1126/science.1232887, 2013.

Emmer, A., Harrison, S., Mergili, M., Allen, S., Frey, H., and Huggel, C.: 70 years of Lake Evolution and Glacial Lake Outburst Floods in the Cordillera Blanca (Peru) and Implications for the Future, Geomorphology, 365, 107 178, https://doi.org/10.1016/j.geomorph.2020.107178, 2020.

Epos-France: Epos-France Broad-band network (RLBP), https://doi.org/10.15778/RESIF.FR, artwork Size: Approximately 200 active stations, 10 GB/day., 33TB in 2025, 1962.

https://doi.org/10.5194/egusphere-2026-971
Preprint. Discussion started: 6 March 2026

Evans, S. G., Bishop, N. F., Fidel Smoll, L., Valderrama Murillo, P., Delaney, K. B., and Oliver-Smith, A.: A re-examination of the mechanism and human impact of catastrophic mass flows originating on Nevado Huascarán, Cordillera Blanca, Peru in 1962 and 1970, Engineering Geology, 108, 96–118, https://doi.org/10.1016/j.enggeo.2009.06.020, 2009.

Garavaglia, F., Le Lay, M., Gottardi, F., Garçon, R., Gailhard, J., Paquet, E., and Mathevet, T.: Impact of model structure on flow simulation and hydrological realism: from a lumped to a semi-distributed approach, Hydrology and Earth System Sciences, 21, 3937–3952, https://doi.org/10.5194/hess-21-3937-2017, 2017.

Gardent, M.: Inventaire et retrait des glaciers dans les alpes françaises depuis la fin du Petit Age Glaciaire, Theses, Université de Grenoble, https://theses.hal.science/tel-01062226, 2014.

Gascoin, S., Soubeyroux, J.-M., Karbou, F., Thirel, G., Sourp, L., Lejeune, Y., Gouttevin, I., and and, S. M.: Évolution du manteau neigeux pendant la sécheresse de 2022 en France, LHB, 110, 2314 174, https://doi.org/10.1080/27678490.2024.2314174, 2024.

Gertsch, E.: Geschiebelieferung alpiner Wildbachsysteme bei Grossereignissen: Ereignisanayse und Entwicklung eines Abschätzverfahrens, Ph.D. thesis, Verlag nicht ermittelbar, 2009.

Gibson, S., Moura, L. Z., Ackerman, C., Ortman, N., Amorim, R., Floyd, I., Eom, M., Creech, C., and Sánchez, A.: Prototype Scale Evaluation of Non-Newtonian Algorithms in HEC-RAS: Mud and Debris Flow Case Studies of Santa Barbara and Brumadinho, Geosciences, 12, https://doi.org/10.3390/geosciences12030134, 2022.

Gimbert, F., Tsai, V. C., and Lamb, M. P.: A physical model for seismic noise generation by turbulent flow in rivers, Journal of Geophysical Research: Earth Surface, 119, 2209–2238, https://doi.org/10.1002/2014JF003201, 2014.

Ginesta, M., Yiou, P., Messori, G., and Faranda, D.: A methodology for attributing severe extratropical cyclones to climate change based on reanalysis data: the case study of storm Alex 2020, Climate Dynamics, 61, 229–253, https://doi.org/10.1007/s00382-022-06565-x, 2023.

Goodling, P. J., Lekic, V., and Prestegaard, K.: Seismic signature of turbulence during the 2017 Oroville Dam spillway erosion crisis, Earth Surface Dynamics, 6, 351–367, https://doi.org/10.5194/esurf-6-351-2018, 2018.

Goutal, N., Lacombe, J., Zaoui, F., and El-Kadi-Abderrezzak, K.: MASCARET: a 1-D open-source software for flow hydrodynamic and water quality in open channel networks, in: River flow, vol. 1, pp. 1169–1174, Taylor & Francis Group London, UK, 2012.

Gras, S.: Considérations sur les anciens lits de déjection des torrents des Alpes et sur leur liaison avec le phénomène erratique, Bulletin de la Société de Statistique des Sciences naturelles et des Arts industriels du département de l'Isère, Tome IV, 421–441, 1847.

Gulley, J. D., Benn, D. I., Müller, D., and Luckman, A.: A Cut-and-Closure Origin for Englacial Conduits in Uncrevassed Regions of Polythermal Glaciers, Journal of Glaciology, 55, 66–80, https://doi.org/10.3189/002214309788608930, 2009.

Haeberli, W., Schaub, Y., and Huggel, C.: Increasing risks related to landslides from degrading permafrost into new lakes in de-glaciating mountain ranges, Geomorphology, 293, 405–417, https://doi.org/10.1016/j.geomorph.2016.02.009, permafrost and periglacial research from coasts to mountains, 2017.

Hazeleger, W., van den Hurk, B. J. J. M., Min, E., van Oldenborgh, G. J., Petersen, A. C., Stainforth, D. A., Vasileiadou, E., and Smith, L. A.: Tales of future weather, Nature Climate Change, 5, 107–113, https://doi.org/10.1038/nclimate2450, 2015.

Hersbach, H., Bell, B., Berrisford, P., Hirahara, S., Horányi, A., Muñoz-Sabater, J., Nicolas, J., Peubey, C., Radu, R., Schepers, D., Simmons, A., Soci, C., Abdalla, S., Abellan, X., Balsamo, G., Bechtold, P., Biavati, G., Bidlot, J., Bonavita, M., De Chiara, G., Dahlgren, P., Dee, D., Diamantakis, M., Dragani, R., Flemming, J., Forbes, R., Fuentes, M., Geer, A., Haimberger, L., Healy, S., Hogan, R. J., Hólm, E., Janisková, M., Keeley, S., Laloyaux, P., Lopez, P., Lupu, C., Radnoti, G., de Rosnay, P., Rozum, I., Vamborg, F., Villaume, S., and Thépaut, J.-N.: The ERA5 global reanalysis, Quarterly Journal of the Royal Meteorological Society, 146, 1999–2049, https://doi.org/10.1002/qj.3803, 2020.

https://doi.org/10.5194/egusphere-2026-971
Preprint. Discussion started: 6 March 2026

Hervouet, J. and Haren, L. V.: Floodplain processes, chap. Recent advances in numerical methods for fluid flow, John Wiley, 1996.

Huggel, C., Haeberli, W., Kääb, A., Bieri, D., and Richardson, S.: An assessment procedure for glacial hazards in the Swiss Alps, Canadian Geotechnical Journal, 41, 1068–1083, https://doi.org/10.1139/t04-053, 2004.

Hungr, O., Morgan, G. C., and Kellerhals, R.: Quantitative analysis of debris torrent hazards for design of remedial measures, Canadian Geotechnical Journal, 21, 663–677, https://doi.org/10.1139/t84-073, 1984.

Imperatori, W. and Mai, P.: The role of topography and lateral velocity heterogeneities on near-source scattering and ground-motion variability, Geophysical Journal International, 202, 2163–2181, https://doi.org/10.1093/gji/ggv281, _eprint: https://academic.oup.com/gji/article-pdf/202/3/2163/1696573/ggv281.pdf, 2015.

IPCC-AR6: Weather and Climate Extreme Events in a Changing Climate, p. 1513–1766, Cambridge University Press, 2023.

Jacquemart, M., Weber, S., Chiarle, M., Chmiel, M., Cicoira, A., Corona, C., Eckert, N., Gaume, J., Giacona, F., Hirschberg, J., Kaitna, R., Magnin, F., Mayer, S., Moos, C., van Herwijnen, A., and Stoffel, M.: Detecting the impact of climate change on alpine mass movements in observational records from the European Alps, Earth-Science Reviews, 258, 104 886, https://doi.org/10.1016/j.earscirev.2024.104886, 2024.

Kääb, A., Reynolds, J. M., and Haeberli, W.: Glacier and Permafrost Hazards in High Mountains, pp. 225–234, Springer Netherlands, Dordrecht, https://doi.org/10.1007/1-4020-3508-X_23, 2005.

Kappes, M. S., Keiler, M., von Elverfeldt, K., and Glade, T.: Challenges of analyzing multi-hazard risk: a review, Natural Hazards, 64, 1925–1958, https://doi.org/10.1007/s11069-012-0294-2, 2012.

Keiler, M., Knight, J., and Harrison, S.: Climate change and geomorphological hazards in the eastern European Alps, Philosophical Transactions of the Royal Society A: Mathematical, Physical and Engineering Sciences, 368, 2461–2479, https://doi.org/10.1098/rsta.2010.0047, 2010.

Kreitz, M.: Les gouttes froides de mai 2024, La Météorologie, pp. 74–79, https://doi.org/10.37053/lameteorologie-2024-0062, 2024.

Krischer, L., Megies, T., Barsch, R., Beyreuther, M., Lecocq, T., Caudron, C., and Wassermann, J.: ObsPy: A bridge for seismology into the scientific Python ecosystem, Computational Science & Discovery, 8, 014 003, https://doi.org/10.1088/1749-4699/8/1/014003, 2015.

Kuhn, M. and Olefs, M.: Elevation-Dependent Climate Change in the European Alps, https://doi.org/10.1093/acrefore/9780190228620.013.762, 2020.

Kääb, A. and and, W. H.: Evolution of a High-Mountain Thermokarst Lake in the Swiss Alps, Arctic, Antarctic, and Alpine Research, 33, 385–390, https://doi.org/10.1080/15230430.2001.12003445, 2001.

Lanzoni, S., Gregoretti, C., and Stancanelli, L. M.: Coarse-grained debris flow dynamics on erodible beds, Journal of Geophysical Research: Earth Surface, 122, 592–614, https://doi.org/https://doi.org/10.1002/2016JF004046, 2017.

Lavers, D. A., Simmons, A., Vamborg, F., and Rodwell, M. J.: An evaluation of ERA5 precipitation for climate monitoring, Quarterly Journal of the Royal Meteorological Society, 148, 3152–3165, https://doi.org/10.1002/qj.4351, 2022.

Lavorel, R. and Champon, M.: Un an après la destruction de leur village, les habitants veulent rentrer chez eux, Reporterre, available at: https://reporterre.net/Un-an-apres-la-destruction-de-La-Berarde-les-habitants-veulent-rentrer (Accessed : January 6th, 2026).

Le Roux, E., Evin, G., Eckert, N., Blanchet, J., and Morin, S.: Elevation-dependent trends in extreme snowfall in the French Alps from 1959 to 2019, The Cryosphere, 15, 4335–4356, https://doi.org/10.5194/tc-15-4335-2021, 2021.

Le Roy, M., Deline, P., Carcaillet, J., Schimmelpfennig, I., and Ermini, M.: 10Be exposure dating of the timing of Neoglacial glacier advances in the Ecrins-Pelvoux massif, southern French Alps, Quaternary Science Reviews, 178, 118–138, https://doi.org/https://doi.org/10.1016/j.quascirev.2017.10.010, 2017.

https://doi.org/10.5194/egusphere-2026-971
Preprint. Discussion started: 6 March 2026

Legay, A., Magnin, F., and Ravanel, L.: Rock temperature prior to failure: Analysis of 209 rockfall events in the Mont Blanc massif (Western European Alps), Permafrost and Periglacial Processes, 32, 520–536, https://doi.org/10.1002/ppp.2110, 2021.

Liébault, F., Melun, G., Piton, G., Chapuis, M., Passy, P., and Tacon, S.: Channel change during catastrophic flood: Example of Storm Alex in the Vésubie and Roya valleys, Geomorphology, 446, 109 008, https://doi.org/https://doi.org/10.1016/j.geomorph.2023.109008, 2024.

Lu, Y., Stehly, L., Paul, A., and Group, A. W.: High-resolution surface wave tomography of the European crust and uppermost mantle from ambient seismic noise, Geophysical Journal International, 214, 1136–1150, 2018.

Lützow, N., Veh, G., and Korup, O.: A Global Database of Historic Glacier Lake Outburst Floods, Earth System Science Data, 15, 2983–3000, https://doi.org/10.5194/essd-15-2983-2023, 2023.

Magnin, F., Ravanel, L., Bodin, X., Deline, P., Malet, E., Krysiecki, J.-M., and Schoeneich, P.: Main Results of Permafrost Monitoring in the French Alps through the PermaFrance Network over the Period 2010–2022, Permafrost and Periglacial Processes, 35, 3–23, https://doi.org/10.1002/ppp.2209, 2024.

Mainieri, R., Blanc, A., Astrade, L., Baratier, A., Berthet, J., Deline, P., Le Roy, M., Misset, C., De Montety, F., Robert, Y., and Schoeneich, P.: Les aspects géomorphologiques de la crue torrentielle du torrent des Étançons à la Bérarde du 21 juin 2024, Géomorphologie : relief, processus, environnement, 31, https://doi.org/10.4000/14ipc, 2025.

Malgwi, M. B., Fuchs, S., and Keiler, M.: A Generic Physical Vulnerability Model for Floods: Review and Concept for Data-Scarce Regions, Natural Hazards and Earth System Sciences, 20, 2067–2090, https://doi.org/10.5194/nhess-20-2067-2020, 2020.

Mani, P., Allen, S., Evans, S. G., Kargel, J. S., Mergili, M., Petrakov, D., and Stoffel, M.: Geomorphic Process Chains in High-Mountain Regions—A Review and Classification Approach for Natural Hazards Assessment, Reviews of Geophysics, 61, e2022RG000 791, https://doi.org/https://doi.org/10.1029/2022RG000791, e2022RG000791 2022RG000791, 2023.

Marchi, L. and D'Agostino, V.: Estimation of debris-flow magnitude in the Eastern Italian Alps, Earth Surface Processes and Landforms, 29, 207–220, https://doi.org/10.1002/esp.1027, 2004.

Marchi, L., Brunetti, M. T., Cavalli, M., and Crema, S.: Debris-flow volumes in northeastern Italy: Relationship with drainage area and size probability, Earth Surface Processes and Landforms, 44, 933–943, https://doi.org/10.1002/esp.4546, 2019.

Martini, M., D'Agostino, V., and Piton, G.: Geomorphic activity and related large wood recruitment during debris flows and debris Floods: Storm Alex in the Vésubie valley (France), CATENA, 257, 109 180, https://doi.org/10.1016/j.catena.2025.109180, 2025.

Masson, V., Le Moigne, P., Martin, E., Faroux, S., Alias, A., Alkama, R., Belamari, S., Barbu, A., Boone, A., Bouyssel, F., Brousseau, P., Brun, E., Calvet, J.-C., Carrer, D., Decharme, B., Delire, C., Donier, S., Essaouini, K., Gibelin, A.-L., Giordani, H., Habets, F., Jidane, M., Kerdraon, G., Kourzeneva, E., Lafaysse, M., Lafont, S., Lebeaupin Brossier, C., Lemonsu, A., Mahfouf, J.-F., Marguinaud, P., Mokhtari, M., Morin, S., Pigeon, G., Salgado, R., Seity, Y., Taillefer, F., Tanguy, G., Tulet, P., Vincendon, B., Vionnet, V., and Voldoire, A.: The SURFEXv7.2 land and ocean surface platform for coupled or offline simulation of earth surface variables and fluxes, Geoscientific Model Development, 6, 929–960, https://doi.org/10.5194/gmd-6-929-2013, 2013.

Mergili, M., Pudasaini, S. P., Emmer, A., Fischer, J.-T., Cochachin, A., and Frey, H.: Reconstruction of the 1941 GLOF Process Chain at Lake Palcacocha (Cordillera Blanca, Peru), Hydrology and Earth System Sciences, 24, 93–114, https://doi.org/10.5194/hess-24-93-2020, 2020.

Mizuyama, T., Kobashi, S., and Ou, G.: Prediction of debris flow peak discharge, in: Internationales symposion: Interpraevent, pp. 99–108, 1992.

https://doi.org/10.5194/egusphere-2026-971
Preprint. Discussion started: 6 March 2026

Moezzi, M., Janda, K. B., and Rotmann, S.: Using stories, narratives, and storytelling in energy and climate change research, Energy Research & Social Science, 31, 1–10, https://doi.org/10.1016/j.erss.2017.06.034, narratives and Storytelling in Energy and Climate Change Research, 2017.

Monteiro, D. and Morin, S.: Multi-decadal analysis of past winter temperature, precipitation and snow cover data in the European Alps from reanalyses, climate models and observational datasets, The Cryosphere, 17, 3617–3660, https://doi.org/10.5194/tc-17-3617-2023, 2023.

Mool, P., Wangda, D., Bajracharya, S. R., Joshi, S. P., Kunzang, K., and Gurung, D. R.: Inventory of Glaciers, Glacial Lakes and Glacial Lake Outburst Floods: Monitoring and Early Warning Systems in the Hindu Kush-Himalayan Region - Bhutan, International Centre for Integrated Mountain Development (ICIMOD), https://doi.org/10.53055/icimod.373, 2001.

Morel, M., Piton, G., Kuss, D., Evin, G., and Le Bouteiller, C.: Statistical modeling of sediment supply in torrent catchments of the northern French Alps, Natural Hazards and Earth System Sciences, 23, 1769–1787, https://doi.org/10.5194/nhess-23-1769-2023, 2023.

Noetzli, J., Isaksen, K., Barnett, J., Christiansen, H. H., Delaloye, R., Etzelmüller, B., Farinotti, D., Gallemann, T., Guglielmin, M., Hauck, C., Hilbich, C., Hoelzle, M., Lambiel, C., Magnin, F., Oliva, M., Paro, L., Pogliotti, P., Riedl, C., Schoeneich, P., Valt, M., Vieli, A., and Phillips, M.: Enhanced warming of European mountain permafrost in the early 21st century, Nature Communications, 15, 10 508, https://doi.org/10.1038/s41467-024-54831-9, 2024.

Nuth, C. and Kääb, A.: Co-Registration and Bias Corrections of Satellite Elevation Data Sets for Quantifying Glacier Thickness Change, The Cryosphere, 5, 271–290, https://doi.org/10.5194/tc-5-271-2011, 2011.

Ogier, C., Fischer, M., Werder, M. A., Huss, M., Hupfer, M., Jacquemart, M., Gagliardini, O., Gilbert, A., Hösli, L., Thibert, E., Vincent, C., and Farinotti, D.: Definition, Formation and Rupture Mechanisms of Water Pockets in Alpine Glaciers: Insights from an Updated Inventory for the Swiss Alps, Journal of Glaciology, 71, e82, https://doi.org/10.1017/jog.2025.43, 2025.

Ogier, C., Werder, M. A., Gagliardini, O., Santin, I., Moser, R., Hugonnet, R., Blanc, A., and Farinotti, D.: Potential glacier contributions to the 2024 La Bérarde flood, EGUsphere, 2026, 1–26, https://doi.org/10.5194/egusphere-2026-466, 2026.

ONF-RTM: Données relatives à la Restauration des Terrains de Montagne (RTM), BDRTM, data retreived from https://geo-onf.opendata.arcgis.com/maps/760c436f2736431fb0cae21c14c7414b/about, 2025.

Paquet, E. and and, M.-T. L.: Retour d'expérience et perspectives d'exploitation des Nivomètres à Rayonnement Cosmique d'EDF, La Houille Blanche, 92, 113–119, https://doi.org/10.1051/lhb:200602015, 2006.

Peleg, N., Koukoula, M., and Marra, F.: A 2°C warming can double the frequency of extreme summer downpours in the Alps, npj Climate and Atmospheric Science, 8, 216, https://doi.org/10.1038/s41612-025-01081-1, 2025.

Perrin, C., Michel, C., and Andréassian, V.: Improvement of a parsimonious model for streamflow simulation, Journal of Hydrology, 279, 275–289, https://doi.org/10.1016/S0022-1694(03)00225-7, 2003.

Pescaroli, G. and Alexander, D.: Understanding Compound, Interconnected, Interacting, and Cascading Risks: A Holistic Framework, Risk Analysis, 38, 2245–2257, https://doi.org/10.1111/risa.13128, 2018.

Pörtner, H.-O., Roberts, D. C., Masson-Delmotte, V., Zhai, P., Tignor, M., Poloczanska, E., Weyer, N., et al.: The ocean and cryosphere in a changing climate, IPCC special report on the ocean and cryosphere in a changing climate, 1155, 10–1017, 2019.

Rabatel, A. and Klee, X.: Mise à jour de l'inventaire des glaciers des Alpes françaises à partir de données Sentinel-2 de 2022, Rapport d'action, Plan d'Actions pour la Prévention des Risques d'Origine Glaciaire et périglaciaire, France, rapport d'action dans le cadre du Plan d'Actions pour la Prévention des Risques d'Origine Glaciaire et périglaciaire, 2023a.

https://doi.org/10.5194/egusphere-2026-971
Preprint. Discussion started: 6 March 2026

Rabatel, A. and Klee, X.: Mise à jour de l'inventaire des glaciers des Alpes françaises à partir de données Sentinel-2 de 2022. Rapport d'action du Plan d'Actions pour la Prévention des Risques d'Origine Glaciaire et périglaciaire (PAPROG), Tech. rep., Institut des Geosciences de l'Environement, 2023b.

Reinthaler, J. and Paul, F.: Reconstructed glacier area and volume changes in the European Alps since the Little Ice Age, The Cryosphere, 19, 753–767, https://doi.org/10.5194/tc-19-753-2025, 2025.

Rickenmann, D.: Empirical Relationships for Debris Flows, Natural Hazards, 19, 47–77, https://doi.org/10.1023/A:1008064220727, 1999.

Rickenmann, D. and Koschni, A.: Sediment loads due to fluvial transport and debris flows during the 2005 flood events in Switzerland, Hydrological Processes, 24, 993–1007, https://doi.org/10.1002/hyp.7536, 2010.

Rickenmann, D. and Zimmermann, M.: The 1987 debris flows in Switzerland: documentation and analysis, Geomorphology, 8, 175–189, https://doi.org/10.1016/0169-555X(93)90036-2, 1993.

Sattar, A., Cook, K. L., Rai, S. K., Berthier, E., Allen, S., Rinzin, S., de Vries, M. V. W., Haeberli, W., Kushwaha, P., Shugar, D. H., Emmer, A., Haritashya, U. K., Frey, H., Rao, P., Gurudin, K. S. K., Rai, P., Rajak, R., Hossain, F., Huggel, C., Mergili, M., Azam, M. F., Gascoin, S., Carrivick, J. L., Bell, L. E., Ranjan, R. K., Rashid, I., Kulkarni, A. V., Petley, D., Schwanghart, W., Watson, C. S., Islam, N., Gupta, M. D., Lane, S. N., and Bhat, S. Y.: The Sikkim flood of October 2023: Drivers, causes, and impacts of a multihazard cascade, Science, 387, eads2659, https://doi.org/10.1126/science.ads2659, 2025.

Sauquet, E., Evin, G., Siauve, S., Aissat, R., Arnaud, P., Bérel, M., Bonneau, J., Branger, F., Caballero, Y., Colléoni, F., Ducharne, A., Gailhard, J., Habets, F., Hendrickx, F., Héraut, L., Hingray, B., Huang, P., Jaouen, T., Jeantet, A., Lanini, S., Le Lay, M., Magand, C., Mimeau, L., Monteil, C., Munier, S., Perrin, C., Robelin, O., Rousset, F., Soubeyroux, J.-M., Strohmenger, L., Thirel, G., Tocquer, F., Tramblay, Y., Vergnes, J.-P., and Vidal, J.-P.: A large transient multi-scenario multi-model ensemble of future streamflow and groundwater projections in France, EGUsphere, 2025, 1–41, https://doi.org/10.5194/egusphere-2025-1788, 2025.

Scherrer, S. C., Fischer, E. M., Posselt, R., Liniger, M. A., Croci-Maspoli, M., and Knutti, R.: Emerging trends in heavy precipitation and hot temperature extremes in Switzerland, Journal of Geophysical Research: Atmospheres, 121, 2626–2637, https://doi.org/10.1002/2015JD024634, 2016.

Schmandt, B., Aster, R. C., Scherler, D., Tsai, V. C., and Karlstrom, K.: Multiple fluvial processes detected by riverside seismic and infrasound monitoring of a controlled flood in the Grand Canyon, Geophysical Research Letters, 40, 4858–4863, https://doi.org/10.1002/grl.50953, 2013.

Schneuwly-Bollschweiler, M. and Stoffel, M.: Hydrometeorological triggers of periglacial debris flows in the Zermatt valley (Switzerland) since 1864, Journal of Geophysical Research: Earth Surface, 117, https://doi.org/10.1029/2011JF002262, 2012.

Schraml, K., Thomschitz, B., McArdell, B. W., Graf, C., and Kaitna, R.: Modeling debris-flow runout patterns on two alpine fans with different dynamic simulation models, Natural Hazards and Earth System Sciences, 15, 1483–1492, https://doi.org/10.5194/nhess-15-1483-2015, 2015.

Shugar, D. H., Jacquemart, M., Shean, D., Bhushan, S., Upadhyay, K., Sattar, A., Schwanghart, W., McBride, S., de Vries, M. V. W., Mergili, M., Emmer, A., Deschamps-Berger, C., McDonnell, M., Bhambri, R., Allen, S., Berthier, E., Carrivick, J. L., Clague, J. J., Dokukin, M., Dunning, S. A., Frey, H., Gascoin, S., Haritashya, U. K., Huggel, C., Kääb, A., Kargel, J. S., Kavanaugh, J. L., Lacroix, P., Petley, D., Rupper, S., Azam, M. F., Cook, S. J., Dimri, A. P., Eriksson, M., Farinotti, D., Fiddes, J., Gnyawali, K. R., Harrison, S., Jha, M., Koppes, M., Kumar, A., Leinss, S., Majeed, U., Mal, S., Muhuri, A., Noetzli, J., Paul, F., Rashid, I., Sain, K., Steiner, J., Ugalde, F., Watson, C. S., and Westoby, M. J.: A massive rock and ice avalanche caused the 2021 disaster at Chamoli, Indian Himalaya, Science, 373, 300–306, https://doi.org/10.1126/science.abh4455, 2021.

https://doi.org/10.5194/egusphere-2026-971
Preprint. Discussion started: 6 March 2026

Soergel, D., Pedersen, H. A., Stehly, L., Margerin, L., Paul, A., and Group, A. W.: Coda-Q in the 2.5–20 s period band from seismic noise: application to the greater Alpine area, Geophysical Journal International, 220, 202–217, 2020.

Sommer, C., Malz, P., Seehaus, T. C., Lippl, S., Zemp, M., and Braun, M. H.: Rapid glacier retreat and downwasting throughout the European Alps in the early 21st century, Nature Communications, 11, 3209, https://doi.org/10.1038/s41467-020-16818-0, 2020.

Stoffel, M. and Beniston, M.: On the incidence of debris flows from the early Little Ice Age to a future greenhouse climate: A case study from the Swiss Alps, Geophysical Research Letters, 33, 2006GL026 805, https://doi.org/10.1029/2006GL026805, 2006.

Stoffel, M. and Corona, C.: Future winters glimpsed in the Alps, Nature Geoscience, 11, 458–460, https://doi.org/10.1038/s41561-018-0177-6, 2018.

Stoffel, M., Lièvre, I., Conus, D., Grichting, M. A., Raetzo, H., Gärtner, H. W., and Monbaron, M.: 400 Years of Debris-Flow Activity and Triggering Weather Conditions: Ritigraben, Valais, Switzerland, Arctic, Antarctic, and Alpine Research, 37, 387–395, https://doi.org/10.1657/1523-0430(2005)037[0387:YODAAT]2.0.CO;2, 2005.

Stoffel, M., Allen, S. K., Ballesteros-Cánovas, J. A., Jakob, M., and Oakley, N.: Climate Change Effects on Debris Flows, pp. 273–308, Springer International Publishing, Cham, https://doi.org/10.1007/978-3-031-48691-3_10, 2024.

Takahashi, T.: Mechanical Characteristics of Debris Flow, Journal of the Hydraulics Division, 104, 1153–1169, https://doi.org/10.1061/JYCEAJ.0005046, 1978.

Thibert, E., Dkengne Sielenou, P., Vionnet, V., Eckert, N., and Vincent, C.: Causes of Glacier Melt Extremes in the Alps Since 1949, Geophysical Research Letters, 45, 817–825, https://doi.org/10.1002/2017GL076333, 2018.

Tomasetto, L., Boué, P., Ardhuin, F., Stutzman, E., Xu, Z., De Plaen, R., and Stehly, L.: WMSAN Python Package: From Oceanic Forcing to Synthetic Cross-correlations of Microseismic Noise, EathArXiv, 2024.

Torricelli, E.: Opera geometrica, In-quarto, 1644.

Tramblay, Y., Arnaud, P., Artigue, G., Lang, M., Paquet, E., Neppel, L., and Sauquet, E.: Changes in Mediterranean flood processes and seasonality, Hydrology and Earth System Sciences, 27, 2973–2987, https://doi.org/10.5194/hess-27-2973-2023, 2023.

Tramblay, Y., Thirel, G., Strohmenger, L., Evin, G., Corre, L., Heraut, L., and Sauquet, E.: Evolution of flood generating processes under climate change in France, Hydrology and Earth System Sciences, 29, 7023–7039, https://doi.org/10.5194/hess-29-7023-2025, 2025.

Tsai, V. C., Minchew, B., Lamb, M. P., and Ampuero, J.-P.: A physical model for seismic noise generation from sediment transport in rivers, Geophysical Research Letters, 39, https://doi.org/10.1029/2011GL050255, 2012.

Turkington, T., Remaître, A., Ettema, J., Hussin, H., and van Westen, C.: Assessing debris flow activity in a changing climate, Climatic Change, 137, 293–305, https://doi.org/10.1007/s10584-016-1657-6, 2016.

UNESCO: Convention Concerning the Protection of the World Cultural and Natural Heritage, 1972.

Valéry, A., Andréassian, V., and Perrin, C.: 'As simple as possible but not simpler': What is useful in a temperature-based snow-accounting routine? Part 2 – Sensitivity analysis of the Cemaneige snow accounting routine on 380 catchments, Journal of Hydrology, 517, 1176–1187, https://doi.org/10.1016/j.jhydrol.2014.04.058, 2014.

Vericat, D., Wheaton, J. M., and Brasington, J.: Revisiting the Morphological Approach, chap. 5, pp. 121–158, John Wiley & Sons, Ltd, https://doi.org/10.1002/9781118971437.ch5, 2017.

Vernay, M., Lafaysse, M., Monteiro, D., Hagenmuller, P., Nheili, R., Samacoïts, R., Verfaillie, D., and Morin, S.: The S2M meteorological and snow cover reanalysis over the French mountainous areas: description and evaluation (1958–2021), Earth System Science Data, 14, 1707–1733, https://doi.org/10.5194/essd-14-1707-2022, 2022.

https://doi.org/10.5194/egusphere-2026-971
Preprint. Discussion started: 6 March 2026

Vincent, C., Garambois, S., Thibert, E., Lefèbvre, E., Le Meur, E., and Six, D.: Origin of the outburst flood from Glacier de Tête Rousse in 1892 (Mont Blanc area, France), Journal of Glaciology, 56, 688–698, https://doi.org/10.3189/002214310793146188, 2010.

Vionnet, V., Brun, E., Morin, S., Boone, A., Faroux, S., Le Moigne, P., Martin, E., and Willemet, J.-M.: The detailed snowpack scheme Crocus and its implementation in SURFEX v7.2, Geoscientific Model Development, 5, 773–791, https://doi.org/10.5194/gmd-5-773-2012, 2012.

Voellmy, A.: Über die Zerstörungskraft von Lawinen, Schweizerische Bauzeitung, Sonderdruck aus dem 73, Jahrgang, pp. 1–25, 1955.

Welfringer, T., Liébault, F., Laigle, D., and Kuss, D.: Sediment yields during a catastrophic flood: Example of the Vésubie tributaries during Storm Alex, Géomorphologie : relief, processus, environnement, 31, https://doi.org/10.4000/14nmk, 2025.

Wilhelm, B., Rapuc, W., Amann, B., Anselmetti, F. S., Arnaud, F., Blanchet, J., Brauer, A., Czymzik, M., Giguet-Covex, C., Gilli, A., Glur, L., Grosjean, M., Irmler, R., Nicolle, M., Sabatier, P., Swierczynski, T., and Wirth, S. B.: Impact of warmer climate periods on flood hazard in the European Alps, Nature Geoscience, 15, 118–123, https://doi.org/10.1038/s41561-021-00878-y, 2022.

Zahs, V., Hämmerle, M., Anders, K., Hecht, S., Sailer, R., Rutzinger, M., Williams, J. G., and Höfle, B.: Multi-temporal 3D point cloud-based quantification and analysis of geomorphological activity at an alpine rock glacier using airborne and terrestrial LiDAR, Permafrost and Periglacial Processes, 30, 222–238, https://doi.org/https://doi.org/10.1002/ppp.2004, 2019.

Zemp, M., Jakob, L., Dussaillant, I., Nussbaumer, S. U., Gourmelen, N., Dubber, S., A, G., Abdullahi, S., Andreassen, L. M., Berthier, E., Bhattacharya, A., Blazquez, A., Boehm Vock, L. F., Bolch, T., Box, J., Braun, M. H., Brun, F., Cicero, E., Colgan, W., Eckert, N., Farinotti, D., Florentine, C., Floricioiu, D., Gardner, A., Harig, C., Hassan, J., Hugonnet, R., Huss, M., Jóhannesson, T., Liang, C.-C. A., Ke, C.-Q., Khan, S. A., King, O., Kneib, M., Krieger, L., Maussion, F., Mattea, E., McNabb, R., Menounos, B., Miles, E., Moholdt, G., Nilsson, J., Pálsson, F., Pfeffer, J., Piermattei, L., Plummer, S., Richter, A., Sasgen, I., Schuster, L., Seehaus, T., Shen, X., Sommer, C., Sutterley, T., Treichler, D., Velicogna, I., Wouters, B., Zekollari, H., Zheng, W., and Team, T. G.: Community estimate of global glacier mass changes from 2000 to 2023, Nature, 639, 382–388, https://doi.org/10.1038/s41586-024-08545-z, 2025.

Zimmermann, F., McArdell, B. W., Rickli, C., and Scheidl, C.: 2D Runout Modelling of Hillslope Debris Flows, Based on Well-Documented Events in Switzerland, Geosciences, 10, https://doi.org/10.3390/geosciences10020070, 2020.

Zscheischler, J., Westra, S., van den Hurk, B. J. J. M., Seneviratne, S. I., Ward, P. J., Pitman, A., AghaKouchak, A., Bresch, D. N., Leonard, M., Wahl, T., and Zhang, X.: Future climate risk from compound events, Nature Climate Change, 8, 469–477, https://doi.org/10.1038/s41558-018-0156-3, 2018.

Zscheischler, J., Martius, O., Westra, S., Bevacqua, E., Raymond, C., Horton, R. M., van den Hurk, B., AghaKouchak, A., Jézéquel, A., Mahecha, M. D., Maraun, D., Ramos, A. M., Ridder, N. N., Thiery, W., and Vignotto, E.: A typology of compound weather and climate events, Nature Reviews Earth & Environment, 1, 333–347, https://doi.org/10.1038/s43017-020-0060-z, 2020.

https://doi.org/10.5194/egusphere-2026-971
Preprint. Discussion started: 6 March 2026

Appendix A: Appendix

A1 Map and photo after the event

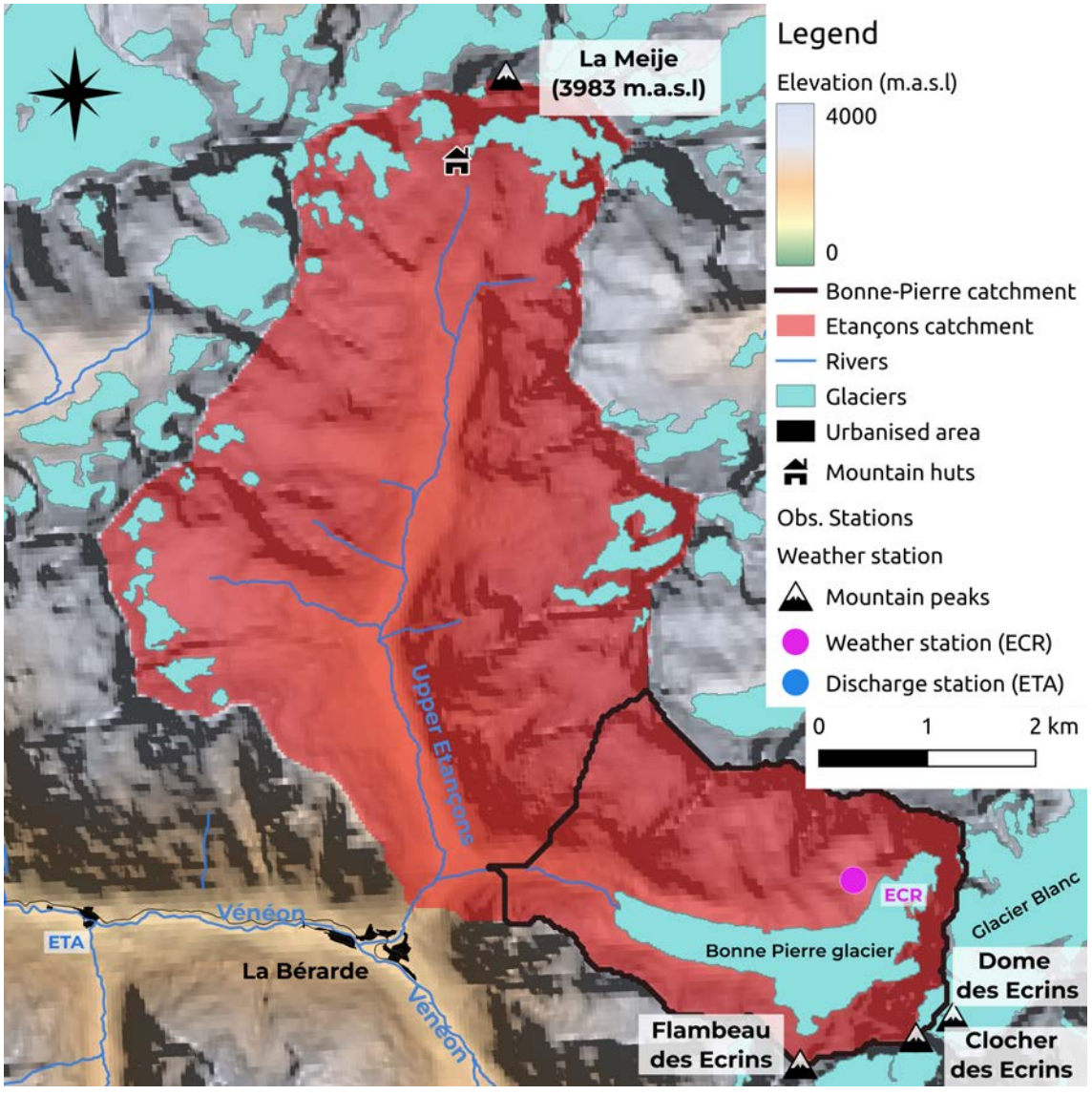

Figure A1. Map showing the Étançons catchment with the Bonne Pierre glacier, the Glacier Blanc, The Étançons torrent, the Vénéon river, in respect to the village of la Bérarde.

https://doi.org/10.5194/egusphere-2026-971
Preprint. Discussion started: 6 March 2026

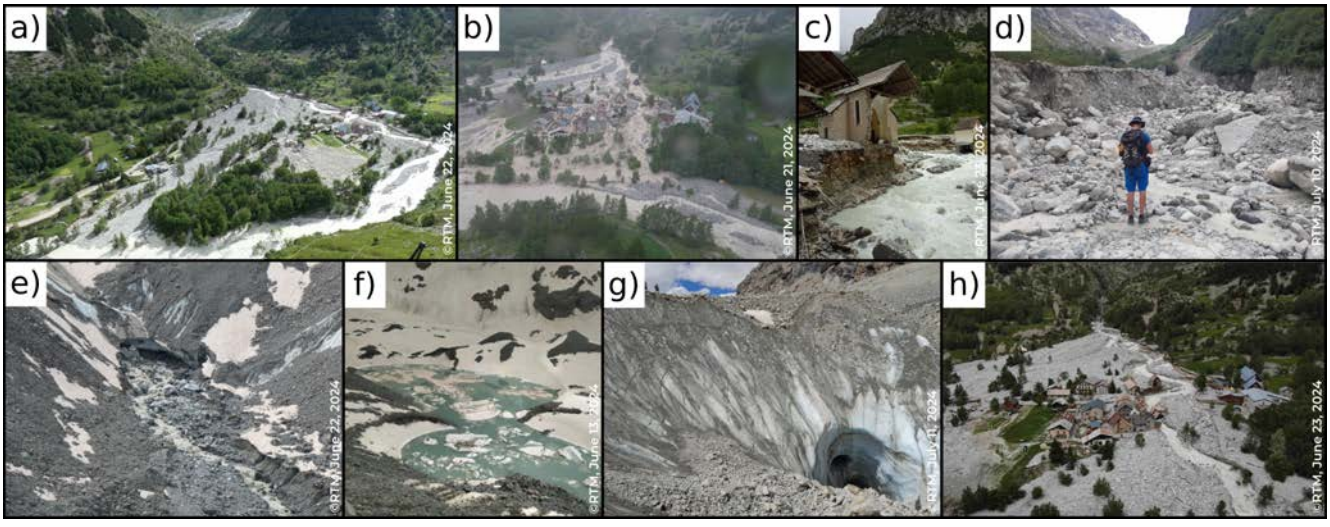

Figure A2. Photos of the area of La Bérarde and above during and after the event. **a)** Aerial view of the village after the flood. The Vénéon river crosses right to left in the foreground. **b)** The village during the flood event on June 21. **c)** The 132 year-old church cut in half by the newly carved path of the Étançons river. **d)** Carved channel around the outlet of the Bonne Pierre glacier. **e)** Outlet of the glacial river of the Bonne Pierre glacier. **f)** Photo of the supra-glacial lake prior to the flood on June 13. **g)** Supra-glacial lake subglacial drainage system. **h)** Village of La Bérarde on June 23 after the flooding event.

https://doi.org/10.5194/egusphere-2026-971
Preprint. Discussion started: 6 March 2026

A2 Natural hazards map

A3 Sediment volume estimates

Sediment budgets were calculated by comparing the two lidar DEMs from IGN LiDAR-HD (18 July 2021) and from the Direction Départementale des Territoires de l'Isère-DDT38 (28 June 2024). We followed the protocols established for this type of event (Liébault et al., 2024). Point clouds were co-registered tile by tile, as systematic errors were not spatially homogeneous, and a DoD (Difference of DEM) raster was then generated. Uncertainty in submerged areas was considered negligible. Sediment budget analysis was restricted to sectors that experienced morphological changes during the June 2024 event. The uncertainty associated with these budgets is proportional to the surface area over which they are calculated. Finally, areas upstream of the Étançons covered by snow were excluded from the analysis, as were potential volumes beneath the glacier. These volumes remain unknown. Thus, these sediment budgets are minimum estimates at the catchment scale.

Due to the heterogeneity of the lidar datasets, we did not compute a site-specific LoD (Level of Detection). The magnitude of the morphological changes observed between the two dates reduces the relevance of a precise LoD calculation. We therefore applied a uniform LoD of 0.1 m, consistent with recent scientific literature for this type of environment (Zahs et al., 2019; Liébault et al., 2024).

A4 Observation network

Table A1 presents a summary of all observation stations fully or partially used for this analysis. These stations are part of different owner such as Météo-France, Electricité de France (EDF), or Observatoire des Sciences de l'Univers de Grenoble (OSUG).

https://doi.org/10.5194/egusphere-2026-971
Preprint. Discussion started: 6 March 2026

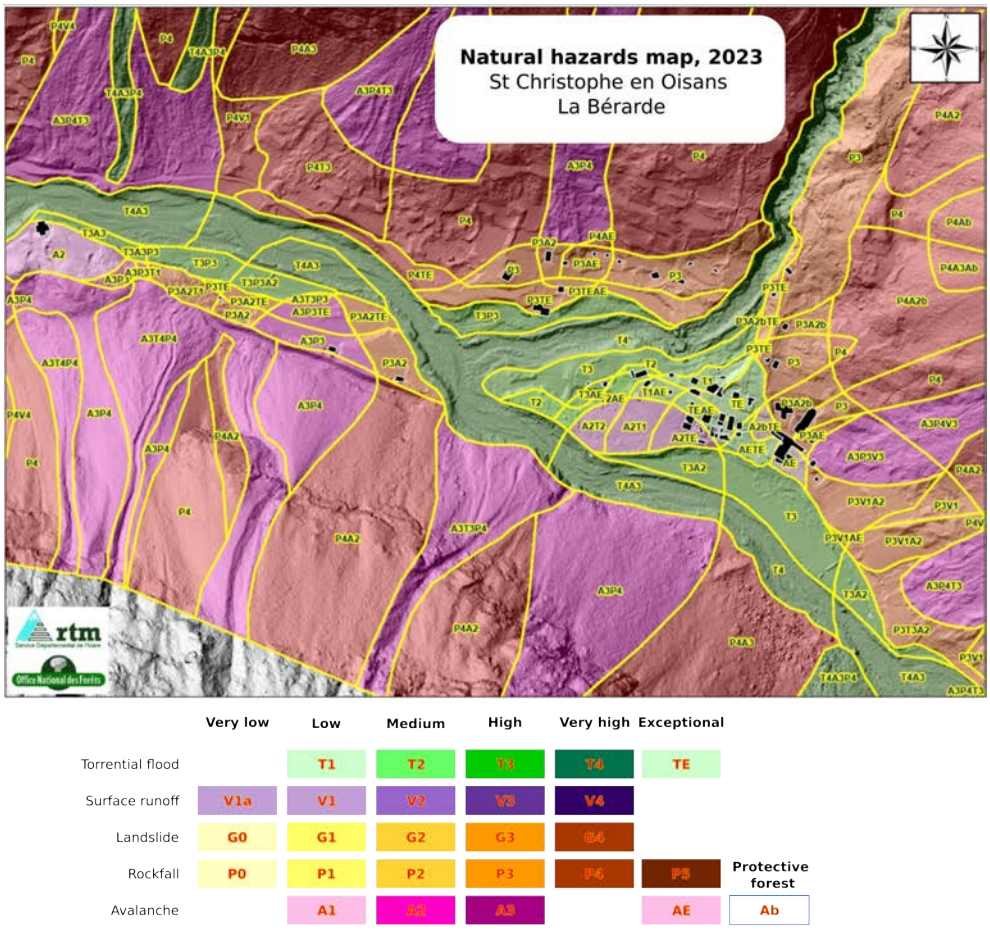

Figure A3. Natural hazards map from July 2023 for the locality of La Bérarde. The coloring indicates the type of hazards and its relative probability. Note that the color reflect the dominant hazards, and the alphanumeric codes corresponds to each type of hazards and may include several hazards. For instance, the alphanumeric code for the area where the church was, is TEAE corresponding to *exceptional torrential flood* (*a.k.a.* debris flood) and *exceptional avalanche*.

https://doi.org/10.5194/egusphere-2026-971
Preprint. Discussion started: 6 March 2026

Acronym	Name	Lon/lat	Elevation [m a.s.l.]	Variable available
ECR	Nivose Écrins	6.346°E, 44.937°N	2978	Air temperature, wind, snow depth
CHR	Saint Christophe en Oisans	6.188°E, 44.945°N	1560	Precipitation, wind, air temperature
CEZ	Cézanne	6.415°E, 44.917°N	1875	Precipitation, wind, air temperature
ETA	Les Étages	6.252°E, 44.937°N	1582	Discharge
PDL	Plan du Lac	6.145°E, 44.979°N	1173	Discharge
ROU	Pont Rouge	6.013°E, 45.116°N	714	Discharge
PRA	Prapic	6.424°E, 44.670°N	2500	Snow water equivalent
PEL	Pelvoux	6.479°E, 44.876°N	1270	Precipitation, air temperature, snow depth
PES	Pont Escoffier	6.069°E, 45.003°N	766	Precipitation
MON	Monetier	6.545°E, 44.971°N	1460	Precipitation, air temperature, snow depth
ARE	Villard d'Arène	6.336°E, 45.041°N	1665	Precipitation, air temperature wind, snow depth
CHA	La Grave	6.285°E, 45.054°N	1790	Precipitation, air temperature
LAC	Lac Noir	6.225°E, 45.051°N	2450	
VAL	Chapelle Valgaudemar	6.195°E, 44.810°N	1264	Precipitation, air temperature, snow depth
OGSA	Col du Lautaret	6.401°E, 45.037°N	2110	Seismic
OGAG	L'Argentière la Bessée	6.560°E, 44.788°N	1308	Seismic
OGVG	Saint-Maurice-en-Valgaudemar	6.112°E, 44.815°N	1046	Seismic
MH-FTU	Montain Hut Font Turbat	6.179°E, 44.865°N	2177	48 h precipitation
MH-PEL	Montain Hut Pelvoux	6.406°E, 44.882°N	2694	48 h precipitation
MH-ECR	Montain Hut Écrins	6.383°E, 44.947°N	3127	48 h precipitation
MH-PRM	Montain Hut Promontoire	6.303°E, 44.998°N	3026	48 h precipitation

Table A1. Description of the observation network used in the reanalysis of the event.

https://doi.org/10.5194/egusphere-2026-971
Preprint. Discussion started: 6 March 2026

Table A2. Geospatial data

Date YYYY-mm-dd	Type	Resolution (m)*	Ortho	DEM
2003-07-15	Aerial	0.5	x	
2009-08-05	Aerial	0.5	x	
2012-07-15	Aerial	0.5	x	
2015-08-05	Aerial	0.5	x	
2016-07-19	Spot6	1.5	x	
2018-08-12	Pléiades	0.5	x	x
2019-08-25	Spot6	1.5	x	
2021-07-21	lidar	1.0		x
2021-08-16	Spot6	1.5	x	
2023-08-07	Spot6	1.5	x	
2024-07-04	Pneo	0.3	x	x
2024-10-28	lidar	1.0		x

* All ortho-mosaics were resampled to 1m

https://doi.org/10.5194/egusphere-2026-971
Preprint. Discussion started: 6 March 2026

A5 Climatology

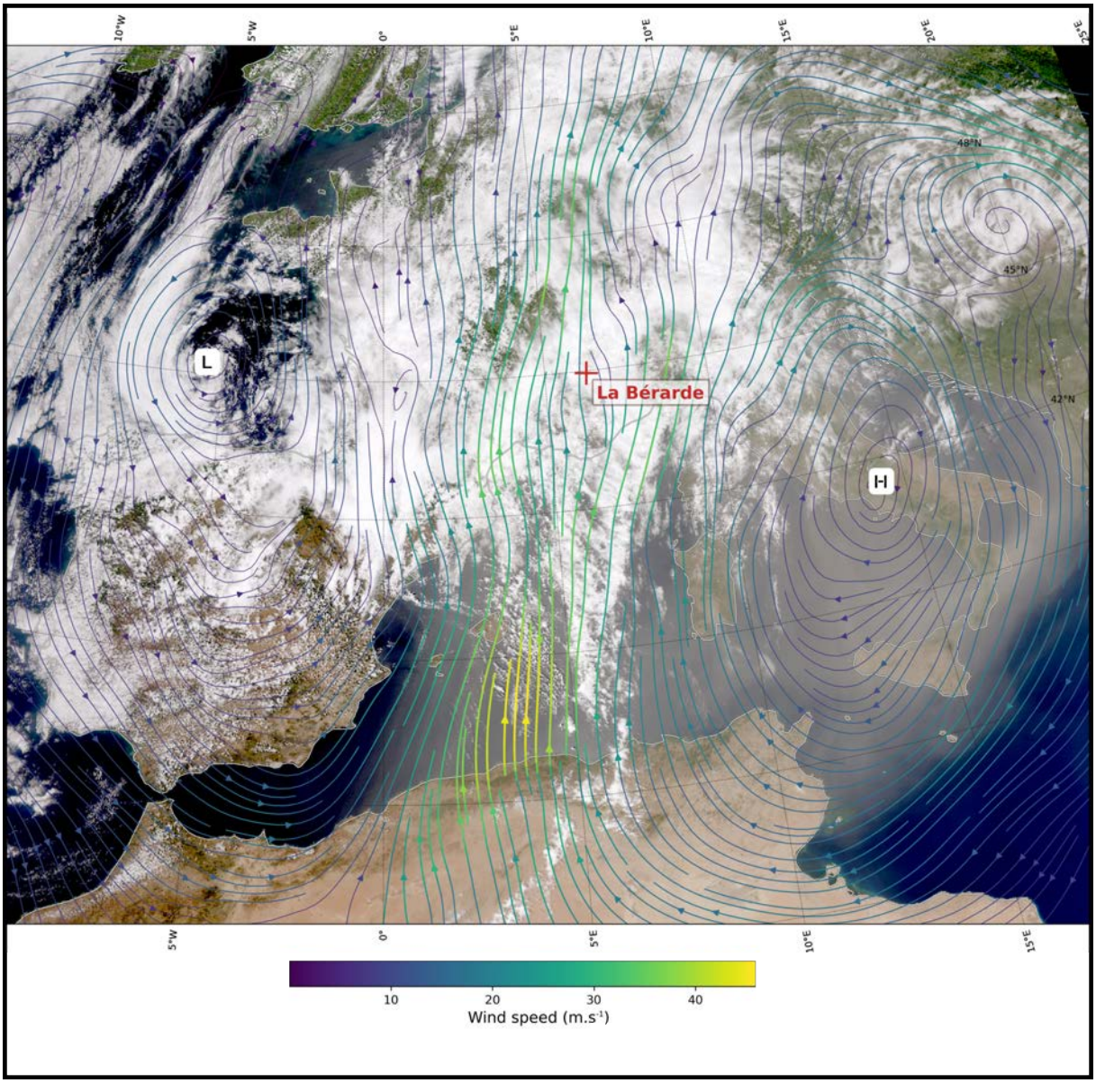

Figure A4. Visible image from NOAA-20 satellite (June 20, 2024 12:32 UTC) overlaid with the ERA5 reanalysis wind field at 500 hPa (June 20, 2024 12:00 UTC)($\approx 5500\ m\ a.s.l.$). Projection is stereographic.

https://doi.org/10.5194/egusphere-2026-971
Preprint. Discussion started: 6 March 2026

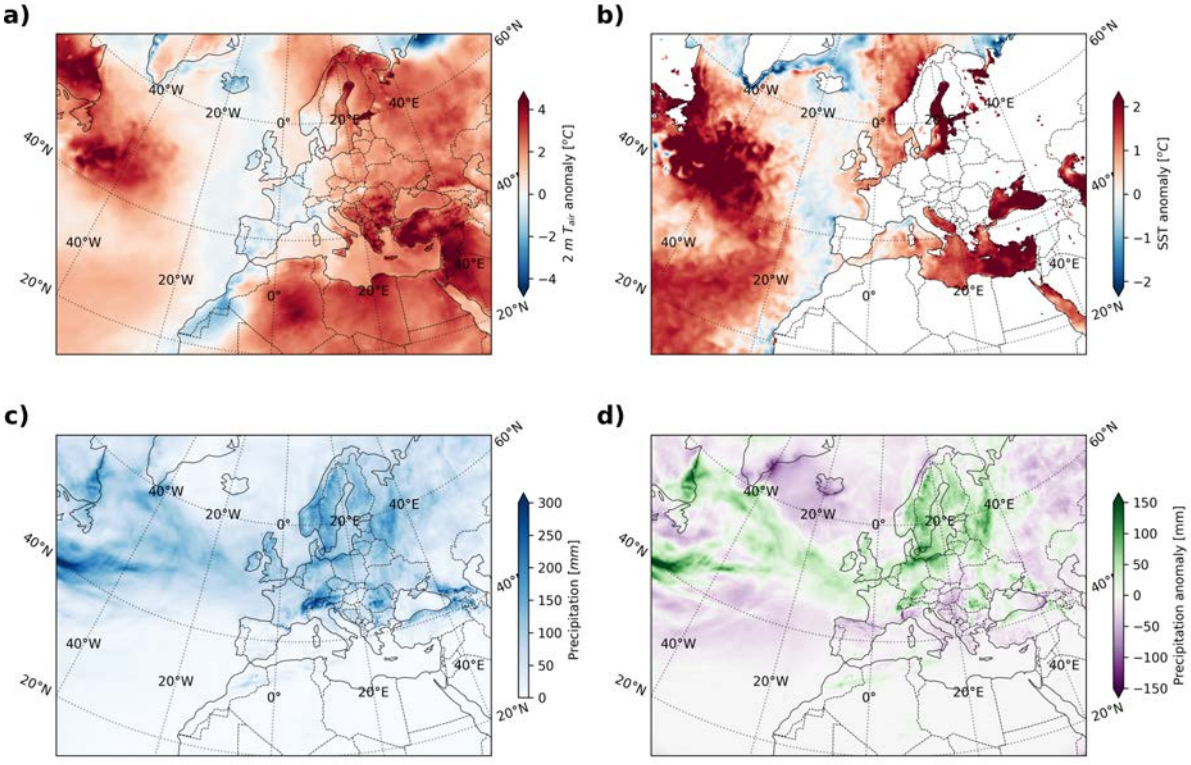

Figure A5. June 2024 climatology based on the ERA5 reanalysis data considering the reference period 1991-2020. **a)** 2-m air temperature anomaly. **b)** Sea surface temperature anomaly (SST). **c)** Total precipitation. **d)** Total precipitation anomaly.

https://doi.org/10.5194/egusphere-2026-971
Preprint. Discussion started: 6 March 2026

Table A3. Precipitation observed from June 19 to June 21 at the mountain huts in the vicinity of La Bérarde.

Acronym	Name	Lon/lat	Elevation [m a.s.l.]	48 h Precipitation [mm]
MH-FTU	Montain Hut Font Turbat	6.179°E, 44.865°N	2177	110
MH-PEL	Montain Hut Pelvoux	6.406°E, 44.882°N	2694	127
MH-ECR	Montain Hut Écrins	6.383°E, 44.947°N	3127	113.5
MH-PRM*	Montain Hut Promontoire	6.303°E, 44.998°N	3026	100

* *Mountain hut located within the Étançons catchment with testimony of bucket overfilling at the peak precipitation with intense winds.*

A6 Snowmelt

The snowmelt analysis is mainly based on S2M (Vernay et al., 2022), from which we extracted estimates of liquid precipitation (*i.e.* rain), and snowmelt (water exiting the snowpack at its bottom minus the rain input), and the combination of both water sources. S2M provides data since 1959 based on a downscaling scheme (SAFRAN) that abstract each mountain range into an idealized geometry of two pyramids of 8 sides (*i.e.* aspects) and of slopes 20° and 40° respectively, for every 300 m altitudinal bands. Using the atmospheric forcings, the snowpack at each tile of these two pyramids can be simulated with in-depth detailed physics.

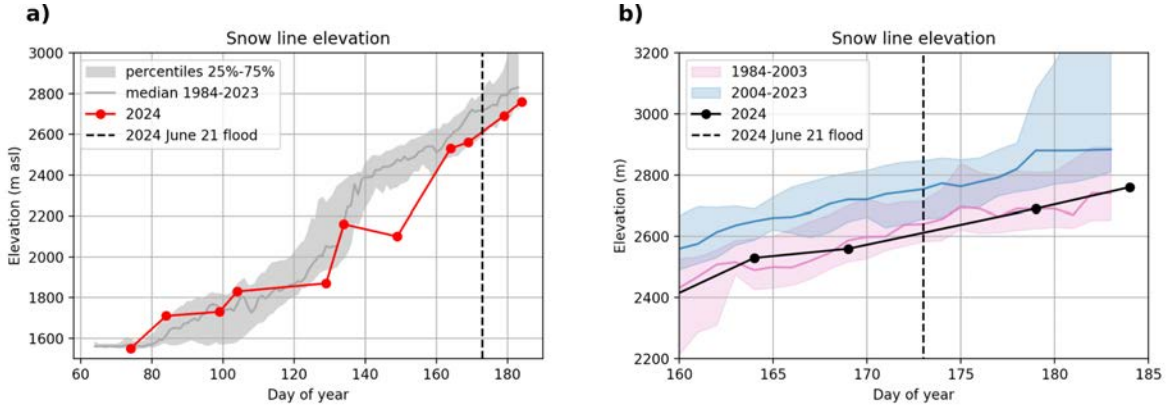

Figure A6. Seasonal snowline elevation at the Étançons catchment estimated from Sentinel-2, SPOT and Landsat imagery (Barrou Dumont et al., 2024) **a)** Evolution of the spring 2024 snowline in respect to 1984-2023 statistics. Notice how in spring 2024, the snow line remains around the 25 % percentile line from the years 1983-2023. **b)** Zoom on the date of the event contextualized against the periods 1984-2003 (pink) and 2004-2023 (blue). We see the snow coverage was equivalent to an average snow cover of the period 1983-2003.

https://doi.org/10.5194/egusphere-2026-971
Preprint. Discussion started: 6 March 2026

Table A4. 48 h time window corresponding to peak melt, peak rain and peak melt plus rain. Hours correspond to the start of the corresponding 48 h time window. In bold, the peak instantaneous peak contribution of melt plus rain. Return periods are computed based on a GEV model, more detail in section 6.2. A26.

		Return Levels [mm]			**Return Periods [years]**		
Hour (UTC)	Main contribution	Rain	Melt	Total runoff	Rain	Melt	Total runoff
2024-06-19 08:00	Melt	44.8	93.8	138.6	1.3-1.5	23-64	20-41
2024-06-20 05:00	Melt+Rain	**85.1**	**86.9**	**172**	**5.6-7.6**	**14-25**	**45-165**
2024-06-21 00:00	Rain	92.5	57.6	150.2	7.3-11	1.5-1.7	28-68

A6.1 Snowmelt sensitivity analysis

Locally, the rain has been underestimated within the S2M scheme due to averaging of precipitation over the entire Météo-France massif of the Écrins (Fig. 6d). Indeed, for the June 19, 12:00 to June 21 12:00 UTC, we estimated from S2M a rainfall of 85 mm and a snowmelt of 75 mm. This is to be compared to the rainfall observed at CHR of 104 mm. Rain brings sensible heat to the snowpack, an energy that contributes to melting the snow. Therefore an additional amount of rain may increase the snowmelt estimate.

To test how sensitive were our results, we adjusted the precipitation (*i.e.* rain) to match those of CHR with a 10 mm incrementally added before June 20, 12:00, and a 24 mm also incrementally added for the precipitation during the night from June 20-21. In total, it is an additional of 34 mm rain added over the course of the event. This correction is done equivalently across all altitudinal bands (Fig. A7).

With this correction, only 1.2 mm extra snowmelt is observed.

https://doi.org/10.5194/egusphere-2026-971
Preprint. Discussion started: 6 March 2026

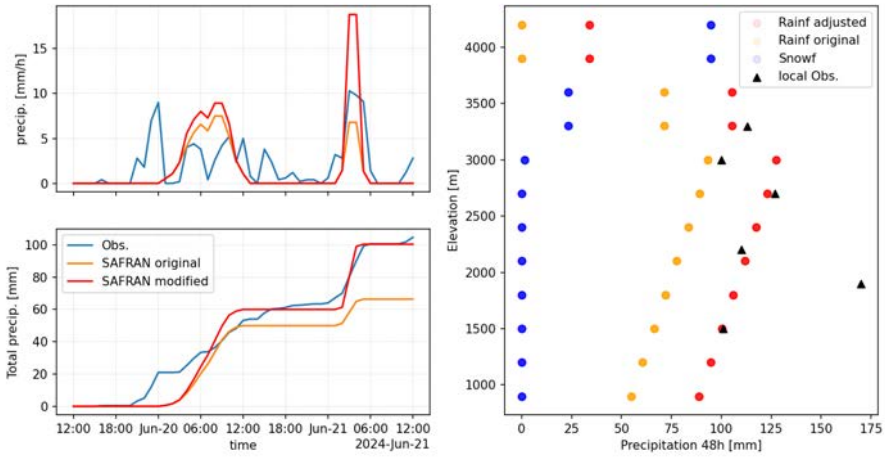

Figure A7. Adjustments to perform the sensitivity analysis to take into account the extra rainfall locally observed in the are of the Étançons catchment in respect to the larger mountain massif of the Écrins. **a)** the hourly precipitation at CHR, before and after correction of the S2M timeseries. **b)** same as a) but cumulative. **c)** altitudinal gradient correction in respect to local observations (*e.g.* mountain huts).

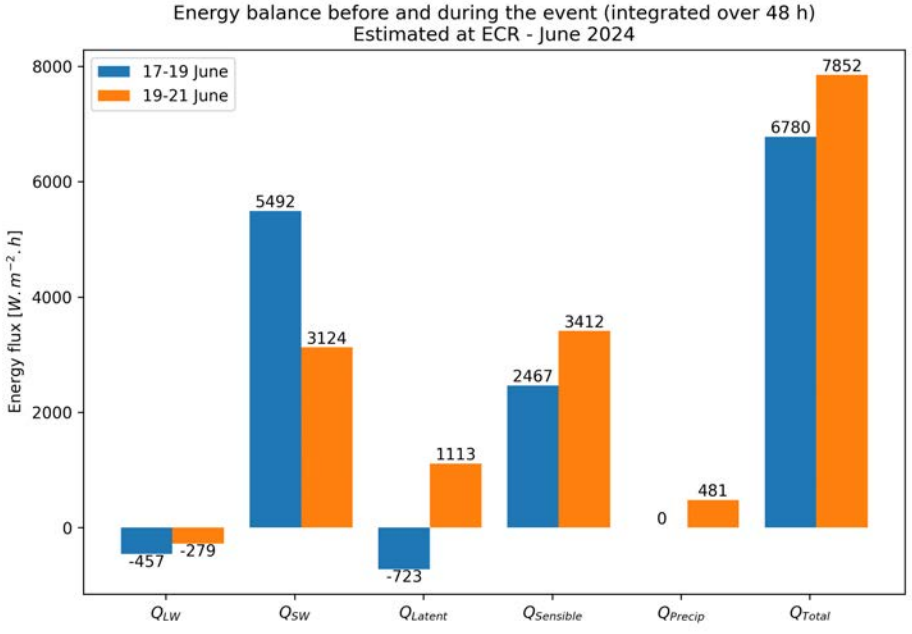

Figure A8. Surface energy balance at the Écrins weather station (ECR) integrated over 48 h for the two periods, before (blue) and during (orange) the June 2024 event. Notice the drop in shortwave, reversal in latent heat transfer and the increase in sensible heat.

https://doi.org/10.5194/egusphere-2026-971
Preprint. Discussion started: 6 March 2026

A7 Glacier and glacial lake

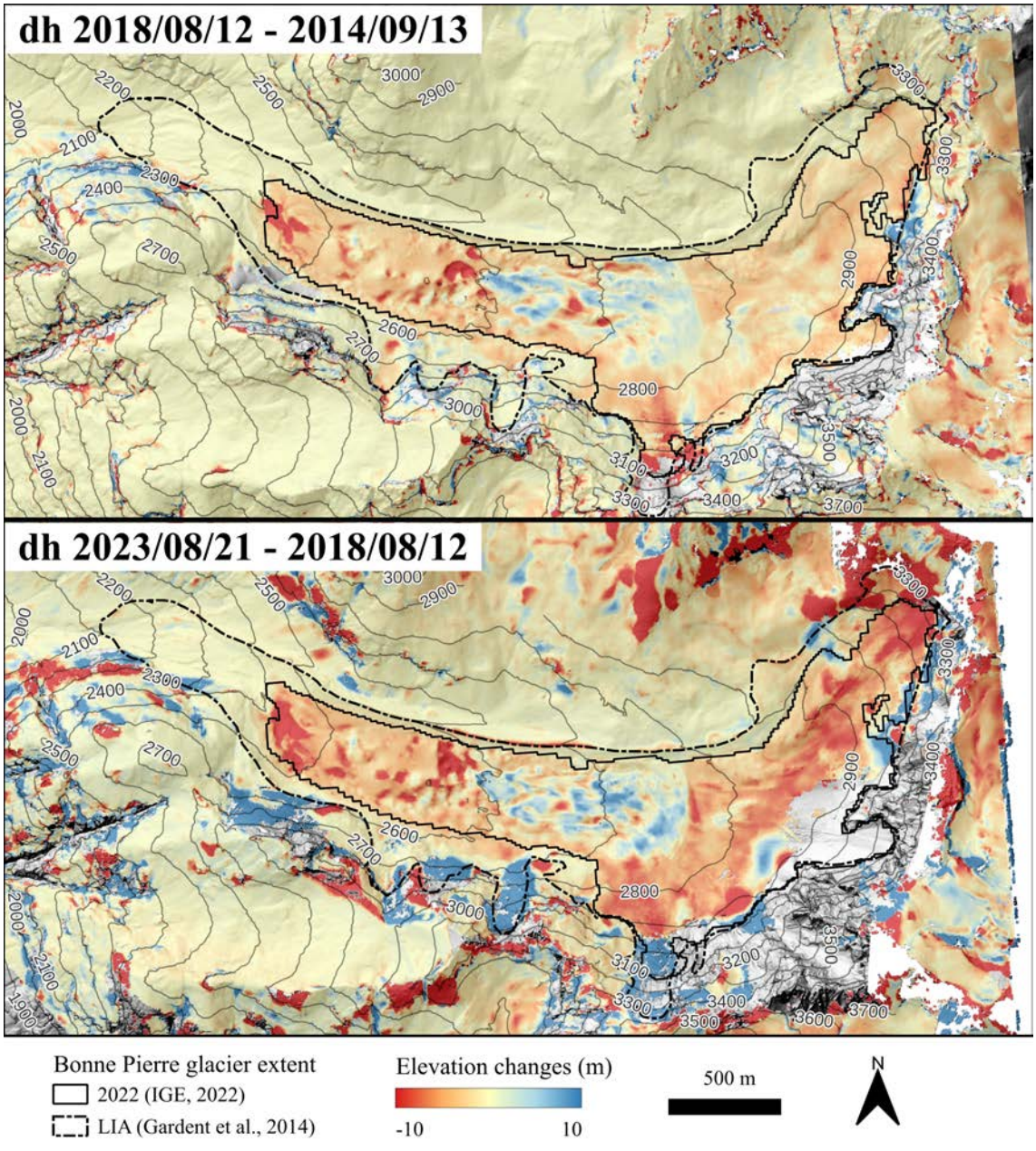

Figure A9. Elevation changes map pf Bonne Pierre glacier for two different periods 2018-2014 and 2023-2018. Digital Surface Models (DSM) were obtained from stereo correlation of Pléiades satellite images (2.4).

https://doi.org/10.5194/egusphere-2026-971
Preprint. Discussion started: 6 March 2026

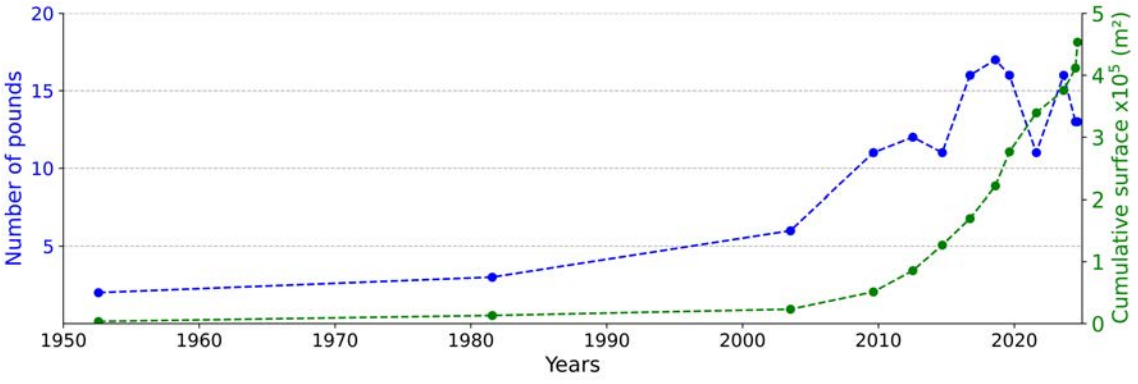

Figure A10. Temporal evolution (frequency and cumulative surface) of supra-glacial ponds on Bonne Pierre glacier since 1950.

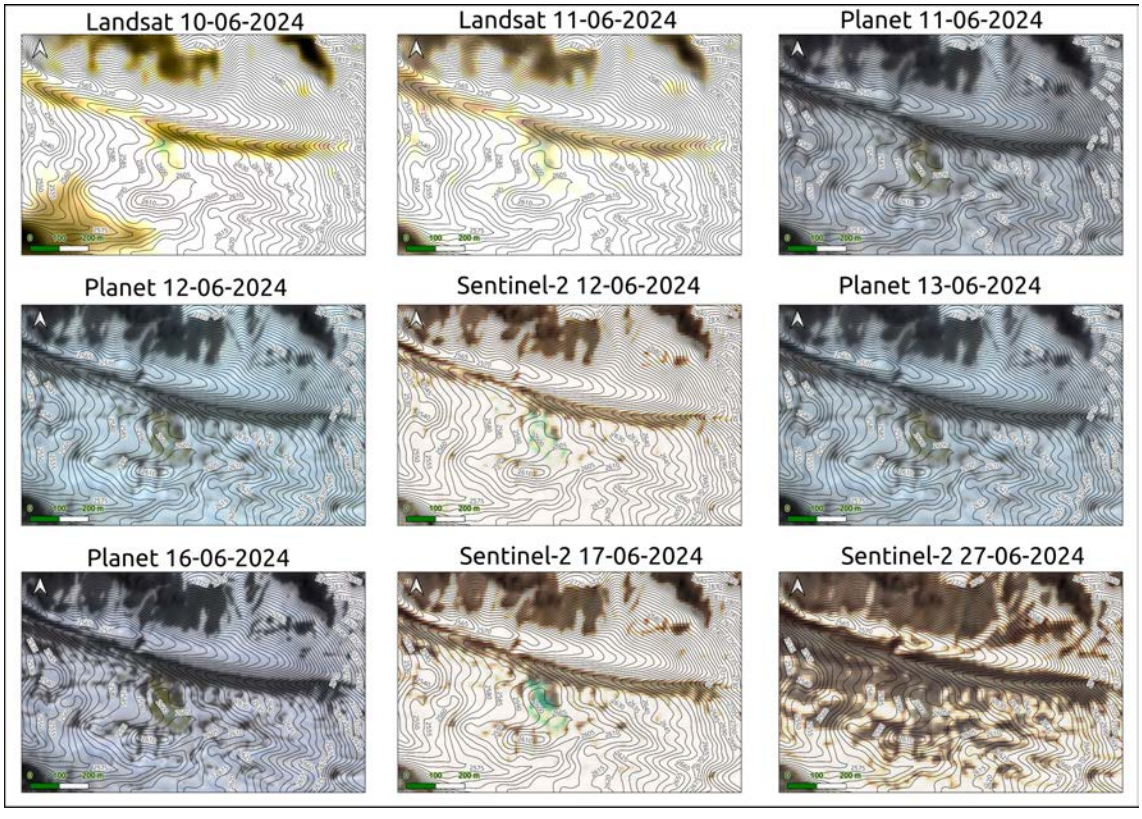

Figure A11. Temporal evolution of the Bonne Pierre glacier surface for the month of June 2024 based on imagery from Sentinel-2, Landsat 9, and Planet satellites. The lake appears to fill up throughout the month of June and is observed empty on June 27.

https://doi.org/10.5194/egusphere-2026-971
Preprint. Discussion started: 6 March 2026

Figure A12. Picture taken by Adrien le Bouquetin (CC BY-NC-ND 3.0) on June 18, 2024 at 08:16 UTC. The supra-glacial lake is visible just on the right of the climber's head, along the longitudinal moraine. Picture retrieved on February 4, 2026 from the online forum Campto-Camp.org

A8 Discharge measurements

The station "Les Etages" (ETA) is a hydrometric station operated by EDF since 1951. Sub-hourly data are available since 1983. The station is regularly gauged, between 6 and 8 times a year, when the access road is open. The discharge measurements explore hydraulic control up to approximately 30 m^3/s. Beyond this point, the rating curve is based on 1D hydraulic modeling. The discharge measurements show very unstable hydraulic control at low streamflow. The rating curve changes on average every year. The spring melt causes solid transport, which is responsible for the drift of the rating curve. Medium and high streamflows are less variable when the general slope of the riverbed becomes the main hydraulic control.

Water-levels superior to 2 m occur on average twice a year (Figure A13a). This water-level represents a discharge between 29 and 35 m^3/s according to the historical rating curves. For four years (2008, 2017, 2020, and 2023), the station logged flooding events reaching a maximum water-level closed to 2.40 m (corresponding to discharges around 50 m^3/s). These four flooding

https://doi.org/10.5194/egusphere-2026-971
Preprint. Discussion started: 6 March 2026

events never damaged the station, and did not disturbed the recording at the station. However, the flood event of June 2024 destroyed the station. The DREAL sensor located outside the gauging well was torn off when the water reached about 2.50 m. The DTG sensor was better secured inside the gauging well. The last recorded and transmitted water-level value would have reached 2.87 m (Figure A13b). This had never been recorded before. According to the current rating curve, discharge would have reached approximately 80 m^3/s, though this value is extremely uncertain, due to the important solid transport during the June 2024 event.

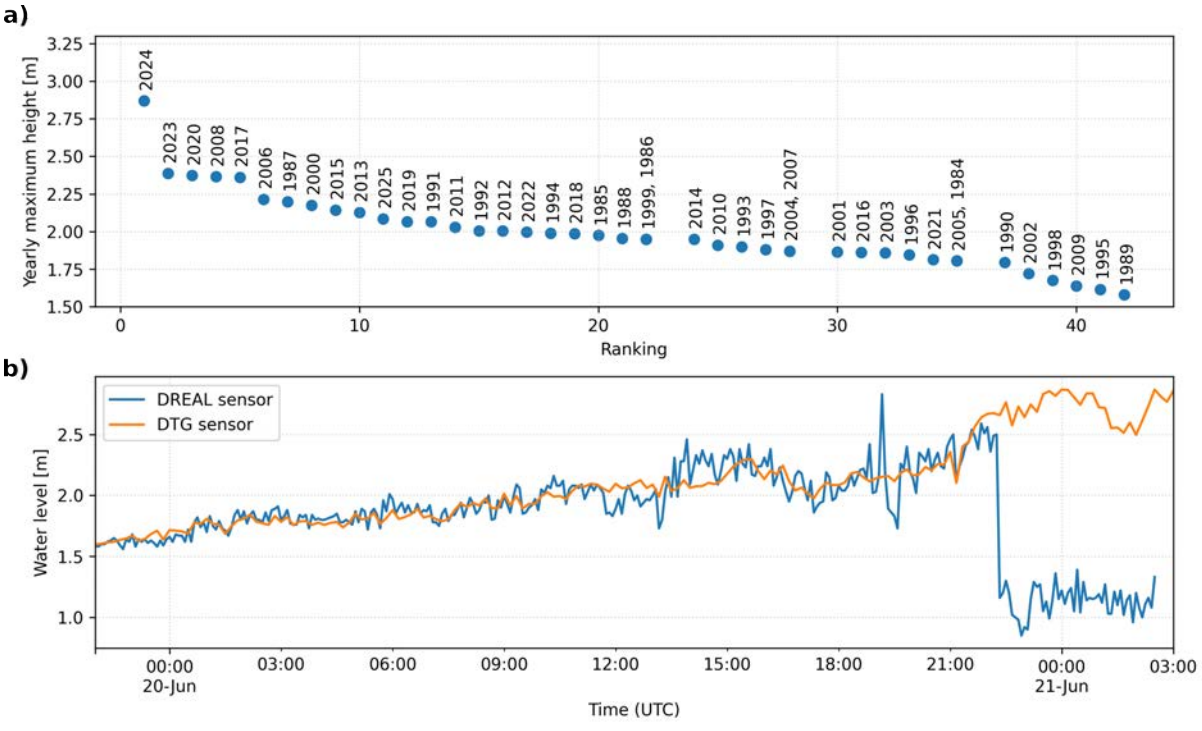

Figure A13. Water-level measurement at the discharge station from "Les Etages" (ETA) **a)** Yearly hourly water-level maximum ranked since 1984 **b)** Logged Sub-hourly water-level at ETA during the 20 and 21 June 2024 (EDF-DTG main sensor in orange, DREAL sensor in blue)

https://doi.org/10.5194/egusphere-2026-971
Preprint. Discussion started: 6 March 2026

A9 Hydraulic modeling

The 2D hydraulic modeling conducted with Telemac highlights the significant influence of bathymetric changes on discharge estimation during the June 2024 flood event. Simulations based on pre-flood and post-flood digital terrain models (DTMs) reveal substantial morphological alterations, including erosion up to 1.5 m and widespread sediment deposition, which strongly affect flow patterns and roughness coefficients. Using the pre-flood DTM, the peak discharge was estimated between 95 and 110 m^3/s, whereas the post-flood DTM yielded values ranging from 85 to 95 m^3/s. This 25 m^3/s discrepancy underscores the uncertainty introduced by dynamic channel morphology during extreme events. Furthermore, the assumption of a uniform Strickler coefficient across the channel proved limiting, as roughness likely varied both spatially and temporally throughout the flood. All simulations were performed using Strickler coefficients within a realistic range of 8 to 12, consistent with field observations. These findings confirm that incorporating updated bathymetry is essential for improving the reliability of 2D models in complex alpine environments.

A10 Hydrological method details

To estimate the spatial and temporal dynamic of rainfall over the Vénéon catchment for the June 2024 event, we used the ANTILOPE reanalysis dataset consisting of the hourly precipitation field from June 19 to June 21 18:00 UTC (48 h). The ANTILOPE precipitation field reanalysis from Météo-France (Champeaux et al., 2011) merges radar and ground observations. Although, surrounded by some of the highest mountains of the French Alps, the Vénéon catchment is reasonably reached by the signal from the Mont Colombis meteorological radar, located about 50 km south of La Bérarde. It is to be noted also that the radar from the Mont Moucherotte, was in maintenance at the time of the event, explaining partially some of the incomplete precipitation fields.

The ANTILOPE precipitation fields are smoothed and then scaled to minimize the difference with the neighboring hourly precipitation ground rain gauges. The resulting errors of the ground rain gauges closest to the catchment are then propagated with Inverse Distance Weighting. The total 48-h areal precipitation on the Vénéon catchment is estimated at 127 mm.

To improve the modeling results, we performed a careful updating of the model forcing data until few days before of the flood. Between October 2023 and June 2024, small offsets (less than $\pm$ 2°C) for some periods are added to the air temperature input of the model to minimize the difference between the global (i.e. catchment averaged) Snow Water Equivalent (SWE) modeled by both MORDOR (Garavaglia et al., 2017) and S2M (Vernay et al., 2022).

Figure A14 shows that the 2023-2024 snow water equivalent (SWE) of the snowpack is coherently represented by these two different models in respect to the *in-situ* observations (PRA). Both models are based on very distinct concepts and share few inputs. It is to be noted that no correction of the input precipitation is needed. In the same figure, the SWE modeled by MORDOR for one of its altitude bands is compared to the SWE measured at the Prapic Cosmic Ray Snow Gauge (Paquet and and, 2006), located about 30 km south of La Bérarde at the altitude of 2480 m, showing also a good agreement.

The modeling of the June 2024 flood is finally done using as inputs the 48-h sequence of reanalysis precipitation and air temperature at ECR. As for the 2023-2024 season, some temporary offsets are added (from -4°C to +1.2°C) to the ECR

https://doi.org/10.5194/egusphere-2026-971
Preprint. Discussion started: 6 March 2026

temperature between June 16 and June 22 to improve the match between the modeled discharge and the measurements at ETA. These temperature corrections mostly affect the modeled snowmelt during the beginning of the flood.

A second rainfall-runoff modeling chain, using the hourly CemaNeige snow accumulation and melt (Valéry et al., 2014) and GR4H hydrological (Perrin et al., 2003) models within the airGR R package (Coron et al., 2017, 2023) was deployed. It confirmed the general understanding of the event that was depicted thanks to the MORDOR model on the hydrological viewpoint. Its results are not presented in this article for the sake of conciseness (see Blanc et al. (2024) for further details).

https://doi.org/10.5194/egusphere-2026-971
Preprint. Discussion started: 6 March 2026

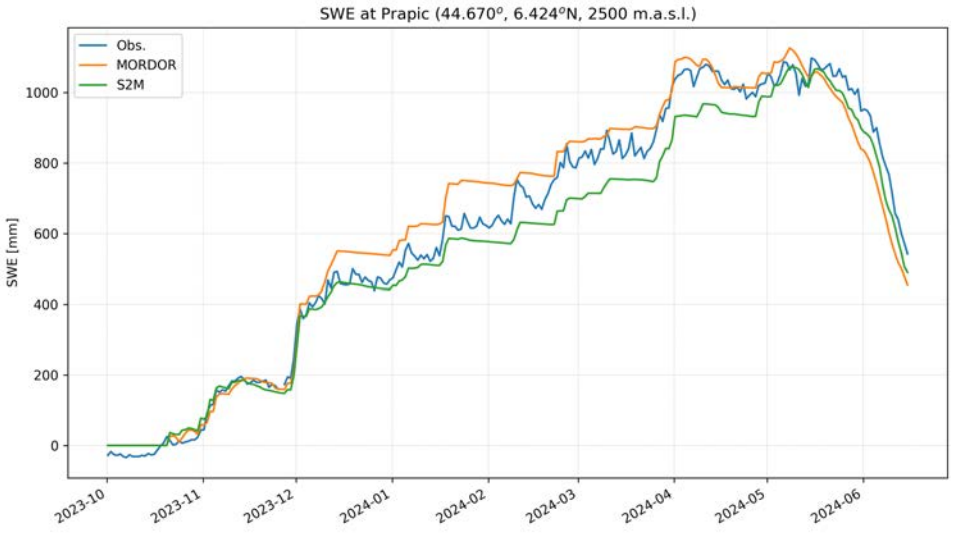

Figure A14. Comparison of Snow Water Equivalent observed at Prapic SWE gauge to the MORDOR and S2M models for the winter season 2023-2024.

https://doi.org/10.5194/egusphere-2026-971
Preprint. Discussion started: 6 March 2026

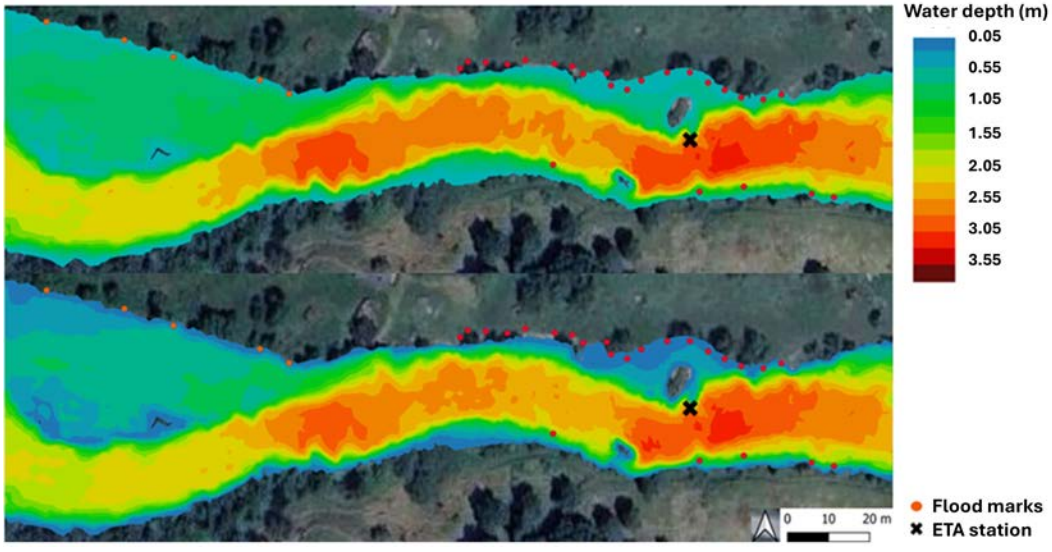

Figure A15. Examples of water depth modeled by Telemac 2D for a Strickler coefficient of 8 $m^{1/3}.s^{-1}$ and a discharge of 95 $m^3.s^{-1}$ (top), and a Strickler coefficient of 12 $m^{1/3}.s^{-1}$ and a discharge of 110 $m^3.s^{-1}$, showing good agreement with the flood marks (red dots). The ETA station is located by a black cross

https://doi.org/10.5194/egusphere-2026-971
Preprint. Discussion started: 6 March 2026

A11 Seismic

The Power Spectral Density (PSD), expressed in dB relative to 1 $(m\ s^{-1})^2\ Hz^{-1}$, describes how seismic signal energy is distributed across frequencies. Spectrograms show the evolution of this frequency content over time by calculating the PSD in successive time windows.

The spectrograms of the three stations (Fig. A16 and A17) reveal increased energy in several frequency bands during the event. The 2–10 Hz frequency band, which shows strong variations at OGAG starting from June 20, 2024, appears to be primarily associated with the La Durance River flow, located approximately 1.5 km from the seismic station (Fig. A18). This observation is consistent with previous studies linking high-frequency seismic noise to turbulent flow and river and sediment transport during floods (e.g., Chmiel et al. (2022)).

In contrast, the 0.4–0.5 Hz frequency band shows an energy increase concurrent with a change in the polarization direction of the seismic waves at OGAG, oriented toward La Bérarde during the event (Fig. A19 and A20).

https://doi.org/10.5194/egusphere-2026-971
Preprint. Discussion started: 6 March 2026

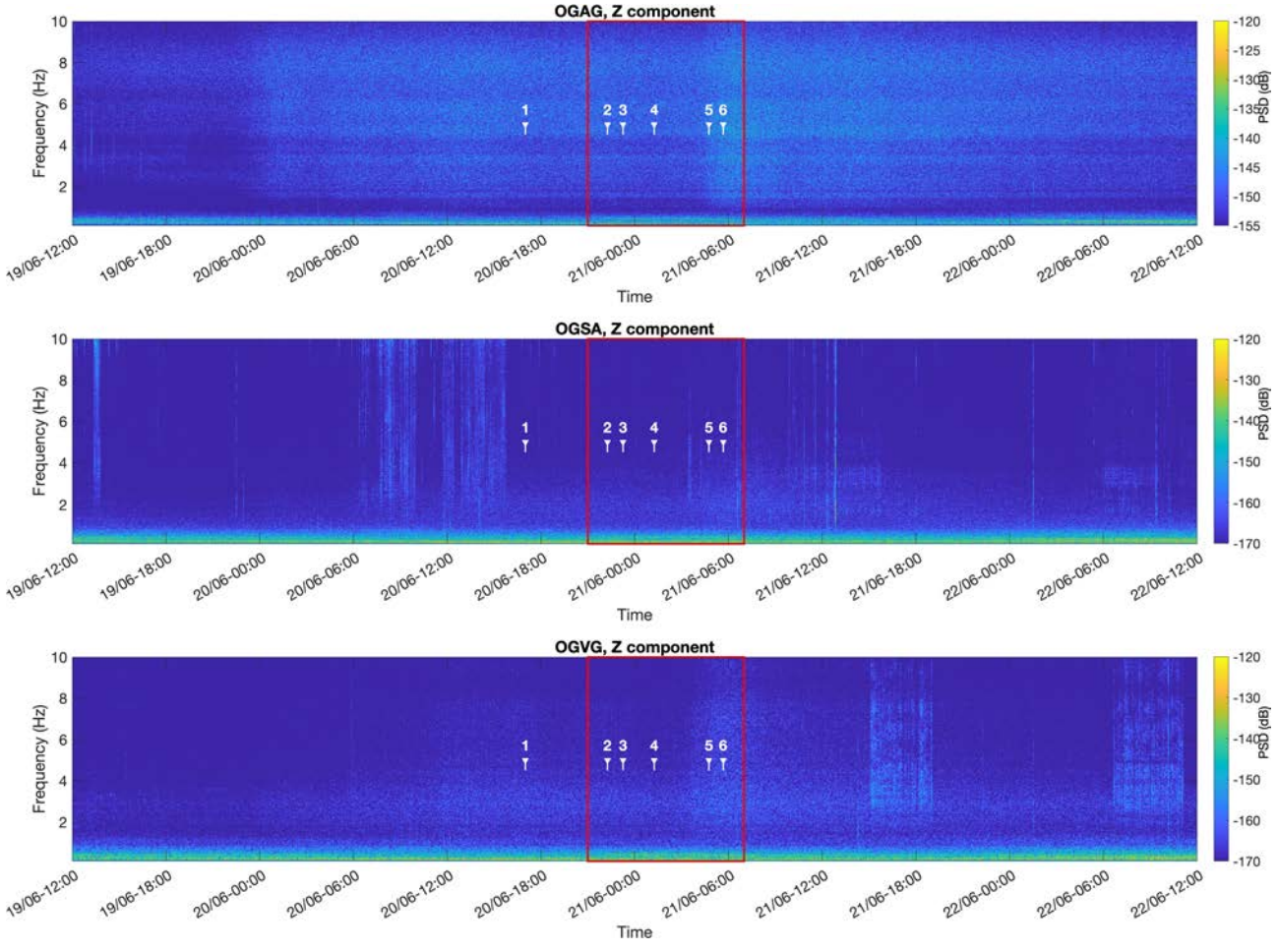

Figure A16. Spectrogram of OGAG, OGVG and OGSA, the three closest permanent seismic station from La Bérarde, between 0.1 and 10 Hz. Red rectangles indicate the period associated with the La Bérarde event, based on discharge measurements from the ETA station and direct observations reported by local residents. 1- First overflowing of the Vénéon at the parking lot ; 2- Overflowing right bank ; 3- Overflowing switches to left bank ; 4- Overflowing switches to right bank ; 5- deposition on right bank and avulsion ; 6- Water reaching sector of the church.

https://doi.org/10.5194/egusphere-2026-971
Preprint. Discussion started: 6 March 2026

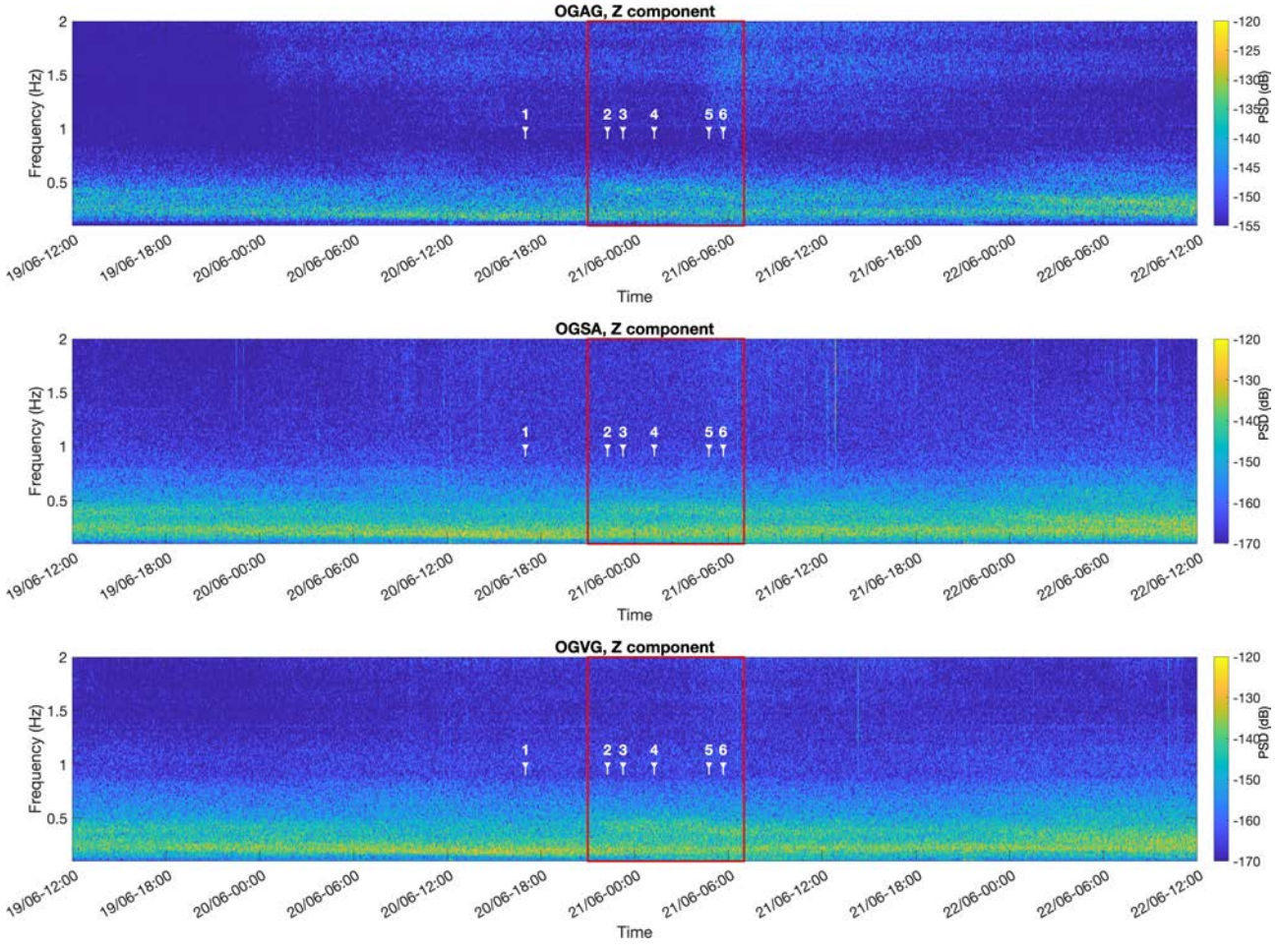

Figure A17. Spectrogram of OGAG, OGVG and OGSA, the three closest permanent seismic station from La Bérarde, between 0.1 and 2 Hz. Red rectangles indicate the period associated with the La Bérarde event, based on discharge measurements from the ETA station and direct observations reported by local residents. 1- First overflowing of the Vénéon at the parking lot ; 2- Overflowing right bank ; 3- Overflowing switches to left bank ; 4- Overflowing switches to right bank ; 5- deposition on right bank and avulsion ; 6- Water reaching sector of the church.

https://doi.org/10.5194/egusphere-2026-971
Preprint. Discussion started: 6 March 2026

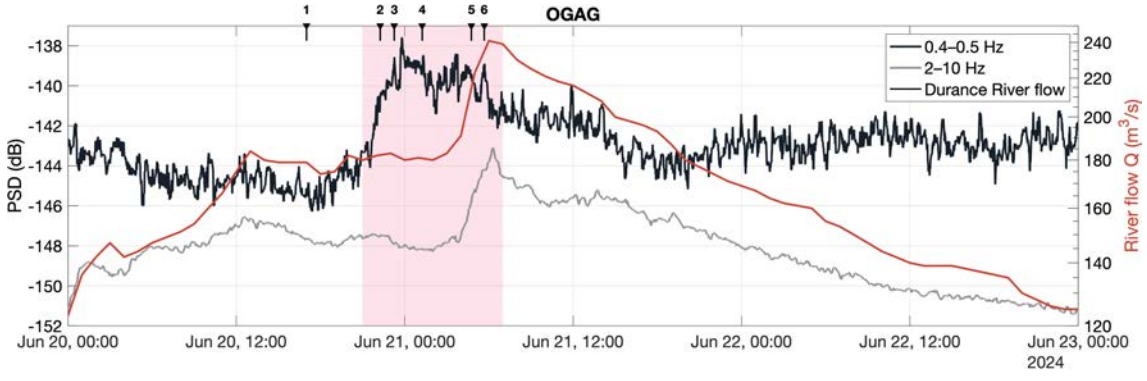

Figure A18. Power Spectral Density (PSD) between 0.4-0.5 Hz and 2-10 Hz for the OGAG seismic station together with the Durance's river flow. OGAG is located 1.5 km away from the Durance river. The pink rectangle indicates the period associated with the La Bérarde event, based on discharge measurements from the ETA station and direct observations reported by local residents. 1- First overflowing of the Vénéon at the parking lot ; 2- Overflowing right bank ; 3- Overflowing switches to left bank ; 4- Overflowing switches to right bank ; 5- deposition on right bank and avulsion ; 6- Water reaching sector of the church.

https://doi.org/10.5194/egusphere-2026-971
Preprint. Discussion started: 6 March 2026

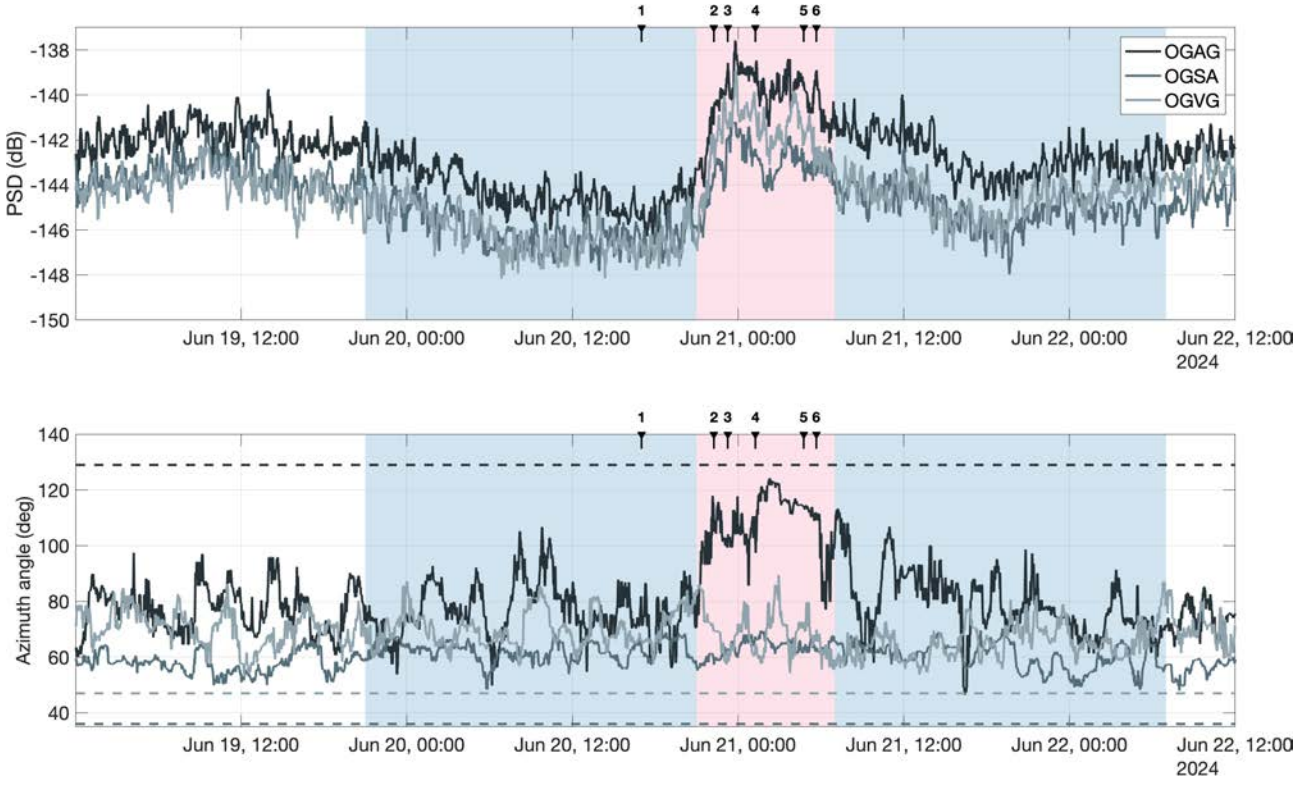

Figure A19. Upper image | PSD between 0.4 and 0.5 Hz for the three closest seismic station to La Bérarde, OGAG, OGSA and OGVG. **Lower image |** Orientation of the particle motion given between 0 and 180° for the same three seismic stations. Dashed lines represent the azimuth of la Bérarde compared to each stations. The pink area indicates the period associated with the La Bérarde event, based on discharge measurements from the ETA station and direct observations reported by local residents, while blue areas represent 24h before and after the event. These time periods are used and mentioned in figure A20 a) and b) respectively. 1- First overflowing of the Vénéon at the parking lot ; 2- Overflowing right bank ; 3- Overflowing switches to left bank ; 4- Overflowing switches to right bank ; 5- deposition on right bank and avulsion ; 6- Water reaching sector of the church.

https://doi.org/10.5194/egusphere-2026-971
Preprint. Discussion started: 6 March 2026

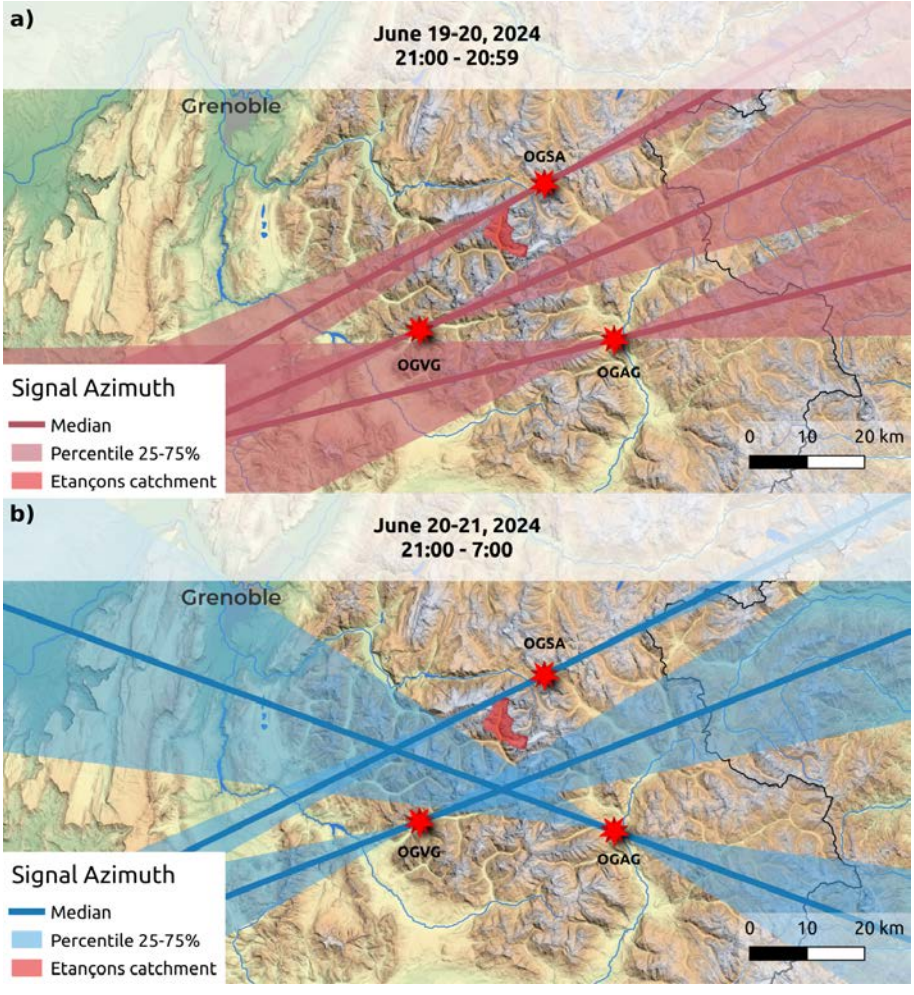

Figure A20. Orientation of the particle motion derived from the seismic signal recorded at OGVG, OGSA, and OGVG, shown during the event **(a)** and outside the event **(b)**. The darker line indicates the median azimuth of particle motion, while the shaded area represents the 25th to 75th percentile range. The azimuth during the rapid discharge was computed as the median over the period from 2024/06/20 21:00 UTC to 2024/06/21 07:00 UTC, while the azimuth outside the event was calculated as the median over the 24-hour periods before and after the event (see blue and pink area in A19).

https://doi.org/10.5194/egusphere-2026-971
Preprint. Discussion started: 6 March 2026

A12 Glacial lake drainage

The volume of the lake is about 100 000 m^3. Its sudden drainage would lead to a peak discharge of around 80 m^3 s^{-1} and a release of the entire stored water volume in about 20 minutes (using the Torricelli law). This high-water discharge flowing on the steep slope stream downstream the glacier (slopes in the range 30-40 %) would have triggered a debris flow. The volume concentration of this debris flow would have been around 50 %, considering flume measurements (Takahashi, 1978; Lanzoni et al., 2017) or field observations (Huggel et al., 2004). Thus, the total volume of the debris flow would be around 200 000 m^3. Using empirical equations relating peak discharge and total debris flow volume reported in the literature for granular debris flow (Mizuyama et al., 1992; Rickenmann, 1999; Bovis and Jakob, 1999), the peak discharge associated with the propagation of this debris flow would be in the range 1800 – 3000 m^3 s^{-1}. The empirical relations used are in the following form:

$$Q_{peak} = a \cdot {V_{debrisflow}}^{b}$$

With Q_{peak} the debris flow peak discharge (m^3 s^{-1}), $V_{debrisflow}$ the total volume of the debris flow (water and sediment, in m^3), a and b empirical coefficients. Rickenmann obtained $a = 0.1$ and $b = 0.83$, Bovis and Jakob obtained $a = 0.05$ and $b = 0.9$ and Mizuyama et al. obtained $a = 0.135$ and $b = 0.78$. Note that considering a granular debris flow here is consistent with the grain size distribution observed on the Bonne Pierre torrent, with high quantities of sand, low quantities of clay and many boulders. The deposits shape of the 2024 flood in the upper Bonne Pierre torrent as well as old deposits also suggest that the Bonne Pierre torrent produces granular debris flows (muddy debris flows are unlikely). Using an empirical equation proposed by Rickenmann (1999) relating the debris flow volume and the propagation length, we can consider that a 200 000 m^3 debris flow would have propagate until the alluvial fan of the Étançons, where the Bérarde village is located (Fig. A21). This empirical relation is in the following form:

$$L = 1.9 \cdot {V_{debrisflow}}^{0.16} \cdot H^{0.83}$$

With L the travel distance (m), $V_{debrisflow}$ debris flow the debris flow volume (m^3) and H the elevation difference (m).

Using an empirical equation for debris flow relating velocity to height (Rickenmann, 1999), we can estimate the range of maximum debris flow height in several locations and compare it to post-flood survey and witnesses' observations.

The simplified Rickenmann friction law is in the form:

$$V = c \cdot {R_h}^{0.67} \cdot S^{0.5}$$

With V the mean velocity (m s^{-1}), c an empirical friction coefficient found to be on average 0.1 s $m^{-1/3}$ for debris flow, R_h the hydraulic radius and S the reach slope. Using this simplified calculation, we obtain a debris flow height in the canyon (part IV) downstream the Bonne Pierre torrent confluence in the range 10-13 m. Post-flood survey gave flood marks in the range 3-3.5 m, which is much lower than the calculated height considering a sudden lake drainage (see Fig. A22 left panel). On the alluvial fan where the Bérarde village is located (calculation is made just upstream the main bridge, see see Fig. A22 right panel), the calculation gives a range of height of 12-17 m. This range is also not consistent with witnesses that did not observe a sudden overflowing at this location. Note that the main bridge has a maximum height of 5.5 m.

https://doi.org/10.5194/egusphere-2026-971
Preprint. Discussion started: 6 March 2026

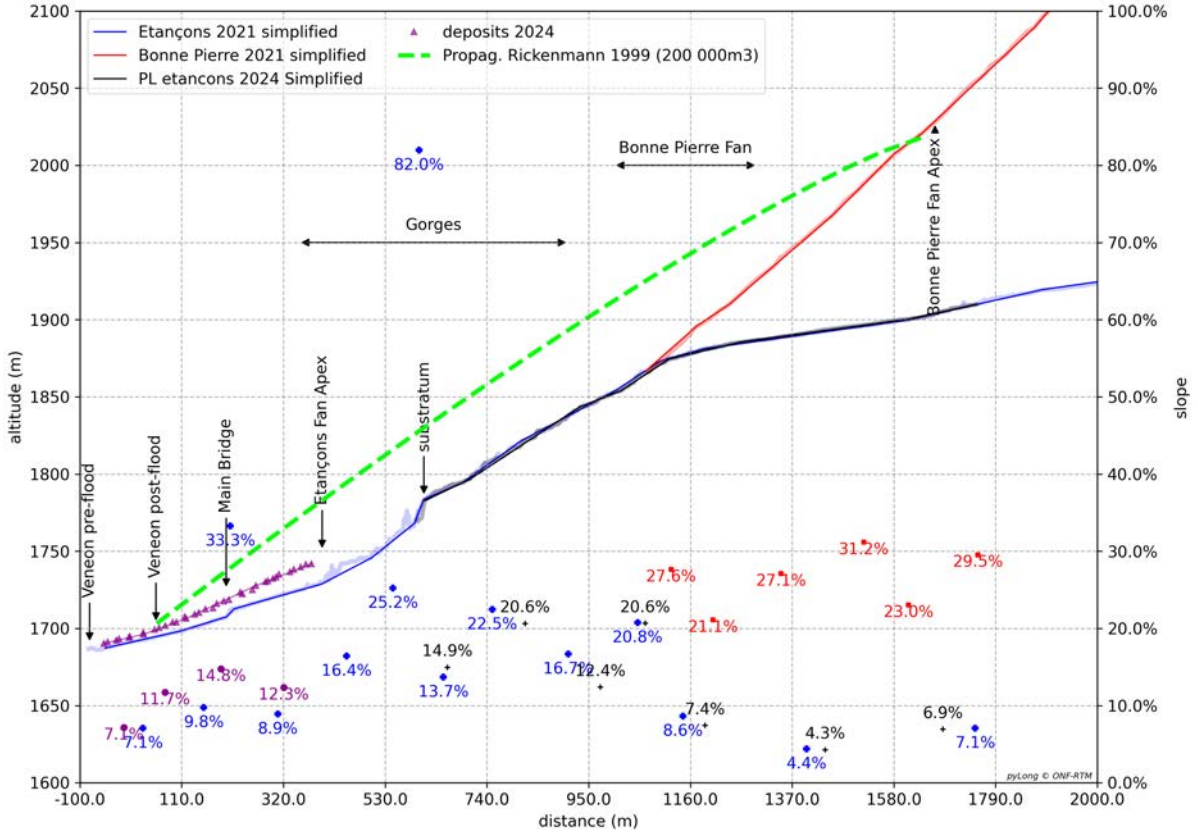

Figure A21. Propagation of a 200 000 m^3 debris flow from the upper Bonne Pierre torrent, using the Rickenmann (1999) empirical equation.

Figure A22. Maximum height observed in the canyon (part IV) after the flood (left). View of the Étançons fan apex and location of the main bridge before the flood (right).

https://doi.org/10.5194/egusphere-2026-971
Preprint. Discussion started: 6 March 2026

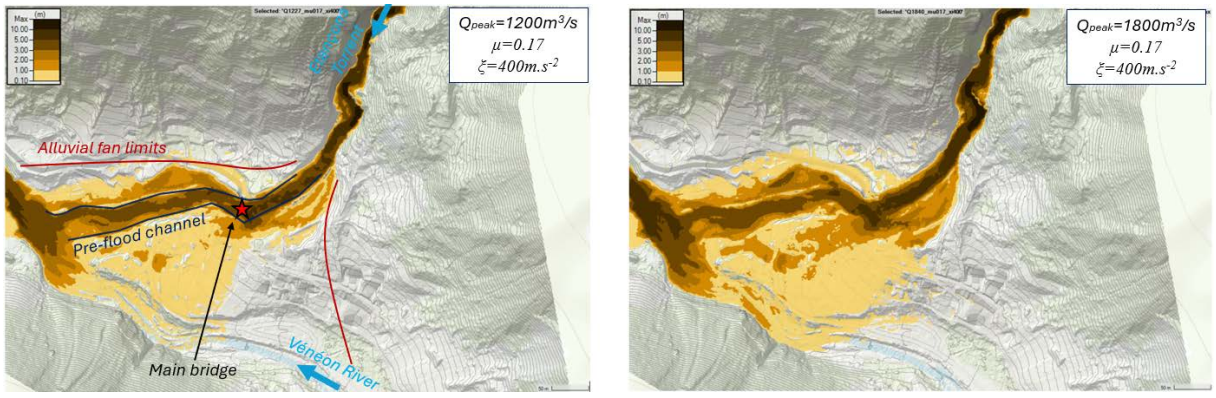

Figure A23. Maximum height obtained by non-Newtonian modeling of a debris flow triggered by a sudden lake drainage. The debris flow volume is 200 000 m^3, the peak discharge is about 1200 m^3 s^{-1} on the left and 1800 m^3 s^{-1} on the right. The Voellmy friction parameters considered are: μ=0.17 and ξ=400 m s^{-2}.

We also performed numerical modeling using bidimensional non-Newtonian model. We considered the Voellmy rheology (Voellmy, 1955) implemented in the non-Newtonian library of the HEC-RAS platform (Gibson et al., 2022). The Voellmy law can be written as follow:

$$\tau = \mu \cdot N + \frac{\rho g V_2}{\xi}$$

With τ the shear stress, μ the coulomb friction coefficient, N the normal stress, ρ the density, g the acceleration due to gravity, V the velocity and ξ the Voellmy turbulence coefficient. We considered the median values of μ and ξ (respectively 0.17 and 400 m s^{-2}) obtained by the back analysis of debris flow cases reported in the literature (Schraml et al., 2015; Aaron and McDougall, 2019; Zimmermann et al., 2020; Choi et al., 2021). This simplified modeling approach confirms that a sudden release of the lake would have led to sudden and large damage on the fan, which is not consistent with what was observed. We thus believe that the sudden drainage of the lake can be excluded.

A13 Chronology

https://doi.org/10.5194/egusphere-2026-971
Preprint. Discussion started: 6 March 2026

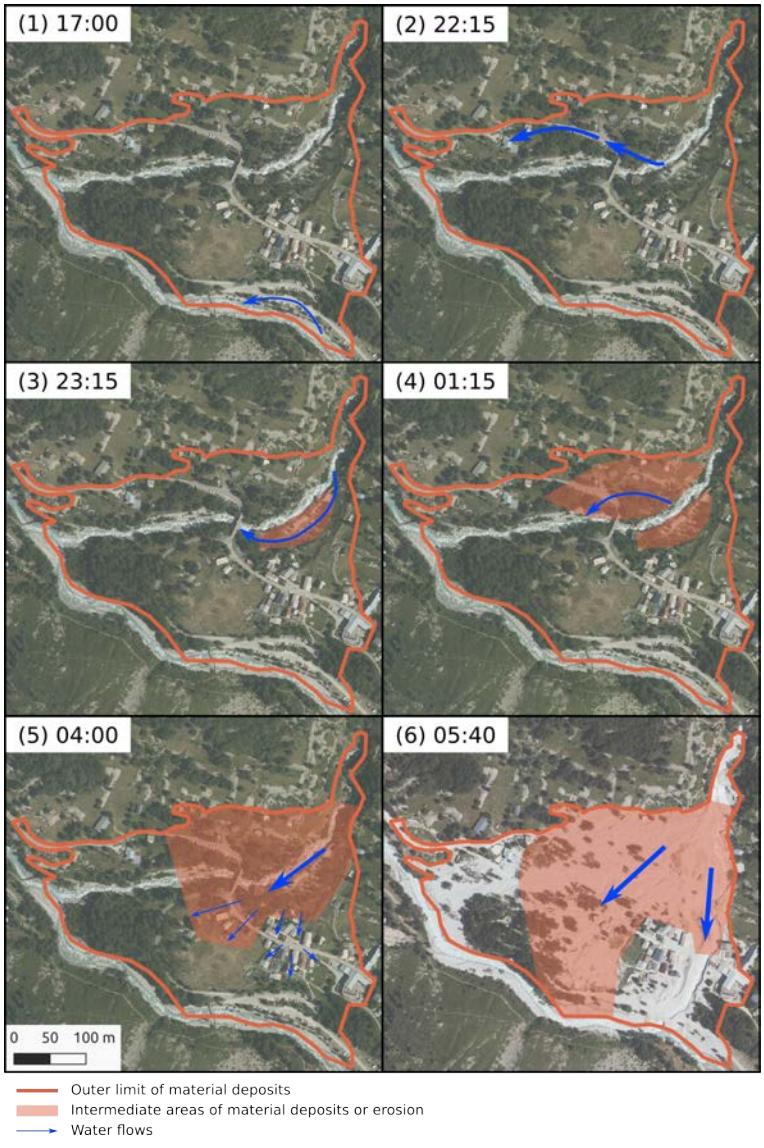

Figure A24. Approximate reconstruction of water overflows and material deposion/erosion events unfolding based on testimonies and, photos and videos. Numbering corresponds to the numbering of Figure 9. Timing and extents are indicative and not exact. Background image for (1)-(5) corresponds to the IGN 2021 Orthophoto. The background image for (6) is from IGN Orthophoto post flood event in 2024.

https://doi.org/10.5194/egusphere-2026-971
Preprint. Discussion started: 6 March 2026

A14 Return periods

The Bayesian framework we used is based on the library PyMC (Abril-Pla et al., 2023). Data are standardized prior to fitting the General Extreme Value distribution. The model has the following structure:

$$\begin{aligned} \mu &\sim Normal(0, 0.5) \\ \sigma &\sim HalfNormal(0, 0.3) \\ \xi &\sim TruncatedNormal(0, 0.2, [-0.6, 0.6]) \\ gev &\sim GEV(\mu, \sigma, \xi) \end{aligned} \tag{A1}$$

with the prior parameters: μ-location, σ-scale, and ξ-shape. The priors μ-location are sampled from a normal distribution of mean zero and standard deviation 0.5. The priors σ-scale are sampled from a half normal distribution of mean 0 and standard deviation 0.3. And the priors ξ-shape are sampled from a truncated normal distribution of mean 0 and standard deviation 0.2, truncated below -0.6 and above 0.6.

The gev is the classical GEV probability distribution function defined as follow:

$$GEV = \frac{1}{\sigma} t(x)^{\xi+1} e^{-t(x)} \qquad \text{where } t(x) = \begin{cases} \left[1 + \xi\left(\frac{x-\mu}{\sigma}\right)\right]^{-1/\xi} & \text{if } \xi \neq 0 \\ exp\left(-\frac{x-\mu}{\sigma}\right) & \text{if } \xi = 0 \end{cases} \tag{A2}$$

Results presented in Figure A25 and A26 are respectively estimated based the time period 1964-2024 and 1959-2024. Hourly timeseries are aggregated to 48 h cumulative precipitation by a rolling sum. Results are quite sensitive to the period of interest. The choice of 48 h was done in respect to rain at which the return period is the most pronounced for the June 2024 event. Shorter or longer integrating time window result in less significative intensity. The uncertainties in return period estimates remain high (see the wide distributions in Figure A26.

https://doi.org/10.5194/egusphere-2026-971
Preprint. Discussion started: 6 March 2026

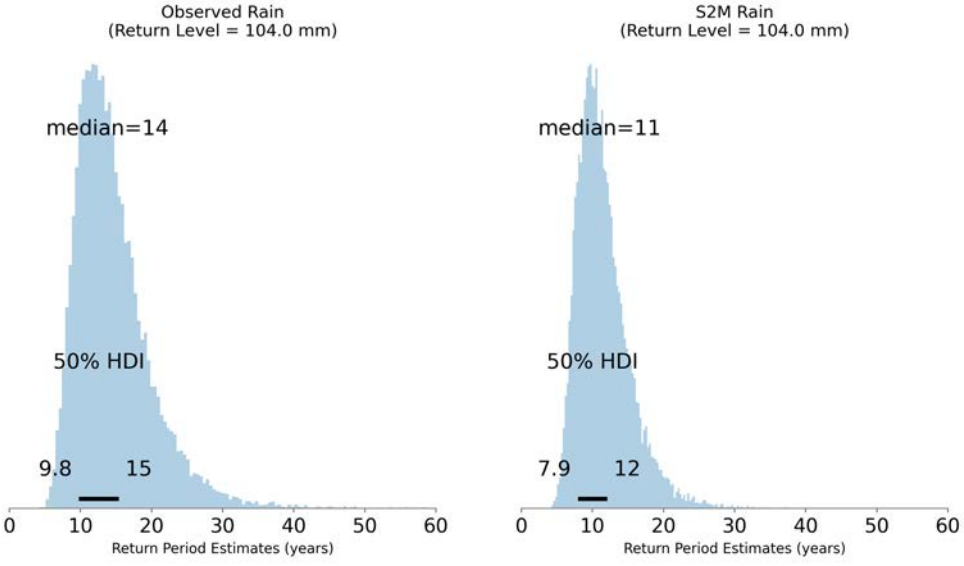

Figure A25. Return period estimates for a rain event of 104 mm in 48h at Saint Christophe en Oisans, based on the precipitation record (left), and the S2M reanalysis (right). The GEV model was trained on the period 1964-2023 using a Bayesian estimator.

https://doi.org/10.5194/egusphere-2026-971
Preprint. Discussion started: 6 March 2026

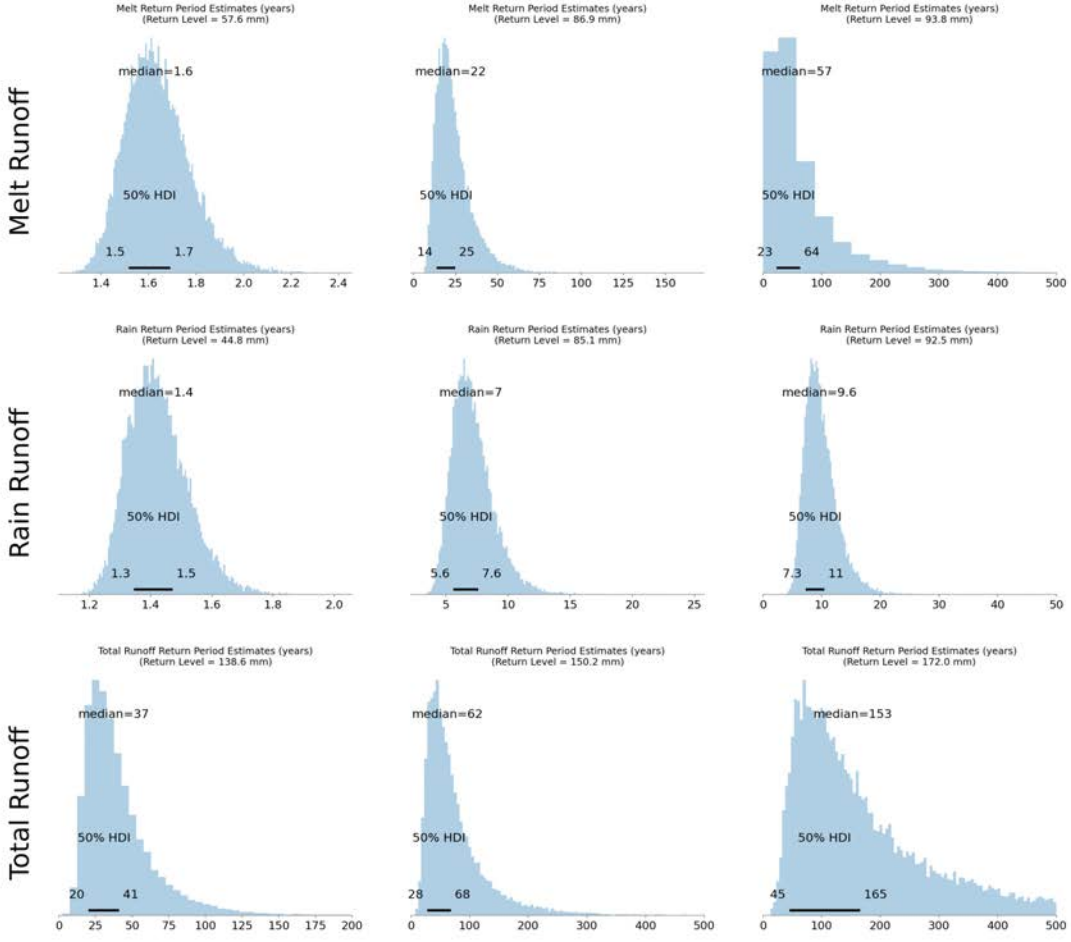

Figure A26. Return period estimates fitting a GEV with Bayesian estimator. The model is fitted on the 01/01/1959 to 20/06/2024 data outputs from the S2M simulation aggregated to the whole Étançons catchment. By row, respectively return period distributions for melt, rain and total runoff (rain + melt) at characteristic return levels for the three 48 h period centered around June 19 08:00 (UTC), June 20 05:00 (UTC), and June 21 00:00 (UTC). Table A4 summarize the corresponding return level and time.